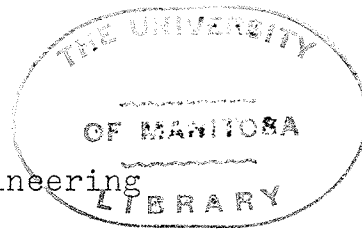


SOME ASPECTS OF CONSOLIDATION FOR
A VARVED LAKE AGASSIZ CLAY

A Thesis
Presented to
the Faculty of Civil Engineering
University of Manitoba



In Partial Fulfillment
of the Requirements for the Degree
Master of Science

by
Richard Terrence Martin
May 1961

ACKNOWLEDGMENTS

I wish to acknowledge my gratitude to Professor A. Baracos, whose impetus and encouragement made this study possible.

I also appreciate the assistance provided by the Division of Building Research of the National Research Council of Canada. In particular, I want to thank Mr. James Hamilton, who arranged the loan of papers from the D.B.R. library and provided many ideas through conversations with me.

My special gratitude to Dean W. H. McEwen, who assisted with the mathematics involved in this study.

Finally, I thank the staff of the Engineering library, and Mr. Henry Wiebe of the Soil Mechanics laboratory for his able assistance.

ABSTRACT

SOME ASPECTS OF CONSOLIDATION FOR A VARVED LAKE AGASSIZ CLAY

The purpose of this study was to measure the common characteristics of compression and consolidation that apply to a typical sample of clay from the Lake Agassiz deposit in Winnipeg. In particular, data was required on the effect of testing techniques, the effect of repeated cycles of loading and unloading on a clay, and the general consolidation and compression properties of the clay parallel to both the vertical and horizontal axes of the clay.

In order to determine the influence of equipment upon the values, two types of consolidation equipment were used; a consolidometer (oedometer), and a triaxial cell. The effects of different testing techniques were found by varying the testing procedure for the consolidometer. Loading cycles were studied by repeatedly loading and unloading consolidometer specimens between various limits. For all tests the specimens were extracted from the same block sample, in order to ensure that the results would always be comparable.

It was found that the results were somewhat unpredictable. Even the initial void ratios of the various specimens cut from the block showed widely varying values. In fact, it was found that two groups of specimens were de-

fined by the initial void ratio: silty ones averaging at 1.58, and clayey ones at 1.75. It was further discovered that the silt affected the consolidation characteristics far more than the compression properties. In fact, the only influence upon the compression properties was the downward displacement of the entire compression curve (e-log p curve).

The effect of the orientation of the laminations was also found to be more significant in the consolidation characteristics than in the compression properties. Apart from a slightly higher overburden pressure for vertical specimens, no difference in the compression properties existed. However, it was found that samples compressed in a direction parallel to the laminations (horizontal samples), yielded permeabilities roughly twice as large as those in vertical samples.

The comparison of results between consolidometer tests and triaxial tests did not prove to be fruitful, but it was possible to show that the testing procedure has no effect upon the compression properties gained from the consolidometer. No attempt was made to discover how testing techniques affected the consolidation characteristics.

It was discovered that cycling caused the hysteresis loops to progress downwards in a fairly regular manner. Moreover, indications were that these loops also flattened a

slight amount. Other analyses indicated that the highest load in the cycle had a major influence upon the amount of downward shift of the consolidation curve.

In the final analysis this thesis was of very general nature, and was intended to be a possible forerunner for future investigations on the various aspects included within it.

TABLE OF CONTENTS

SECTION	PAGE
Glossary of Terms	xiv
I. PURPOSE AND EXTENT OF RESEARCH	1
Purpose and Scope of Research	1
Definition of the Values Sought	2
Organization of the Thesis	4
II. LITERATURE REVIEW	5
Effect of Sample Disturbance	5
Effect of Equipment	7
Effect of Consolidometer Testing Techniques	8
Theory	10
Effect of Triaxial Test Techniques	12
Structure and Swelling	12
III. DESCRIPTION OF THE SAMPLE	16
Location, Removal, and Preservation of the Sample	16
Type of Sample	17
Classification Tests, 18	
IV. TESTING EQUIPMENT AND TECHNIQUES	20
The Consolidometer	20
Loading Devices and Calibrations, 20; Consolidometer Procedure, 22	
Triaxial Cell	26
Pressure Apparatenances, 26; The Cell Assembly, 27; Procedure, 30	

SECTION	PAGE
V. COMPRESSION AND CONSOLIDATION PROPERTIES	
IN THE CONSOLIDOMETER	34
Sample Disturbance	34
Remoulded Samples, 35; Typical Laboratory Disturbances, 38	
Compression Properties	41
Sample Irregularities, 41; Initial void ratio variation, 42; Orientation of laminations, 45; Effect of Test Procedure, 47	
Consolidation Characteristics	52
Effect of Fitting Methods, 53; Calculation of Errors, 57; Permeability, 58; Coefficient of Consolidation, 60	
Summary	60
VI. CONSOLIDATION TEST IN A TRIAXIAL CELL . . .	64
The Theory of Combined Axial and Radial Consolidation	64
Evaluation of Hydraulic Gradients, 65; Pore Volume Change, 65; Basic Differential Equation, 68; Theorem Combining Radial and Axial Consolidation, 69; Solution of the Differential Equation, 71; Boundary Conditions, 74; Time Factors, 76; Degree of Consolidation, 76	
Results of Triaxial Consolidation	79
Compressibility by Triaxial Con- solidation, 83; Consolidation Characteristics in the Triaxial Cell, 86	
Difficulties with the Triaxial Method . .	91
VII. EFFECTS OF LOADING CYCLES	95
Effect of Cycling upon Compression Properties	95

SECTION

PAGE

Effect upon Compression Curves, 95; Magnitude and Causes of Curve- Shift, 99; Flaking of the Sample, 106; Flattening of the Loops, 107	
Effects of Cycling upon Consolidation	
Characteristics	109
Summary	113
VIII. SWELLING PROPERTIES	114
Determination of Swelling Indices	114
Explanation of Rebound Curves, 114; Swelling-Time Curves, 118; The Swelling Index, 120	
Factors Influencing Swelling	124
Sample Disturbance during Swelling, 124; Cycling in the Field, 124; Orientation of Laminations, 125; Drying of the Samples, 127	
Summary	127
IX. SUMMARY OF CONCLUSIONS	129
BIBLIOGRAPHY	133
APPENDIX A	137
APPENDIX B	142
INDEX	150

LIST OF TABLES

TABLE		PAGE
I.	Classification Characteristics of the Clay	19
II.	Average Degree of Consolidation for Various Time Factor Values	80
III.	(a) e Vs. p Computation for TM 39	87
	(b) T_v and T_h Computations for TM 39.	88
IV.	Effects of Cycling upon Void Ratio and Rebound	101

LIST OF FIGURES

FIGURE		PAGE
1	Consolidometers and Loading Devices	21
2	Typical Apparatus Deflections	23
3	The Cutting Tools and Brass Rings for Consolidometer Specimens	28
4	Details of Drains in Triaxial Cell	28
5	Two Views of Assembled Triaxial Cell . . .	29
6	Compression Curves for Remoulded Samples .	36
7	Compression Index Vs. Moisture Content . .	37
8	Reconstruction of the Field Compression Curve from a Low Pressure	39
9	Frequency Curve of Initial Void Ratio Variation in the Block Sample	43
10	Typical Compression Curves for Two Groups of Specimens	44
11	Log p Versus e/e_0	46
12	Compression Curves for Various Types of Loading	48
13	Determination of Overburden Pressure by Two Methods	51
14	A Comparison of Actual and Theoretical Deflection-Log Time Curves	54
15	A Comparison of Actual and Theoretical Deflection-Root of Time Curves	56

FIGURE	PAGE	
16	Void Ratio Vs. Permeability for Horizontal, Vertical, and Remoulded Specimens	59
17	e/e_0 Vs. Permeability for Horizontal, Vertical, and Remoulded Samples	59
18	Coefficient of Consolidation Vs. Pressure .	61
19	Pressure Distribution with Three Dimensional Drainage through a Cylindrical Specimen	66
20	Consolidation-Time Curves for Axial and Radial Drainage	81
21	Consolidation-Square Root of Time Curves for Axial and Radial Drainage	82
22	Compression Curves in the Triaxial Cell. . .	84
23	Triaxial Consolidation-Time Curves	90
24	Deflection-Time Curves for 115 psi Pressure on TM 39	94
25	Typical Compression Curve for TM 31	97
26	Two Compression Curves created by Cycling. .	98
27	Effect of Load Cycles upon Void Ratio . . .	100
28	Curve-Shift Versus Number of Cycles for Large and Small Load Increments	100
29	Effect upon Curve-Shift of Minor Cycles within the Major Loop	105
30	Effect of Void Ratio upon the Curve-Shift .	105

FIGURE

PAGE

31	Effect of Cycling upon the Coefficient of Compressibility	108
32	Effect of Cycling upon the Coefficient of Consolidation	110
33	Effect of Cycling upon the Coefficient of Permeability	111
34	Rebound Curves from Various Void Ratios . .	115
35	Typical Swelling-Log Time Curves for TM26 .	119
36	Arithmetic Swelling-Time Relationship for TM 26	121
37	Swelling-Root of Time Plots for TM 26 . . .	122
38	Swelling Index Vs. e_r/e_o	123
39	Swelling Caused by Dessication	126
40	Complete Swelling Curves for TM 26	143
41	Complete Swelling Curves for TM 27	144
42	Two Sets of Swelling Curves for TM 17 . . .	147
43	Swelling-Time Curve Variation with Cycling of TM 20	149

GLOSSARY OF TERMS

A number of symbols, that are not standard, have appeared in this thesis. In the following pages they have been listed and explained. In addition, a number of terms which are commonly accepted at the University of Manitoba are listed and defined in order to dispel any doubts regarding their meanings.

- A area perpendicular to direction of flow, and a constant of integration in section VI
- a coefficient of compressibility:
 a_h - perpendicular to vertical axis or parallel to the laminations.
 a_v - parallel to vertical axis (vertical specimen)
- B constant of integration in section VI
- C coefficient of consolidation:
 C_h - horizontally and C_v vertically
- C_r swelling index (slope of rebound curve per log cycle of an e-log p plot)
- CI compression index (slope of compression curve per log cycle of an e-log p plot)
- E relative error in a computation (%)
- e void ratio (volume voids/volume solids)
- e_0 initial void ratio (often the field value)
- e_r the void ratio at the beginning of rebound
- exp base for natural logarithms (2.718282)
- $F(r)$ function of r ($F'(r)$ - first derivative)
- H length of vertical drainage path
- dH increase or decrease of specimen height
- h pressure head in water (unit pressure/density of water)
- i hydraulic gradient ($\delta h/\delta L$)
- J represents a Bessel Function:
 J_0 - of zero order, J_1 - of order one.
- k coefficient of permeability:
 k_h - horizontally
 k_r - radially from vertical axis
 k_v or k_z - vertically
- M a number ($\pi n/2$)
- m order of Bessel Function and a number ($\frac{n-1}{2}$)
- n any positive integer
- p intergranular pressure:
 p_0 - of overburden
 p_0' - of preconsolidation

- dp increment of pressure ($p_2 - p_1$) wherein:
 p_2 - recently applied load
 p_1 - previously applied load
 dp/p_1 - load increment ratio
- Q total flow past any section:
 Q_r - radially and Q_z - axially
- q rate of flow past any section
- R outer radius of a cylindrical specimen
- r radius of any section in a cylinder
- T time factor:
 $T_h (T_r)$ - horizontally (radially)
 $T_v (T_z)$ - vertically
- t time
- U degree of total consolidation:
 U_r - degree of radial consolidation
 U_z - degree of vertical consolidation
 U_{zr} - degree of consolidation at (z, r)
- U' average degree of consolidation
- u pore pressure (u_0 after load applied)
 u_z (function of pore pressure in terms of z and t)
- V volume
- dV volume change
- w moisture content
- z depth below top of specimen
- γ unit density (γ_w - of water)
- δ represents an increment (e.g. δt , increment of time)
- ρ number of loading cycles between two pressures
- σ curve-shift (downward displacement of the e -log p curve
 at a particular pressure due to the loading cycles)
- $\phi(t)$ function of time
- ω root of Bessel Function of zero order
 ω_k - root number k

SECTION I

PURPOSE AND EXTENT OF RESEARCH

The clays in the vicinity of Winnipeg are lacustrine deposits that were formed on the bed of Lake Agassiz following the last ice age. They are formed in varves of silt and clay and the latter are believed to be of dispersed structure, as defined by Lambe.¹ Unlike the more orthodox clays of flocculated structure, upon which a great deal of research has been conducted, Winnipeg clays are highly swelling, very compressible, and anisotropic. These differences create a need for research along the lines of investigation performed by others on the orthodox clays.

I. PURPOSE AND SCOPE OF RESEARCH

The purpose of this study was to measure the common characteristics of compression and consolidation that apply to a typical sample of clay from the Lake Agassiz deposit. In addition, it was desired to ascertain the effects of techniques of testing and the previous load history upon these results.

In order to ascertain the effects of the techniques of testing, a great deal of review of literature was nec-

¹T. W. Lambe, "The Structure of Inorganic Soil," The Proceedings of the American Society of Civil Engineers, 1953, Vol. 79, No. 315.

essary. This provided information on how such things as load increments and time affected the results of consolidation tests. In addition, it was decided to attempt to consolidate some specimens in a triaxial cell, because it was believed that the latter created less disturbance of the clay. In order to discover the effects of loading history, some "cycling tests" were run. These tests are similar to the consolidometer tests except that the loads are added and subtracted in repeated cycles, in an effort to duplicate what could occur in the field.

The determination of the consolidation and compression characteristics of the local clays will provide engineers with a crude criterion for use in determining settlements and seepage in beds of varved clay near Winnipeg. Moreover, the study of the cycling characteristics will advance the understanding of the behaviour of these clays in the field.

II. DEFINITION OF THE VALUES SOUGHT

The compression characteristics describe the change in void ratio with pressure. The most popular notation is a graph with void ratio plotted as an ordinate to an arithmetic scale and pressure as an abscissa plotted on a logarithmic scale. The curve has hereinafter been referred to as the e -log p or compression curve. Sometimes

the notation takes the form of an e-p curve, which is the same as e-log p except that it is plotted on a straight arithmetic scale. The compression properties that are derived from such curves are;

- 1) The compression index (CI), which is the slope of the straight line portion of the e-log p plot.
- 2) The coefficient of compressibility (a), which is the slope of the chord between two points on the e-p curve.
- 3) The swelling index (C_r), which is the slope of the swelling portion, rather than the compression branch on the e-log p curve.
- 4) The overburden pressure (p_0) and the preconsolidation load (p_0').

Because Winnipeg clays are anisotropic, measurements of these particular values in both the vertical and horizontal directions (designated by subscripts v and h respectively) have been made.

The consolidation characteristics are the coefficient of consolidation (C), which is a constant required for the solution of the theoretical time-deflection analysis, as given by Terzaghi,² and the coefficient of permeability (k)

²Karl Terzaghi, Theoretical Soil Mechanics, (John Wiley and Sons, Inc., New York, 1943), p. 271.

which is the constant involved in Darcy's Law for the flow of water through a soil. Again the aforementioned designation for the vertical and horizontal cases has been used.

III. ORGANIZATION OF THE THESIS

As an introduction to the main section of the thesis, a review of the literature relating to consolidation testing has been presented in Section II. Section III has described the sample that was used and given some of its general properties of classification. Finally, Section IV dealt with the testing equipment and the techniques that they required.

In the body of the thesis the results of the various tests have been presented. Section V gave the results of the standard consolidation test and made an attempt to assess the validity of them as undisturbed results by comparing them with remoulded samples. The consolidation characteristics obtained from the triaxial cell have been presented together with pertinent theory in Section VI. Section VII dealt with the effects of cycling. The swelling characteristics have been discussed in Section VIII.

A summary of the conclusions has been placed in Section IX.

SECTION II

LITERATURE REVIEW

Since the first papers on the subject of consolidation of clays were presented, a good deal of diverse investigation has occurred. It would be impossible to mention all the significant presentations that have been made in this vast field. Therefore, only those papers of significance to this study have been reviewed.

An attempt has been made to outline briefly the significant presentations that refer to the aspects of consolidation and consolidation testing. The effects of sample disturbances, types of equipment, testing techniques, fitting methods, secondary compression, and of structure have been discussed.

I. EFFECT OF SAMPLE DISTURBANCE

In order to ascertain the validity of the consolidation test for such things as the prediction of settlements, it was necessary first, to determine how representative of field conditions the samples, that are used in the laboratory, could be.

In 1942, Rutledge¹ stated that disturbance and remoulding have the following effects:

¹P. C. Rutledge, "Relation of Undisturbed Sampling to Laboratory Testing," paper #2229, A.S.C.E. Transactions, Vol. 109, (1944), p. 1155.

1. Decrease the void ratio at which a soil will carry any given stress.
2. Obscure the previous stress history.
3. Cause the straight line portion of the compression curve to displace downwards from the laboratory virgin compression curve, and to assume a flatter slope.

He further concluded that by extending the swelling line to meet the laboratory virgin compression line, a reasonable value for the preconsolidation pressure can be obtained.

Van Zelst² confirmed the conclusions of Rutledge. He also found that the depth of disturbance in a specimen is a constant value, and consequently, thicker samples give more reliable results. In fact, he concluded that a sample one and one-half inches in thickness is a very good representation of an undisturbed specimen.

Schmertmann³ developed the void ratio reduction patterns that Van Zelst had used, and used these as a trial and error method for sketching the undisturbed compression curve. He set forth the procedure for reconstructing this

²T. W. Van Zelst, "An Investigation of the Factors Affecting Laboratory Consolidation of Clay," Proceedings of Second International Conference on Soil Mechanics and Foundation Engineering, Vol. VII, paper 11C4, p. 52.

³John H. Schmertmann, "The Undisturbed Consolidation Behaviour of Clay," paper #2775, Transactions of American Society of Civil Engineers, Vol. 120, (1955) p. 1201

curve for a vast number of circumstances. However, his methods did not permit swelling of the samples, due to either the release of load, or the completion of saturation in partially dried clays.

His studies also indicated that disturbance gives low values for the coefficient of consolidation in the laboratory. Furthermore, because the coefficient of permeability is a function of the void ratio, he postulated that the partial destruction of the latter would decrease the apparent coefficient of permeability as indicated by laboratory tests.

II. EFFECT OF EQUIPMENT

Two types of apparatus are commonly used for consolidation tests. They are, the consolidometer, and the triaxial cell.

The consolidometer is more frequently used and has been analysed more thoroughly. A great deal of thought and analysis on the effect of friction upon the test values has been done by Taylor.⁴ He found that a correction for friction would lower the compression branches of the e-log p curve; whereas, it would raise and straighten the swell-

⁴Donald W. Taylor, "Research on Consolidation of Clays," Massachusetts Institute of Technology publication of the Department of Civil and Sanitary Engineering, (1942), serial 82.

ing branch. He found that approximately five per cent of the total load increment is lost to friction in the floating ring type of test, which was used in the following thesis by the investigator. Finally, he intimated that the triaxial cell would incur less disturbance during the testing.

In the triaxial cell, the cell pressure is a constant value but in both, the consolidometer and nature, the total lateral pressure decreases as consolidation progresses. This fact makes the coefficient of consolidation, as found by the triaxial method, slightly low, and Rowe⁵ has developed a correction that makes the results comparable to those gained from the consolidometer. In the same paper Rowe analysed the effectiveness of the filter drains that are used in the triaxial method and found that they became ineffective to a certain extent when subjected to cell pressures.

III. EFFECT OF CONSOLIDOMETER TESTING TECHNIQUES

Langer⁶ showed that very slow loading could produce

⁵P. W. Rowe, "Measurement of the Coefficient of Consolidation of Lacrustine Clays," Geotechnique Vol. IX, (1959), p. 107.

⁶Karl Langer, "The Influence of the Speed of Loading Increment on the Pressure Void Ratio Diagram of Undisturbed Laboratory Soils," Proceedings of the First International Conference on Soil Mechanics and Foundation Engineering, No. D9, Vol. II.

very low values for the compression index. Terzaghi⁷ felt that the compression index as produced by natural loading should be about 0.04. However, it was found that in reality, and proved by moisture content profiles, that the value is 0.3 and higher. In order to explain this disparity Terzaghi proposed the solid bond theory, in which bonding occurred during the secondary compression of a clay while it is loaded in nature. However, extremely heavy loads will destroy this bond and cause the compression indices to become as high as they exist in reality.

After this breakdown has occurred, the rate and increment of loading do not have an appreciable influence upon the compression index.⁸

Although the load increment does not affect the compression characteristics, it does have an appreciable influence upon the consolidation characteristics. Taylor⁹ has shown that the coefficient of consolidation increases when larger load increments are used.

⁷Karl Terzaghi, "Undisturbed Clay Samples and Undisturbed Clays," Journal of the Boston Society of Civil Engineers, Vol. XXVIII, No. 3.

⁸J. J. Hamilton and C. B. Crawford, "Improved Determination of Preconsolidation Pressure of a Sensitive Clay," Special technical publication No. 254 published by American Society for Testing Materials.

⁹Taylor, op. cit.

The pressures to which a clay has been loaded in the field and unloaded in the laboratory influence the swelling and recompression respectively. The greater the preconsolidation load, the steeper is the swelling line that is produced; the smaller the relieving load of swelling, the greater is the amount of subsequent recompression.¹⁰

IV. THEORY

The theory of primary consolidation has been well developed and is well known. No attempt has been made to present it here. However, the methods of correlating the actual test-time curves with that determined by the Terzaghi theory¹¹ are somewhat controversial, due to their empirical nature.

The logarithm of time method for fitting was proposed by Casagrande.¹² Taylor,¹³ later proposed a similar presentation using the square root of time. However, Naylor and Doran¹⁴ decided that a plot relating the natural logarithm of time to the degree of consolidation subtracted from

¹⁰R. Haefeli, "On the Compressibility of Preconsolidated Soil Layers," paper 1d4, Vol. I, Proceedings of Second International Conference on Soil Mechanics and Foundation Engineering, p. 42.

¹¹Karl Terzaghi, Theoretical Soil Mechanics, (John Wiley and Sons, Inc., New York, 1943), pp. 265-290.

¹²Donald W. Taylor, Fundamentals of Soil Mechanics, (John Wiley and Sons, Inc., New York, 1948), p. 240

unity (1-U) is a more reliable method, because it permits secondary consolidation to begin at $U = 0.8$ with nothing but primary consolidation before $U = 0.6$. In order to overcome the sharp break at the preconsolidation load of Leda clays, a rate of strain corresponding to .0006 inches per hour has been recommended as an adequate strain for the point at which primary consolidation is completed in this type of clay.¹⁵

The theory regarding the secondary compression is not as well developed as that for the primary. However, a few theories on this compression have been proposed by Taylor.¹⁶ In this treatise he suggested that because undisturbed samples produce greater secondary consolidation than do remoulded samples, secondary consolidation is caused by the disturbance created by primary consolidation. Moreover, he stated that because strata thicknesses are so great in nature as compared to those encountered in the laboratory, a great deal of secondary consolidation will

¹³Donald W. Taylor, Fundamentals of Soil Mechanics, (John Wiley and Sons, Inc., New York, 1948), p. 238.

¹⁴A. H. Naylor and I. G. Doran, "Precise Determination of Primary Consolidation," Proceedings Second International Conference on Soil Mechanics and Foundation Engineering, Vol. I, p. 34.

¹⁵Hamilton and Crawford, op. cit.

¹⁶Taylor, Research on Consolidation of Clays, op. cit.

occur during the process of primary consolidation, which in the field is extremely slow. Therefore, the compressibility (a) is greater, and the coefficient of consolidation is smaller in nature. He further implied that secondary consolidation could occur at the same rate for both thick and thin samples. The ultimate effect of secondary consolidation is to shift the e -log p curve downwards.

V. EFFECT OF TRIAXIAL TEST TECHNIQUES

The amount of literature on this subject is somewhat limited. However, Bishop and Henkel¹⁷ have stated that normally consolidated clays yield higher compressibilities in the triaxial method, and that overconsolidated clays yield compressibilities that are considerably greater. Moreover, the value for the coefficient of consolidation is lower than that for the consolidometer method.

VI. STRUCTURE AND SWELLING

Structure has an effect upon the consolidation as one would expect. In Lacustrine clays it has been found that the value for the horizontal coefficient of consolidation exceeds that for the vertical at low pressures, because the

¹⁷Allan W. Bishop and D. J. Henkel, Measurement of Soil Properties in the Triaxial Test, (Edward Arnold Ltd., 1957)

varves are fairly free running at low stresses.¹⁸ Rowe¹⁹ has indicated that, for samples loaded parallel to the horizontal axis in the consolidometer, the coefficient of consolidation increases with the thickness of the sample.

However, the main importance of structure seems to be in the explanation of swelling phenomenon. A great deal of diverse research has been done on swelling, particularly the swelling of compacted clays, but recently the introduction of clay mineralogy and the concepts of structure have permitted the explanation of the swelling of clays from the undisturbed state.

Grim²⁰ has explained the mineralogical composition of clays and presented a complete outline of the performance of tests using electron microscopes, x-ray diffraction techniques, and differential thermal analyses for determining the type of minerals in a clay, and subsequently, for determining the swelling and compressibility characteristics. In addition to these tests, other tests such as the free-swell test, Atterberg and grain size tests, and swelling tests in

¹⁸W. H. Ward, G. S. Samuels, Muriel E. Butler, "Further Studies of the Properties of London Clay," Geotechnique, (1959), Vol. IX, p. 45.

¹⁹Rowe, op. cit.

²⁰Ralph E. Grim, Clay Mineralogy, (McGraw-Hill Book Co., Inc. 1953).

consolidometers have been discussed by Holtz and Gibbs.²¹

The more general structure which may be termed the orientation, has been studied by Mitchell,²² who has devised techniques for finding this orientation and the regularity of its occurrence throughout a clay specimen.

Bolt²³ has explained that swelling and compressibility are functions of the osmotic pressure which is determined by the soluble salt concentration within the adsorbed water films. He further stated that the solid components of a specimen are not in contact with one another, but are held apart by the repulsive osmotic forces. He indicated that the osmotic differential, which is the difference between the osmotic pressure of the fluid within the sample and that surrounding it, is of prime importance in determining the compressibility and swelling of a clay.

The literature pertaining to the subject under review is quite extensive and it was impossible to mention all

²¹W. G. Holtz and H. J. Gibbs, "Engineering Properties of Expansive Clays," Proceedings of A.S.C.E., October, 1954, Vol. 80, paper 516.

²²James K. Mitchell, "The Fabric of Natural Clays and its Relation to Engineering Properties," Proceedings Highway Research Board, Vol. 35, (1956).

²³G. H. Bolt, "Physico-Chemical Analysis of the Compressibility of Pure Clays," Geotechnique, Vol. VI, No. 2, p. 86.

the contributions that have been made to this subject. However, as many as possible have been mentioned in the foregoing pages, and a number of related texts and papers have been listed in the Bibliography at the end of this thesis.

SECTION III

DESCRIPTION OF THE SAMPLE

In order to obtain results that could be consistently comparable, all the samples were taken from one block of clay obtained in the Winnipeg area. This section has summarized the location, method of extraction, and classification of that sample.

I. LOCATION, REMOVAL, AND PRESERVATION OF THE SAMPLE

The sample was a clay from the eastern Elmwood district of Winnipeg. It came from the 18 ft. depth of the sewer trench of Clyde Road about one and one-quarter miles east of the meandering Red River. Before the excavation of the trench, this area south of Nairn Avenue was virgin prairie. The general ground profile in this vicinity consisted of;

black fertile loam, 0 to 1-1/2 ft.
brown dry organic clay, 1-1/2 to 6 ft.
yellow clayey silt, 6 to 7 ft.
chocolate clay, 7 to 10 ft.
mottled greyish brown clay, 10 to about 13 ft.
mottled brownish grey clay, 13 ft. down.

Fissures in the clay have been observed to extend to the 20 ft. depth.

The sample was extracted during August, 1959, the same day that the trench was opened to the depth of 18 feet.

It was removed in two stages; first, a backhoe with a large bucket chopped a large chunk of clay from the bottom of the trench. This chunk was raised to the surface where it was trimmed by shovel into a 2 ft. cube. It was immediately wrapped in aluminum foil and rushed to the soil mechanics laboratory of the University of Manitoba.

At the laboratory, a thin coating of wax was painted over the aluminum foil. The entire block was placed upon a board and stored in a room in which the humidity was maintained near 100 per cent. Thereafter, the protective coating was not opened until specimens were required. For the next two years specimens were extracted from this block, yet the percentage of saturation was consistently near 100 per cent, and the moisture content varied from $61\frac{1}{2}\%$ in 1959 to $59\frac{1}{2}\%$, and higher in some instances, in 1961.

II. TYPE OF SAMPLE

The sample was predominantly a clay consisting of alternate layers of chocolate and grey colouring, such that at a casual glance it appeared to have a mottled appearance. Although the sample when stored in the humid room was thought to be lying on its underside, it was found later that the laminations sloped at about 45° from what was originally believed to be the horizontal plane. Accordingly, all samples in the vertical direction were taken at 45°

from the vertical axis of the sample.

Classification Tests. The classification tests that were run on this sample were the Atterberg Limits, the grain size, and specific gravity. These tests were run according to what is considered standard procedure by most laboratory manuals. However, in order to preserve the original structure and grain sizes as much as possible, and to prevent extraneous effects due to oxidation, the samples were not permitted to dry. In all cases they were mixed while in a wet condition.

Because the specific gravity was used frequently throughout the calculations, three trials on different portions of the block sample were run. These trials gave good agreement, and despite the fact that it was difficult to determine the temperature of the slurry in the pycnometers, it was believed that the results were as precise as was possible. In the Atterberg Limits test, four good points comprised the flow line, and the plastic limit was an average of two values which agreed very closely. The shrinkage limit test was run on a sample in undisturbed condition, as cut from the block. The grain size test was run on bits and pieces throughout the sample, such that silt pockets and clay laminations were well represented.

The results of the classification tests are shown in Table I.

TABLE I
CLASSIFICATION CHARACTERISTICS OF THE CLAY

Specific gravity	2.79 ± .006
Liquid limit	111.5%
Plastic limit	43.5%
Plasticity index	68%
Equation of flow line. . . w% =	-21.5 log(no.of blows)+141.5
Toughness index	3.1
Shrinkage limit	21.5%
Shrinkage ratio	1.98
Fine silt	11% (M.I.T. grouping)
Clay size	89%
Less than .001 mm.	79%

The high plasticity index classified this clay as a CH type of clay, which is almost impervious, and has high shrinkage, swelling, and compression characteristics. Moreover, the low value for the shrinkage limit indicated that swelling can be rather high if this clay is dried.

The clay content and particles of colloidal size comprised a high percentage of the specimens. Therefore, it was reasonable to expect a great deal of swelling, as shown by these results.

SECTION IV

TESTING EQUIPMENT AND TECHNIQUES

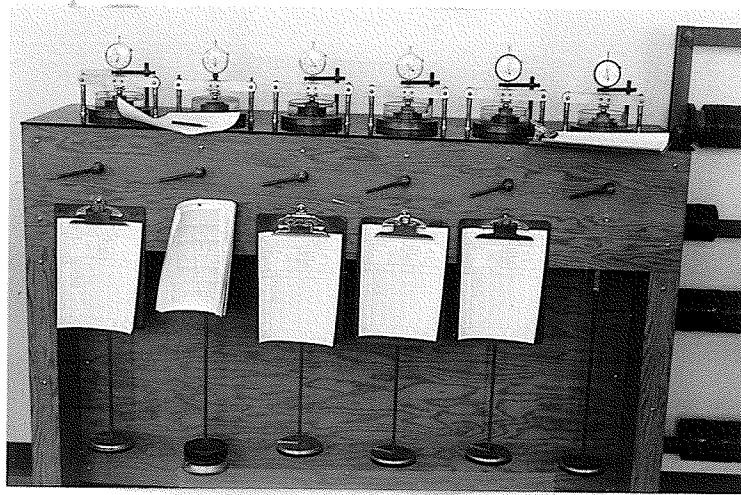
In this section the equipment that was used for the various tests has been described. The technique and corrections that were used have also been explained. In addition, the various series of tests that were run have been listed and described briefly in Appendix A.

I. THE CONSOLIDOMETER

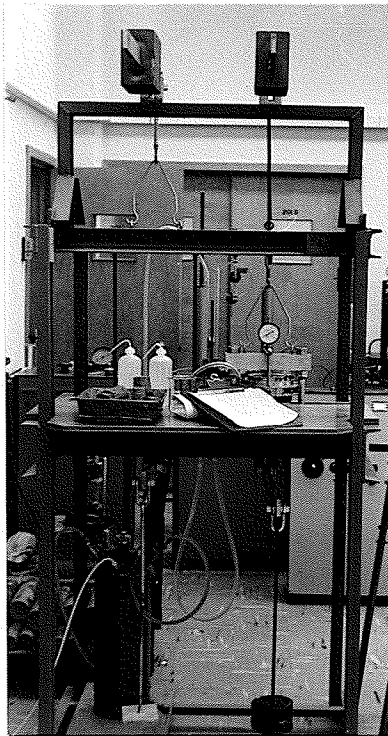
The consolidometer consists of essentially a dish in which distilled water surrounds a ring and loading device, in which the specimen is placed. A dial is attached for the purpose of measuring the deflections. The types of consolidometers used at the University of Manitoba laboratory are shown in Figure 1.

Loading Devices and Calibrations. In addition to the weight of the cap and the ball on the sample, two types of devices for applying loads were employed.

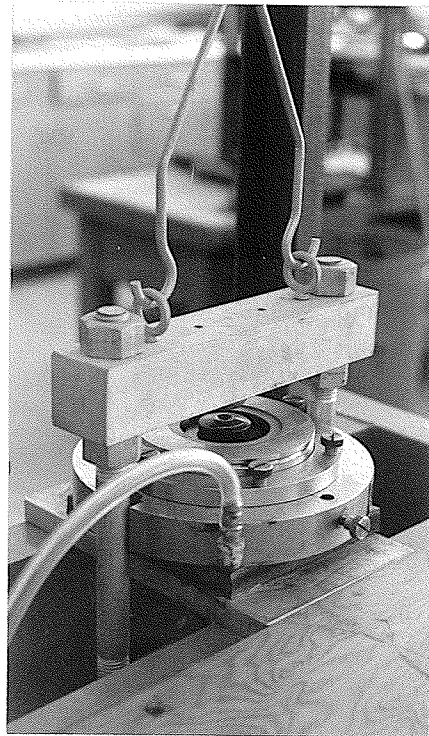
The first type consisted of a drum device. The load was applied to a pan and was transmitted with a mechanical advantage of 10/1 to the specimen by means of a yoke, shown protruding from the cabinet in Figure 1(a). The weight of the pan and yoke were supported by the springs which are also shown. The calibration of these springs indicated that



(a)



(b)



(c)

FIGURE 1.

CONSOLIDOMETERS AND LOADING DEVICES

- (a) First type with mechanical advantage of 10 and load capacity of 40 lbs.
- (b) Second type with mechanical advantage of 8 and unlimited load capacity.
- (c) Detail of second type before beginning of test.

the spring constant was 1.6 lb./in. of deflection for both springs combined. However, during the average consolidation test, the deflection was usually about 0.1 (say 1/4 inch). Therefore, the amount of error caused by the springs was only 0.4 lb., which is insignificant indeed, and no correction has been made for the spring constants in any of the tests.

The second device consisted of a lever with a pan at one end. A weight was applied to this pan and transmitted with a mechanical advantage of 8/1 to the sample by means of a yoke, as shown in Figure 1(b). The weight of the yoke and pan was supported by a counter-weight, which precluded the necessity for a correction.

In both types of equipment a correction was needed to compensate for the deflection that was experienced by the cap and ball, and in some tests by the filter papers also. Some typical deflection curves for the apparatus are shown in Figure 2, page 23.

Consolidometer Procedure. From the block sample a small chunk of clay was cut, either parallel to the vertical axis, or the horizontal axis. This chunk was then cut to size by means of the cutting tool, as shown in Figure 3. (p28) The trimmed specimen was then forced into the ring. One end was trimmed even with the top of the ring, and a small stone of thickness 0.174" was placed on this surface. This

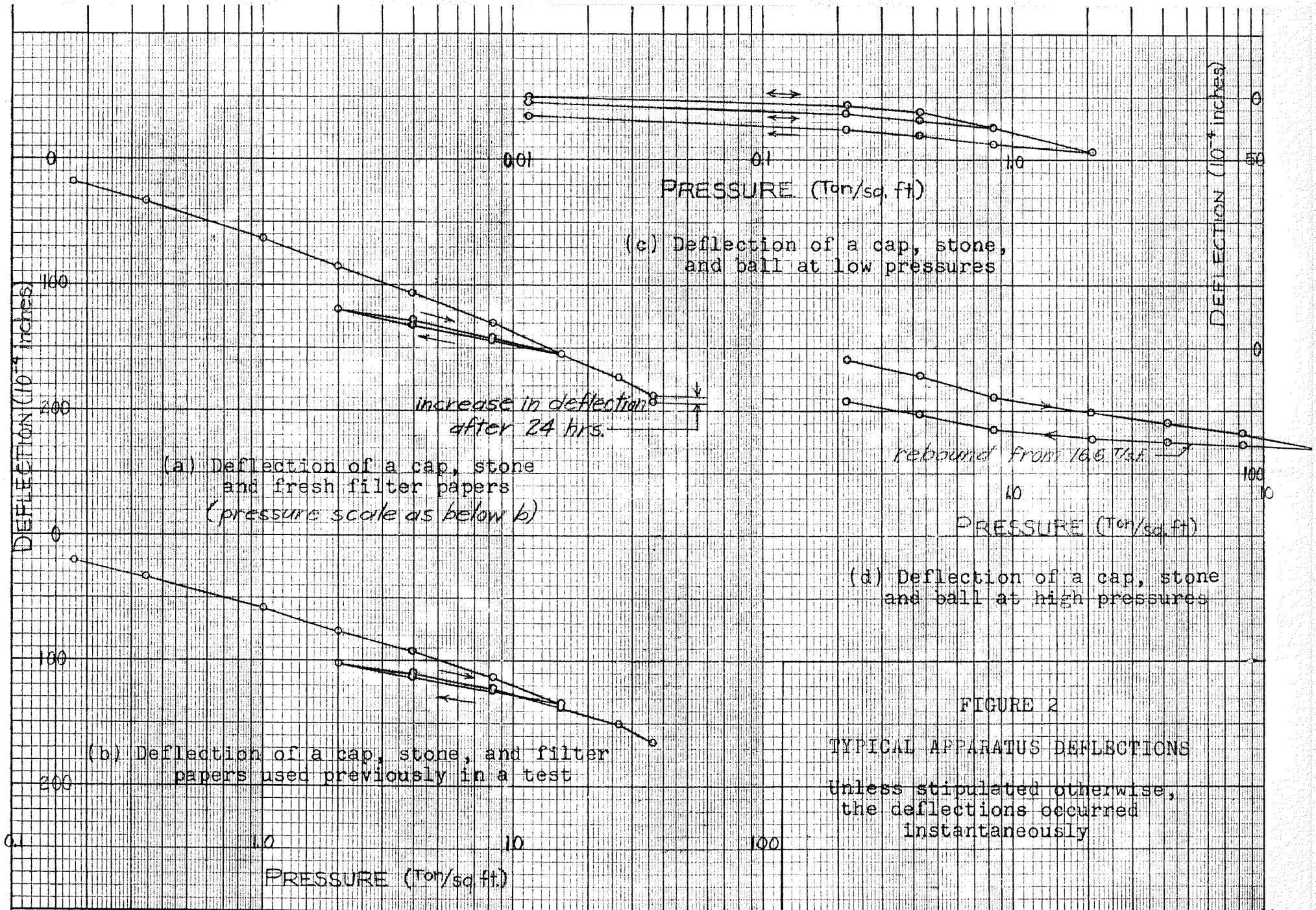


FIGURE 2

TYPICAL APPARATUS DEFLECTIONS

Unless stipulated otherwise, the deflections occurred instantaneously

ring was pushed downwards until its topside became flush with the top of the ring.¹ The bottom surface was then trimmed, using a straight edge. The small stone was removed and the ring and sample weighed and added to the data which already included accurate dimensions and weight of the ring. The cap and bottom stone were then added, such that the thickness of the small stone was allowed for expansion of the specimen. Sometimes filter papers were placed between the sample and the cap or stone, in order to prevent the clogging of the latter by clay.² Slight finger pressure insured a good contact before this portion of the apparatus was placed under the loading device.

In the second type of loading device, the assembly was quite simple. A small weight was applied to the pan after centering all other components, and the test was ready to commence. However, in the first type, a great deal of care was taken to ensure that the loading yoke was centered with respect to the stem of the deflection dial in order to ensure that it did not bear on the stem to cause sticking of the dial during the test. The deflection dials

¹Usually the pressing of the sample into the ring or cutting tool was achieved evenly by means of a hydraulic jack.

²P. L. Newland, and B. H. Allely, "Study of the Consolidation Characteristics of a Clay," Geotechnique, June, 1960, Vol. X, No. 2.

were added and the initial reading taken.

The usual loading technique consisted of applying one half a pound to the pan for 2 minutes before adding water and allowing the sample to swell. The first addition of water did not cover the sample entirely. The top was left dry, in order to permit the escape of gases as the sample was saturated from the bottom. In order to inhibit drying, a ring of filter paper encircling the cap, was kept saturated. After twenty-four hours the sample was fully inundated and swelling was allowed to complete. Loading was then effected at such a rate that the dp/p_1 ratio was unity (load increment/previous load).

During this research a number of special tests that shall be described later were conducted. The no-swell test differed from the standard test insofar as small loads were added, in order to prevent any swelling after water had been added to the dish. This process was terminated when it became apparent that the swelling tendency had ceased to exist. Other tests permitted swelling under no load, and under large loads, but the description of the procedure followed at these times will be described hereafter.

After the final load had been applied and the resulting consolidation completed, the brake was applied in order to prevent any further strain or swelling. The loads on the pan were quickly removed, and the sample, plus ring and

covers, was immediately extracted from the apparatus. It was found that the cap and bottom stone were easily removed on those samples in which filters had been inserted between them and the samples. Having removed these appurtenances, the investigator ran a moisture content test, after the precaution to dry all excess water from the surfaces of the sample and ring had been taken.

II. TRIAXIAL CELL

The triaxial cell consists of the cell, the drains, the membranes, a pressure pump, and the pressure regulator.

Pressure Appurtenances. In order to obtain results that were comparable to those obtained in the consolidometer, it was necessary to impose cell pressures of 16.6 T/s.f., but,

$$1 \text{ T/s.f.} = 13.88 \text{ lb./s.i.}$$

$$\text{or, } 16.6 \text{ T/s.f.} = 230 \text{ lb./s.i.}$$

However, the triaxial equipment will only withstand 250 lb./s.i. and the compressor that delivered the pressure would go to 150 lb./s.i. only. In view of these facts, only half of the pressure (115 p.s.i.) was used in this test. Consequently, the air compressor was set to deliver between 120 to 150 p.s.i..

In order to regulate this high pressure, two regulating devices were used. The first was a commercial type that permitted regulation up to 40 p.s.i.. The second was

a needle type of regulating valve that proved to be effective in holding high pressures. In both cases the pressure variation was insignificant at the gauges.

The gauges were simple Bourdon-type gauges that had been calibrated on a standard dead weight gauge tester, or against a column of mercury. However, these gauges could not be hooked up directly to the cell and an assumption regarding the pressure of the cell with respect to that at the gauge had to be made. In view of the fact that a large number of orifices and expansions occurred together with leakages, the value of 2 p.s.i. was felt to be a reasonable assumption for the loss between the gauge and cell. Consequently, an additional 2 p.s.i. had to be provided at the gauge to ensure that the cell pressure was the value desired.

The pressure of the fluid in the cell exerted an upward thrust on the ram, which had to be compensated because the deflections were measured by way of the ram. The cross sectional area of the ram (1/2" diameter) = 0.1962 s.i. Assuming a 1% loss due to drag of the cell fluid and friction upon the ram, the compensating force required =

$$1.01 \times 0.1962p = 0.198p.$$

$$\text{Therefore, weight on the pan} = \frac{.198}{8}p = 0.025p.$$

The Cell Assembly. The cell is shown in Figures 4 and 5 (pp. 28-29). In addition to the burettes for drainage,



FIGURE 3

The cutting tools and brass rings
for consolidometer specimens.

(two sizes, 1.49" + 2.53").

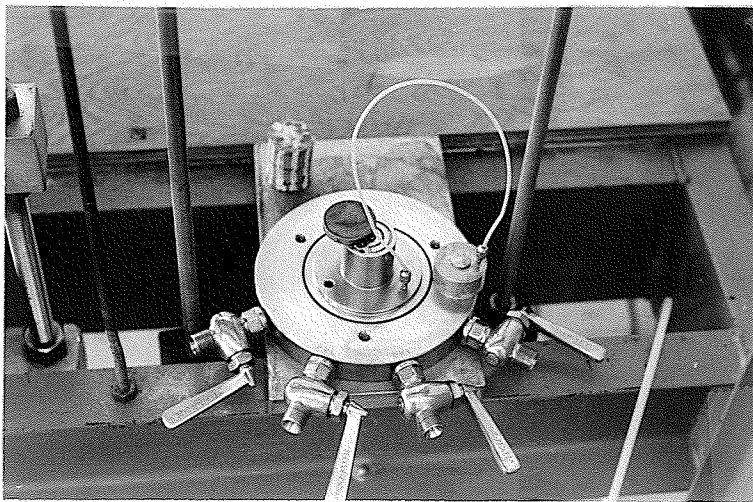
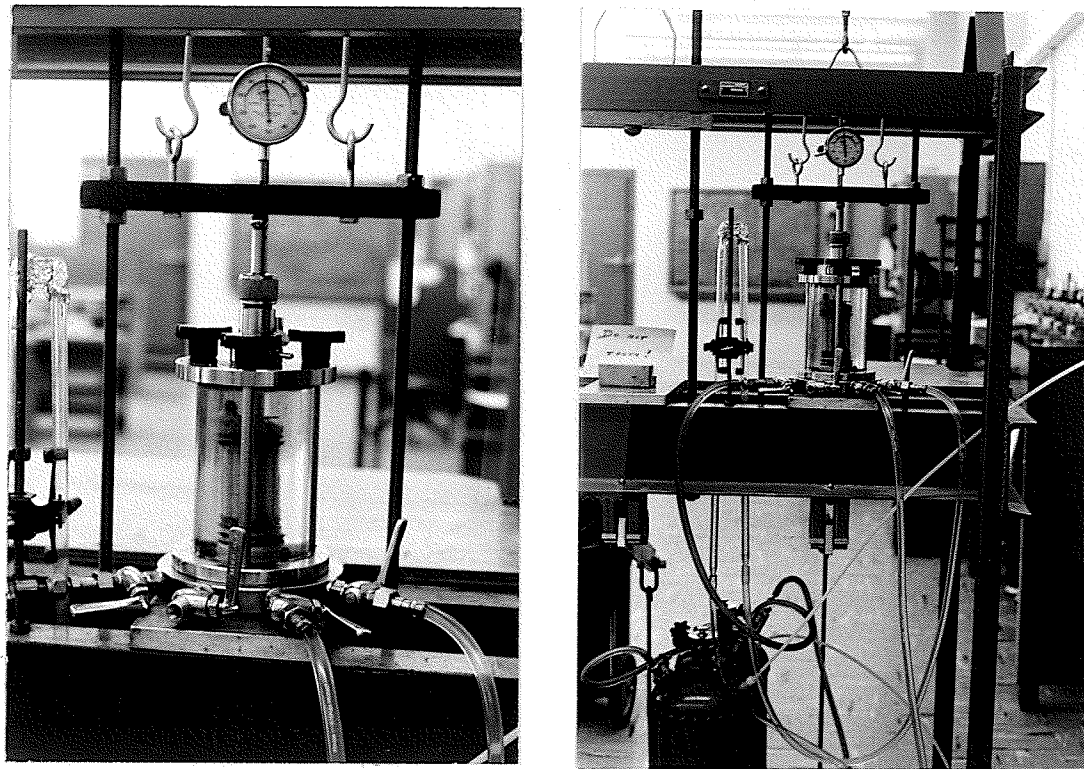


FIGURE 4

Details of drains in Triaxial Cell
showing cap and upper drain with
stone and two lower drains
through the pedestal.



(a)

(b)

FIGURE 5

TWO VIEWS OF ASSEMBLED TRIAXIAL CELL

SHOWING IN

- (a) A close-up of the assembly with the deflection dial, loading yoke, ram, bearing upon the sample lined with filter strips.
- (b) A broad view of the loading device, assembled cell, and tank in which the air pressure is converted into water pressure for the cell.

filter paper, rubber membranes, and silicone grease were necessary apparatus. It was found that two membranes were required. The filter paper was fairly soft for some of the tests, although in the last test some new filter paper that did not soften, when wetted, was obtained.³

The loading device (the pan) was similar to that described as the second type for the consolidometer apparatus and shown in Figure 1(b), page 21. The weight of the loading apparatus was balanced by a counterweight.

Procedure. A chunk of clay about 4" x 3" x 3" was cut parallel to the vertical axis from the block sample. It was then trimmed on a lathe to about 2-1/2" in length x 1-1/2" in diameter.

Before assembling the sample in the cell, the air compressor was turned on and locked, in order to prevent tampering with the pressure system. The apparatus was checked in order to ensure that the drains were free running and that no leaks existed. The stone (grade B) that sat upon the pedestal, and the cap that sat upon the sample, were soaked overnight in de-aired distilled water. The procedure that followed the trimming of the sample was as follows:

³It has been recommended that Whatman's No. 54 filter paper should be used. However, this could not be obtained at the time of testing, although the hard paper used was not much softer.

- 1) A small amount of silicone grease was smeared upon the sides of the cap and the pedestal.
- 2) The sample was weighed and measured.
- 3) Precut strips of filter paper were dipped in de-aired distilled water, and laid lengthwise along the sample. The ends were folded over the top and bottom so that no two filter strips overlapped.
- 4) Two circular pieces of filter paper were dipped in water and placed on the ends of the sample.
- 5) Three O-rings and one membrane were carefully placed over the pedestal.
- 6) The valve controlling the upper drain (see Fig.4 p.28) was opened and water was allowed to trickle through it.
- 7) The second membrane was placed over the cap and secured by an O-ring.
- 8) The cap was placed in an inverted position, and the sample was placed upon it in an upside-down position. The membrane on the cap was carefully rolled over the sample until it almost reached the bottom.
- 9) The stone was placed upon the pedestal, and the sample was set upon it, and the membrane rolled down over them all. It was hoped by this procedure to isolate the air at the bottom of the sample.
- 10) The air was evacuated by opening the auxiliary bottom drain on the pedestal, and allowing water from the regular bottom drain to flow through the stone, forcing as much air as was possible out through the auxiliary drain. All drains were then closed. The sample had then been de-aired as fully as possible.
- 11) Stop-cock grease was smeared over the first membrane, and the second membrane rolled up from the pedestal over it.
- 12) The O-rings at each end of the sample were used to secure the membranes.

- 13) The triaxial cell was assembled around the sample, and the burettes and the deflection dial were set in position.
- 14) The required pressure was built up at the gauge, and fluid was admitted to the cell until it almost filled the cell.
- 15) A film of oil about 1/2" thick was then introduced to the cell, and more fluid was admitted. Then the valve was shut.
- 16) The bleed valve was closed, and initial readings were taken.
- 17) The compensating load was applied to the pan, and as quickly as possible, the cell valve was opened, thus introducing pressure to the specimen. The deflection of the specimen was permitted to continue until it terminated, generally, in about one hour.

At zero time the drains were opened and the readings were then taken in the same manner as would have been used in any consolidation test.

When consolidation had terminated (24 hours were usually allowed), the valves were closed, and the loading procedure was repeated as from step 17 onwards.

When the consolidation test was fully completed, the drains were closed, and the bleed valve was opened until all the oil had been forced out. The weights were removed from the pan and the pressure was shut off. The bleed valve was opened, and the fluid was permitted to drain from the cell. The sample was removed from the apparatus and measured, and the filter strips were peeled off the specimen before a moisture content test was run.

A complete description of the test series has been given in Appendix A, in which the pertinent details of each specimen and additional techniques have been described.

SECTION V

COMPRESSION AND CONSOLIDATION PROPERTIES IN THE CONSOLIDOMETER

In this section attention was given to the usual consolidation and compression properties measured by the consolidometer method. An attempt was made to assess the effects of disturbance upon the results. Furthermore, the type of test and the axis of testing, that is to say, horizontal or vertical, were studied. The correlation of the consolidation characteristics with appropriate parameters have followed a discussion of the fitting methods that were used to find these properties.

I. SAMPLE DISTURBANCE

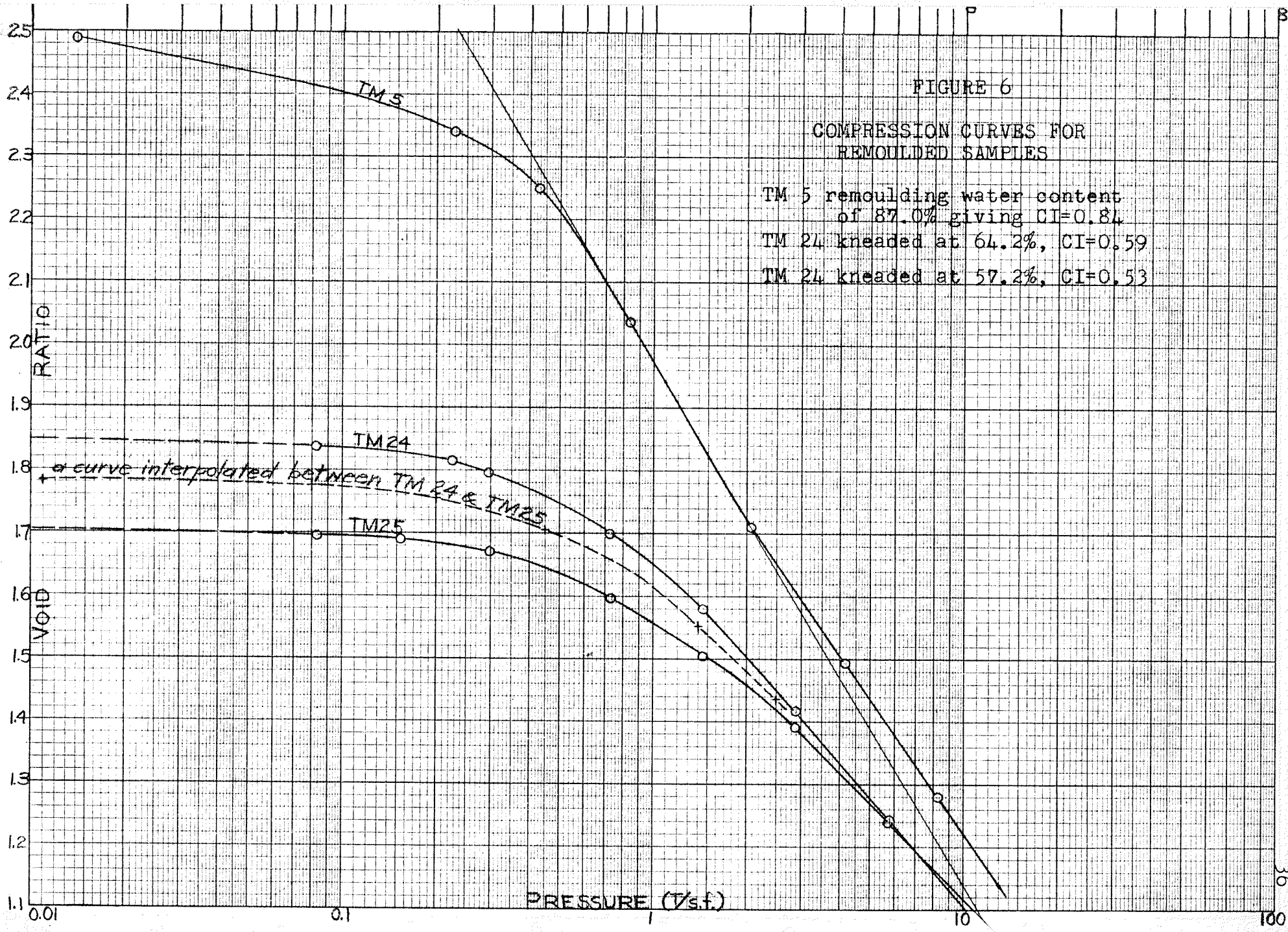
The only method for ascertaining sample disturbance was proposed by Schmertmann.¹ However, Schmertmann's method is not supposed to work for clays that swell. Nevertheless, in his paper he described how a highly pre-loaded clay can be analysed, even though it has swollen due to the decrease in pressure on the clay. In this thesis the

¹John H. Schmertmann, "The Undisturbed Consolidation Behaviour of Clay, " paper #2775 Transactions of American Society of Civil Engineers, Vol. 120, (1955), p. 1201.

investigator proposed to unload a specimen to a very small load (according to the standard test) where the e -log p curve was practically flat. Then it was possible to use a sample remoulded at the moisture content corresponding to that assumed by the sample upon the completion of swelling. This method would seem to be perfectly valid, in view of the fact that Van Zelst² used clays of similar geological origin from nearby Crookston, Minnesota, for his analysis, which was the forerunner of Schmertmann's work.

Remoulded Samples. The results of three consolidometer tests on clays remoulded at three different moisture contents have been revealed in Figure 6. If these samples are assumed to be 100% saturated at the remoulding water content, the relationship shown by the solid line in Figure 7 can be obtained. Even remoulded samples will swell; therefore, the moisture content that corresponded to the void ratio reached after swelling had completed, has been shown by the broken line in Figure 7. The latter relationship has been used to obtain the compression index of a remoulded sample for the disturbance analysis, even though the number of points are few and not perfectly aligned.

²T. W. Van Zelst, "An Investigation of the Factors Affecting Laboratory Consolidation of Clay," Proceedings of Second International Conference on Soil Mechanics and Foundation Engineering, Vol. VII, paper 11C4, p. 52.



Typical Laboratory Disturbance. Specimen TM 13 has been analysed for sample disturbance. The void ratio after swelling was 1.785. The resulting laboratory curve has been plotted in Figure 8. From the broken curve of Figure 7, the compression index for the remoulded sample swollen to a void ratio 1.785 should be 0.57. Moreover, by interpolating between remoulded samples TM 24 and 25, the curve corresponding to the compression index of 0.57 has been drawn as shown in Figure 8.

It was found that the point of intersection of the virgin compression branch of the laboratory curve and the straight line portion of the assumed remoulded sample occurred at 31% of the remoulding void ratio. This figure was somewhat lower than the 36 to 45% range, as given by Schmertmann.³

In order to determine approximately the preconsolidation pressure, it was necessary to extend a swelling line backwards from the point at which the laboratory curve commenced. The slope of this curve was obtained from Figure 38 on page 23 and was taken to be 0.05. Commencing with a trial value of 1.05 for the field virgin compression branch, as Figure 7 indicates the value would be at the liquid limit, a trial and error procedure was followed

³John H. Schmertmann, op. cit.

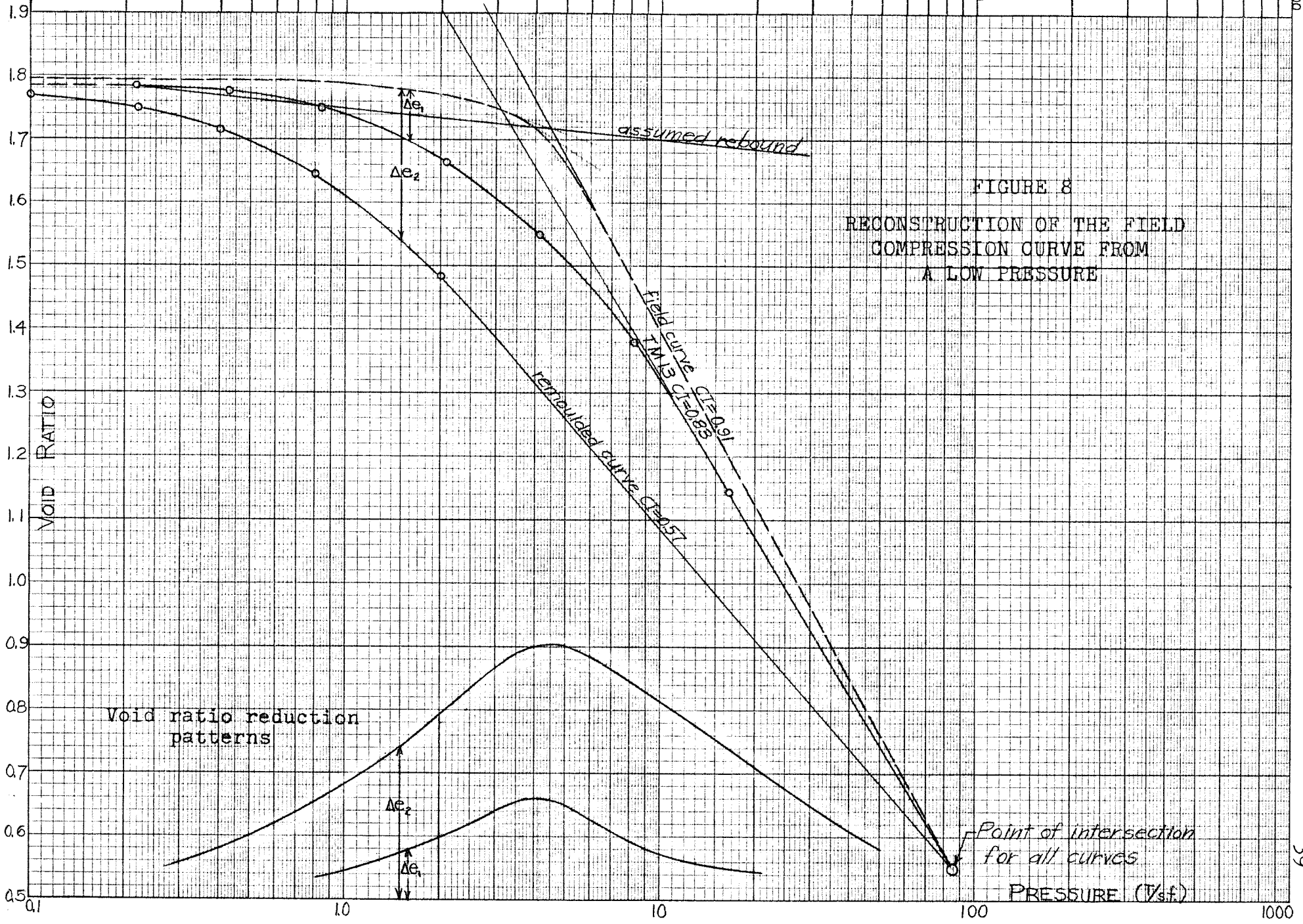


FIGURE 8
 RECONSTRUCTION OF THE FIELD
 COMPRESSION CURVE FROM
 A LOW PRESSURE

until the void ratio reduction patterns as shown in Figure 8 became symmetrical. This final trial was then assumed to be the field compression curve.

It will be noted that at a low pressure it lies slightly above the laboratory curve. This is because the latter is not absolutely flat at this low pressure, but when extended backwards to a very low pressure, it will intersect with the field curve.

According to this field curve the slope of the virgin compression branch should have been 0.91, which would correspond to a liquid limit of 96% in Figure 7. However, the laboratory compression index was 0.83, which would seem to indicate that the effect upon the compression index due to the disturbance was small indeed.

However, the void ratio reduction pattern for the laboratory specimen showed a reduction of 0.16. This was equivalent to 38% of the total possible reduction in void ratio between the field and remoulded samples. This seemed to be a great deal of disturbance, in view of the fact that the specimens were obtained from a block sample which should have provided specimens that were not greatly disturbed. It will be admitted that the use of a cutting tool to trim the sample, rather than a lathe, has incurred some unnecessary disturbance; however, it is difficult to believe that all this disturbance could be attributed

wholly to the trimming method. Moreover, the clays in this area are not known to be sensitive. Consequently, it must be concluded either that these clays cannot be analysed in this manner, due to the peculiarities of their structure, or, that some of the disturbance occurred prior to sampling in the field.

According to the field curve and the swelling line, the preconsolidation pressure for this clay was 4.5 T/s.f.. If one had guessed this value from the laboratory curve, it would have probably been about 5 to 6 T/s.f., but because Casagrande's⁴ construction could not be made for this clay, it was difficult to pin down this value.

II. COMPRESSION PROPERTIES

The effects upon compression properties, specifically the CI, due to sample irregularities and test procedure, have been analysed. The results of nine good tests have been used for finding the average compression index for this particular block of clay.

Sample Irregularities. There were two types of irregularities which were of concern. The first type was

⁴A. Casagrande, "The Determination of the Pre-consolidation Load and its Practical Significance," Proceedings First International Conference on Soil Mechanics, Cambridge, Mass., (1936), Vol. 3, pp. 60-64.



that occurring in the void ratio in small specimens throughout the sample, and the second was that revealed in results gained by loading samples parallel or perpendicular to the laminations.

Initial void ratio variation. It has been found that the initial void ratios of the undisturbed laboratory specimens ranged from 1.54 to 1.82. The average of twenty-five values was 1.72. However, Figure 9 showed that two separate groups existed. The first group, comprising twenty-five percent of the total, varied between 1.54 and 1.62. The average void ratio for this group was 1.58. The second group, comprising seventy-five per cent of the total, varied between 1.66 and 1.82, with the average value being 1.75. The first group was observed to contain either pits of silt (very frequently), or fissures, and quite often both together. Although the silt rarely seemed to be found in significant quantities, it must be concluded that the silt content was the cause of the low void ratios in the first group.

In Figure 10, some curves were plotted to show the effect of the low void ratio on the e -log p curve. It will be noted that the first group lies below that of the second, and even at high pressures, no tendency to converge appeared. All these curves represented samples having initial void ratios within $\pm .01$ of the averages for the

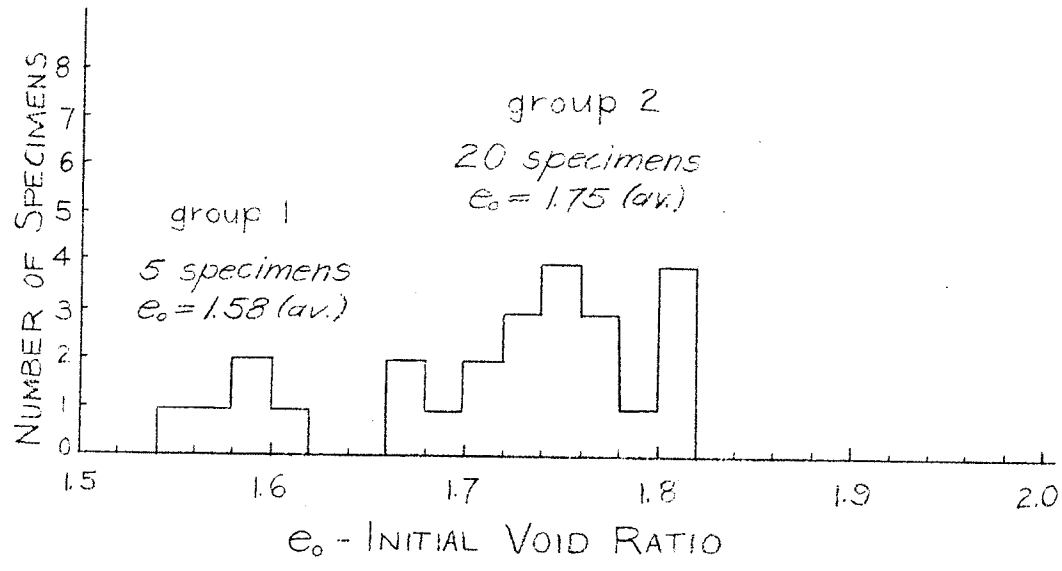


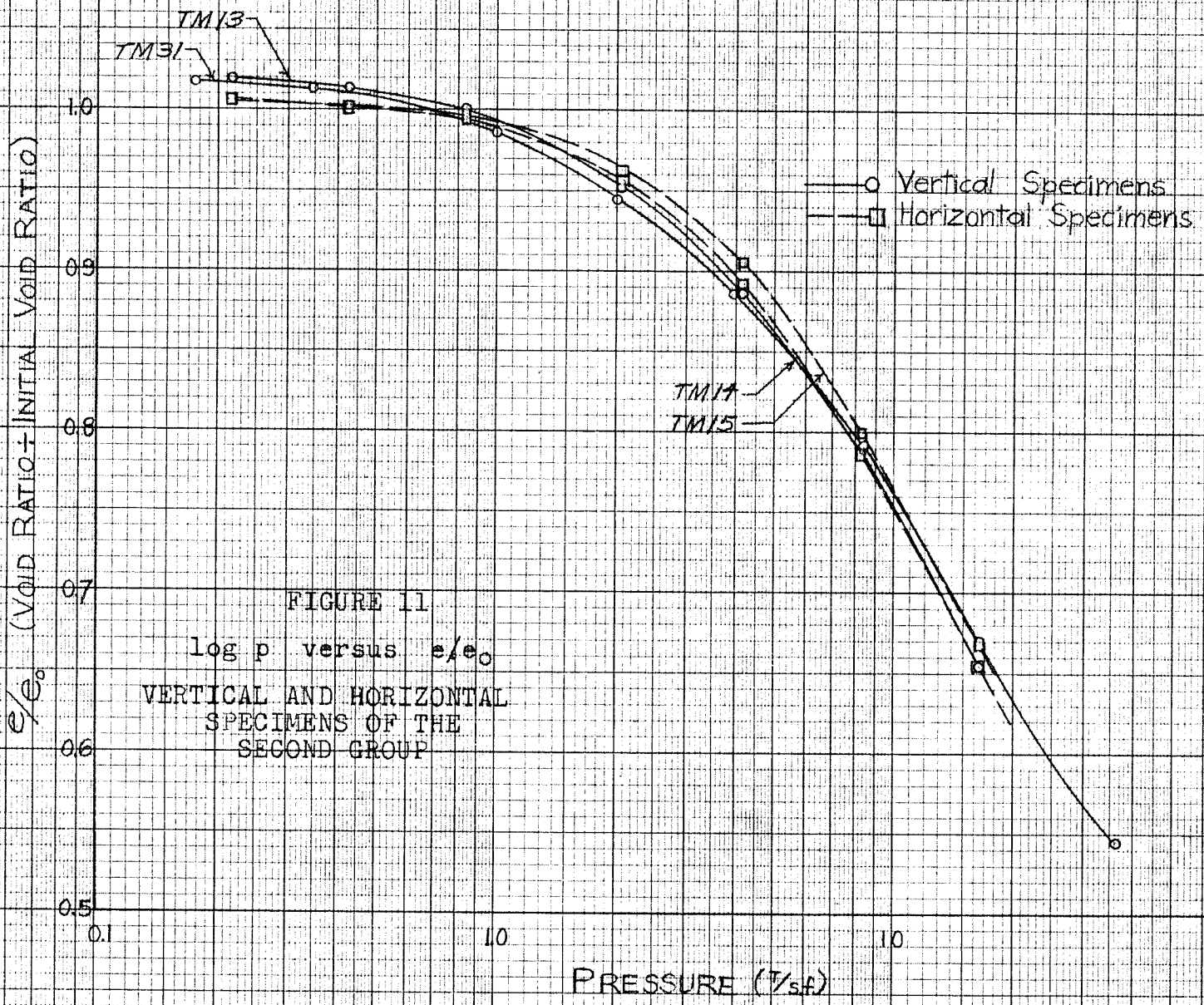
FIGURE 9
FREQUENCY CURVE OF INITIAL
VOID RATIO VARIATION IN
THE BLOCK SAMPLE

respective groups. Furthermore, it will be noted that there is a great deal of disagreement within the groups themselves, although they all seemed to follow the same general pattern, but the compression indices of the two groups do not seem to be much different. No trend was observed in the value of CI in relation to the initial void ratio.

Apart from causing low void ratios, the only influence of the silt seemed to be the downward displacement of the entire compression curve to lower void ratios.

Orientation of laminations. Figure 11 showed the results for samples cut so that the laminations ran vertically through the specimen, as shown by the broken lines (i.e. horizontal specimens), and horizontally in the specimen as shown by the solid lines (vertical specimens). The ordinate, rather than being the void ratio, is the ratio $\frac{e}{e_0}$. This facilitated the comparison between samples of slightly varying values of e_0 . It will be noted that the curves agreed very closely, and it may be concluded that samples loaded parallel to the laminations yielded the same compression curves as samples loaded perpendicularly to the laminations.

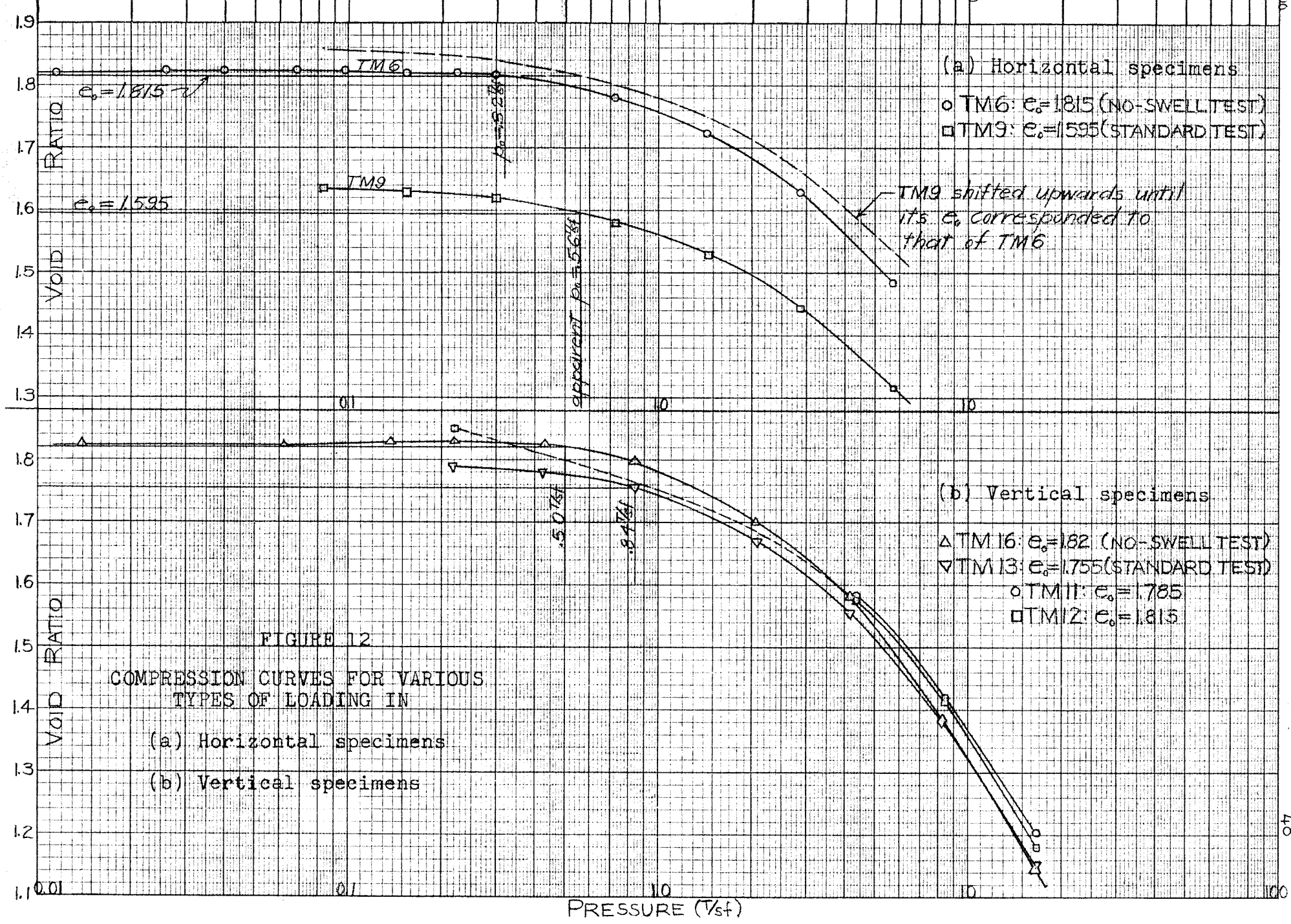
No significant difference can be detected between the CI values or the compression curves between horizontal and vertical samples, provided the initial void ratios were comparable. If the values of e_0 did not compare, the di-



vergence in behaviour was the same in both horizontal and vertical specimens.

Effect of Test Procedures. Figure 12 showed the results of two different kinds of tests for both horizontal and vertical samples. Figure 12(a) represented the horizontal samples TM 6, and TM 9. TM 6 was a no-swell type of test, whereas TM 9 was a freely swelling conventional test. It will be noticed that when TM 9 was shifted upwards to coincide with the initial void ratio of TM 6, the compression curves did not coincide, due to the presence of silt in TM 9. Furthermore, the overburden pressures (p_0) were .32 T/s.f. by the no-swell method and .56 T/s.f. by the conventional test. These represented a ratio of 0.57 to one another.

Figure 12(b) showed similar tests involving TM 16 as a no-swell test, and TM 13 as the conventional. It will be noted that these two samples had similar initial void ratios and consequently, the curves converged at high pressures. This fact would seem to indicate that the type of swelling had no apparent effect upon the virgin compression branch. Also, the overburden pressure for TM 16 was 0.50 T/s.f., and for TM 13, 0.84 T/s.f., representing a ratio of .59 between the two. This value agreed very closely with that obtained for the horizontal samples and would seem to indicate that the silt content in one of



the horizontal specimens had little effect upon the results for the overburden pressure.

Which type of test yields the correct overburden pressure? Only one value is the correct value, and by assuming certain densities of the soil lying above the block sample, an approximate figure for the actual overburden pressure can be obtained.

Assume, γ total = 120 pcf (slightly large to compensate for capillary forces),

therefore, p total = 2,150 psf (at the 18 ft. depth)

Assume, water table at 6 ft. depth because this was a wet year,

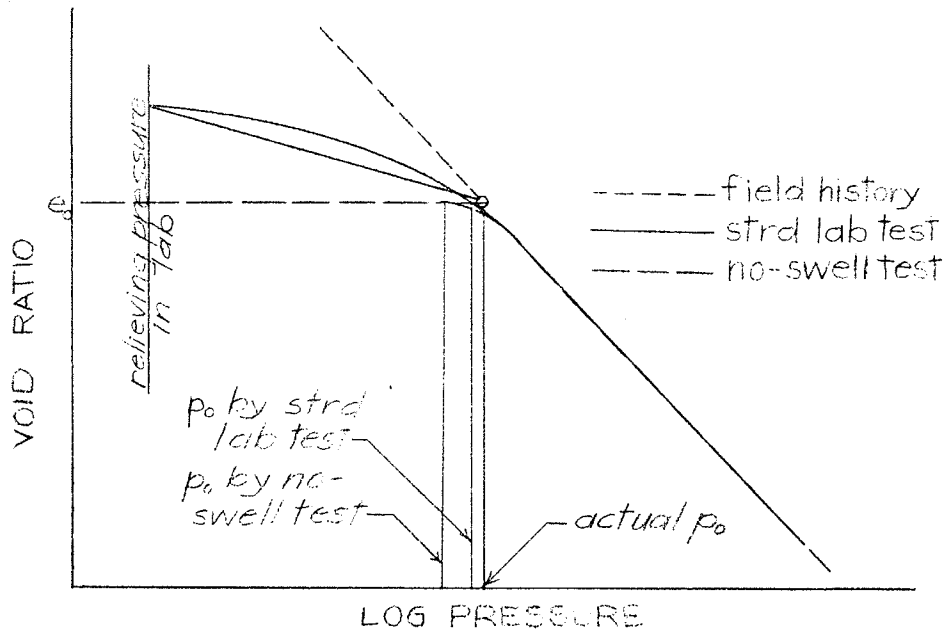
therefore, $18\gamma_w = 1,100$ psf,

and $p_o = 2,150 - 1,100 = 1,050$ psf., or 0.52 T/s.f., is the actual overburden pressure upon the entire block sample. This value agreed well with TM 16 and TM 19, but for the latter specimen it must be remembered that in the "at rest" condition in the field, the ratio of the horizontal pressure to the vertical pressure is usually less than 1.0. Therefore, it is not unreasonable to expect the overburden pressure for the horizontal specimens to be lower than 0.52 T/s.f., and this is the explanation for the lower values of p_o for the two horizontal specimens. Therefore, it would seem that the no-swell type of test gave the truer values for overburden for this particular type of clay, because the no-swell test (TM 16) for the

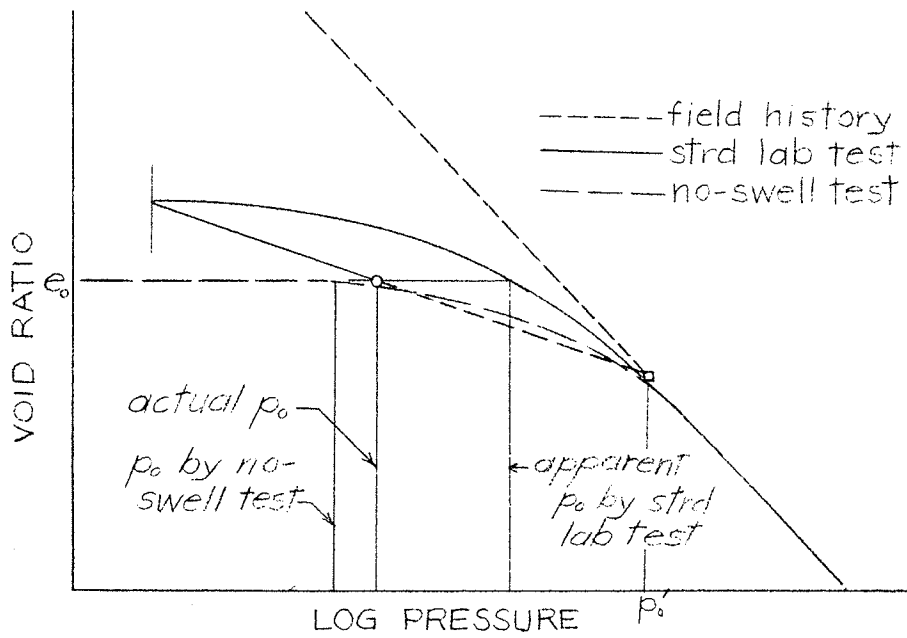
vertical specimens agreed very closely to the actual overburden of 0.52 T/s.f..

A reasonable explanation can be given with the assistance of Figure 13. It can be noticed that for the normally consolidated sample, the recompression curve passes quite close to p_0 , and that the compression for the no-swell type of test also commences at this point. However, for the preloaded clay it can be noticed that the loop does not pass near p_0 , but passes near p_0' , which is the preconsolidation pressure. Consequently, the value of p_0 as given by the standard test for a preloaded clay is not actually the overburden pressure at all. Therefore, the truer value must be that for the no-swell type of test, as the previous computations have already indicated.

Also plotted in Figure 12 are the compression curves for TM 11, which was loaded directly to a pressure of 4.35 T/s.f. from the undisturbed condition in which it was received, and TM 12, which was permitted to swell under a small load before receiving the same treatment. They agreed fairly closely with one another, and also with TM 13 and TM 16. In fact, the agreement was as close as can be expected in view of the disagreement that can arise in samples of the same void ratio, as has been indicated previously in Figure 10, page 44. Not only did the curves agree closely, but also the values of CI agreed well. They were all within a



(a) normally consolidated clays



(b) overconsolidated clays

FIGURE 13

DETERMINATION OF OVERBURDEN PRESSURE BY TWO METHODS

Standard test
No-swell test

range of 0.83 and 0.88. It would seem that the type of loading had little effect upon the curves at high pressures, provided the initial void ratios were in the same general range.

It has been shown that CI is unaffected by variations in the initial void ratio, type of loading, orientation of laminations, and the amount of swelling. Consequently, the results of the nine best tests have been used to find the average value for the compression index, which was $CI = 0.83$, and varied between 0.78 and 0.88. This was the value for both TM 13 and TM 31, the former of which had been justifiably used for the determination of sample disturbance. TM 31 gave a more complete picture of the e-log p curve at high pressures, as has been shown in Figure 25, page 97.

III. CONSOLIDATION CHARACTERISTICS

No attempt has been made to ascertain the effects of disturbance or type of loading upon the consolidation characteristics. These matters have been covered elsewhere⁵. However, two of the most popular fitting methods have been

⁵John H. Schmertmann, op. cit., and Donald W. Taylor, "Research on Consolidation of Clays," Massachusetts Institute of Technology Publication of the Department of Civil and Sanitary Engineering, (1942), serial 82.

analyzed in order to ascertain what differences can be obtained with them. Sample calculations for the consolidation characteristics and the errors in the experimentation have been presented together with the results of numerous tests.

Effect of Fitting Methods. In Figure 14 the results of the deflections plotted against the logarithm of time have been presented for the 8.3 to 16.6 T/s.f. load increment of sample TM 31. The degree of consolidation has been fitted to this curve according to the method proposed by Casagrande. At 50% consolidation:

$$t_{50} = 44 \text{ minutes}$$

dial reading (at U = 50%)	4845
apparatus correction	+ 134
	4979
original dial reading	6000
deflection	= $-.102''$
original thickness	= $.578''$
H ₅₀	= $.476''$

$$C_v = \frac{T_z H^2}{4t_{50}} = \frac{.197(.476)^2}{(44 \times 60) \cdot 4} = 4.24 \times 10^{-6} \frac{\text{sq.in.}}{\text{sec.}}$$

$$a_v = \frac{\text{decrease in dial reading}^{\star}}{\text{height of solids}} \cdot \frac{1}{dp} = \frac{0.212}{8.27} = 25.6 \times 10^{-3} \text{ s.f./T}$$

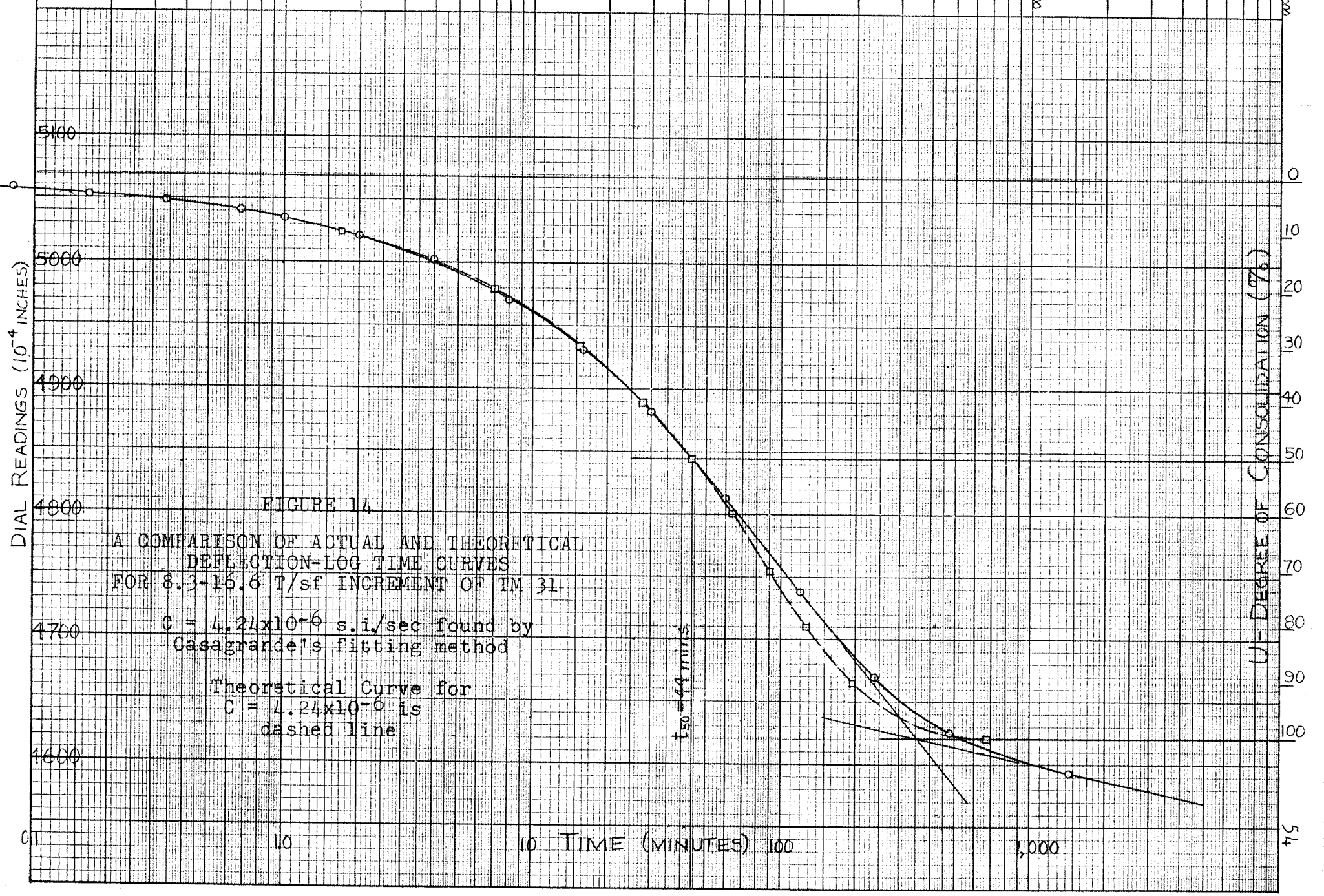
$$\text{or } a_v = 1.85 \times 10^{-3} \text{ sq.in./lb.}$$

$$\text{From Figure 25, page 97, } 1 + e_0^{\star} = 2.43$$

$$\gamma_w = 0.0361 \text{ lb./c.i.}$$

$$\text{Therefore, } k_v = \frac{4.24 \times 1.85 \times .0361 \times 10^{-9}}{2.43} = 0.117 \times 10^{-9} \text{ in./sec.}$$

[★]These figures represent occurrences relating to primary consolidation rather than the whole process including initial and secondary consolidation.



or, $k_v = 0.30 \times 10^{-9}$ cm./sec.

Average e during primary consolidation = 1.33.

Using the value obtained previously for the coefficient of consolidation, the following relationship was obtained:

$$t = 223 T \text{ mins. for this load increment.}$$

By the substitution of appropriate values for the time factor (T), the time corresponding to any degree of consolidation (U) was found and was plotted, as the broken line shown in Figure 14. This line is the theoretical curve corresponding to the value of C_v , as found using this method of fitting.

The deflections were plotted against the square root of time in Figure 15, and the fitting method proposed by Taylor⁶ was used. At 90% consolidation:

$$t_{90} = 138 \text{ minutes}$$

$$\text{Therefore, } C_v = \frac{.848(.476)^2}{138 \times 60 \times 4} = 5.90 \times 10^{-6} \frac{\text{sq. in.}}{\text{sec.}}$$

Using this value for the coefficient of consolidation, the following relationship was obtained:

$$\sqrt{t} = 12.7 \sqrt{T} \text{ (minutes).}$$

Using this relationship, the theoretical curve as shown in Figure 15 was plotted.

⁶Donald W. Taylor, Fundamentals of Soil Mechanics, (John Wiley and Sons, Inc., New York, 1948). p. 238.

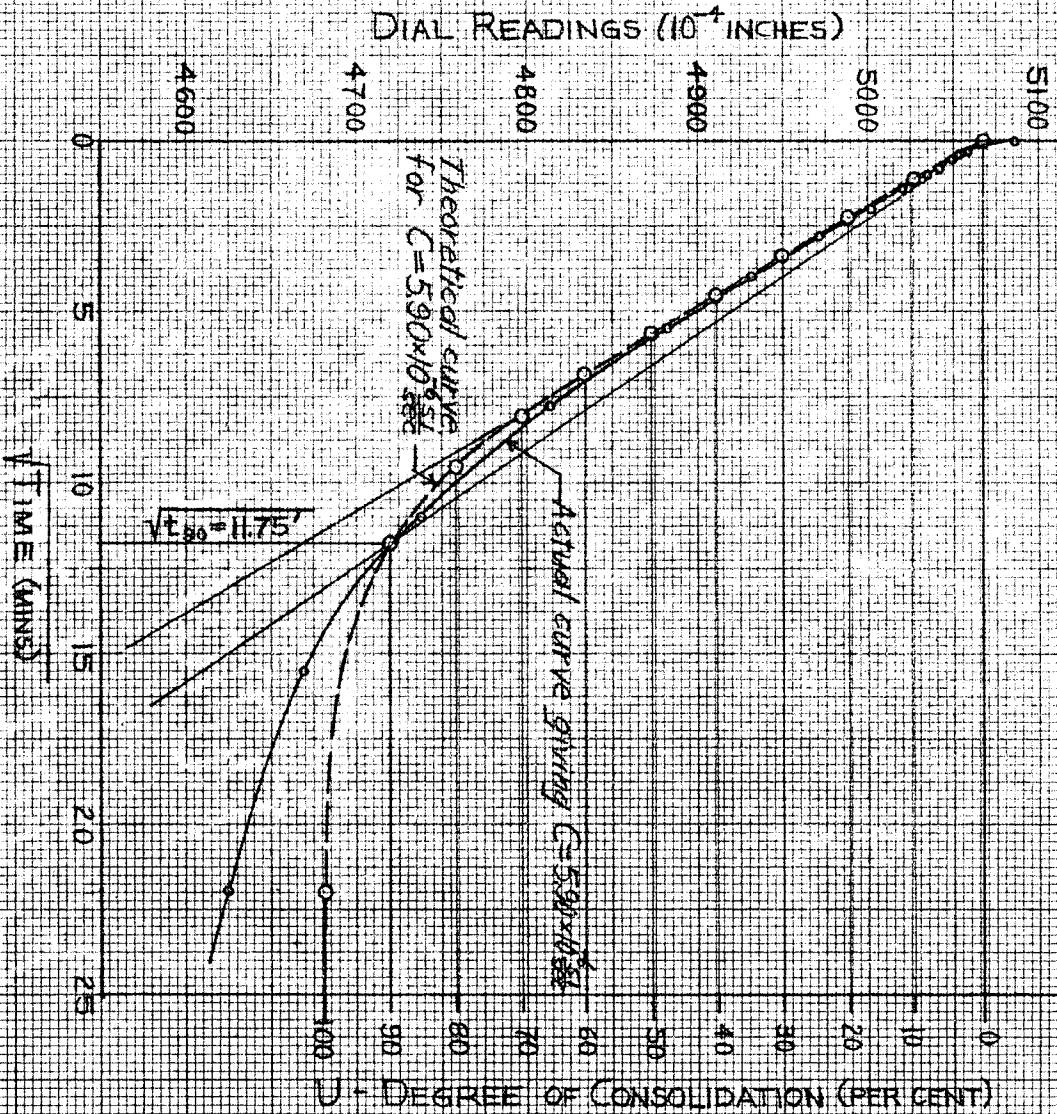


FIGURE 15

A COMPARISON OF ACTUAL AND THEORETICAL DEFLECTION-ROOT OF TIME CURVES
 For the 8.3 - 16.6 t/s.f.
 increment for TM 31

The coefficient of consolidation as found by the second method was 1.39 times that of the first. This represents a good amount of disagreement and it can be expected that other methods of fitting would produce similar disagreements. Therefore, the consolidation characteristics can be expected to be in error by a great deal whichever method of fitting is chosen. The investigator has chosen the Casagrande method, although a comparison of the two showed that the Taylor method fitted a little bit better. The Casagrande method was chosen because it is commonly used at the University of Manitoba, and represents a great deal of saving in time and convenience. All values were calculated using this method, and may be greatly in error, but in relation to one another they will not be in error, because the Casagrande method was used for all specimens.

Calculation of Errors. The errors as calculated hereafter represent the relative errors for the chosen fitting method. The absolute error was not considered. The 2.08 T/s.f. load on TM 19 has been analysed for error, because it was a cycled specimen that could be analysed for error during a cycle, later in the thesis. It was assumed that the $U = 0$, and $U = 100$, points could be found according to the fitting method as close as $\pm .0002$. Therefore, it was determined that $U = 50$ could be obtained as close as $\pm .0003$, which produced t_{50} between 9.6 and 11.2 minutes on

the test time curve. Therefore, $E_t = \frac{.9 \times 100\%}{10.5} = \pm 8.5\%$

Also, $E_{dH} = \pm .0004$ (deflection during primary compression)

$$\text{or } E_{dH} = \frac{.0004 \times 100}{.0158} = \pm 3.2\%$$

$$E_{dp} = \frac{.01 \times 100}{1.24} = \pm .8\%$$

$$E_a = 3.2 + 0.8 = \pm \underline{\underline{4\%}}$$

$$E_{l+e} = \frac{.005 \times 100}{2.75} = \pm .2\%$$

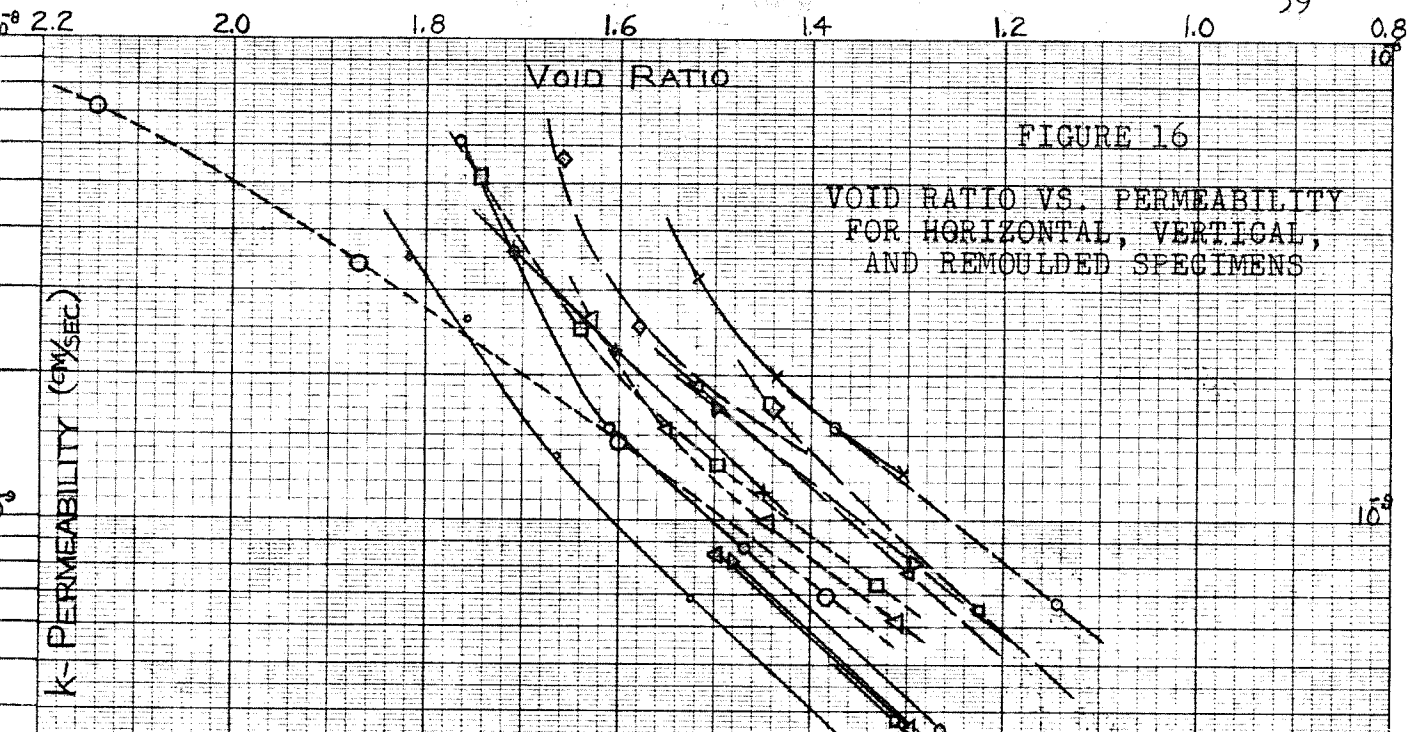
$$E_H^2 = 2 \frac{.0005 \times 100}{.563} = \pm .2\%$$

Therefore, $E_C = E_H^2 + E_t = \pm \underline{\underline{8.7\%}}$

Finally, $E_k = E_C + E_a + E_{l+e} = \pm \underline{\underline{12.9\%}}$

This was the approximate error for all other normal load increments when all factors were taken into consideration.

Permeability. The vertical, horizontal, and remoulded permeabilities were plotted against void ratio in Figure 16. It will be noticed that the horizontal permeabilities were roughly twice as large as the vertical. The permeabilities of the remoulded samples fell about halfway between the two. Only in two cases did the vertical permeability values approach those of the horizontal. For sample TM 17, the curve actually fell within the horizontal range, but it should be recalled that this sample was silty and fissured, and as a consequence, tended to drain faster than a sample devoid of silt pockets. Its curve tended to



LEGEND OF FIG 16 & FIG 17

Vertical specimens ———

TM11 □ TM12 △

TM13 ○ TM16 ▽

TM17 × TM19 +

TM31 •

Horizontal specimens ———

TM7 ○ TM8 □

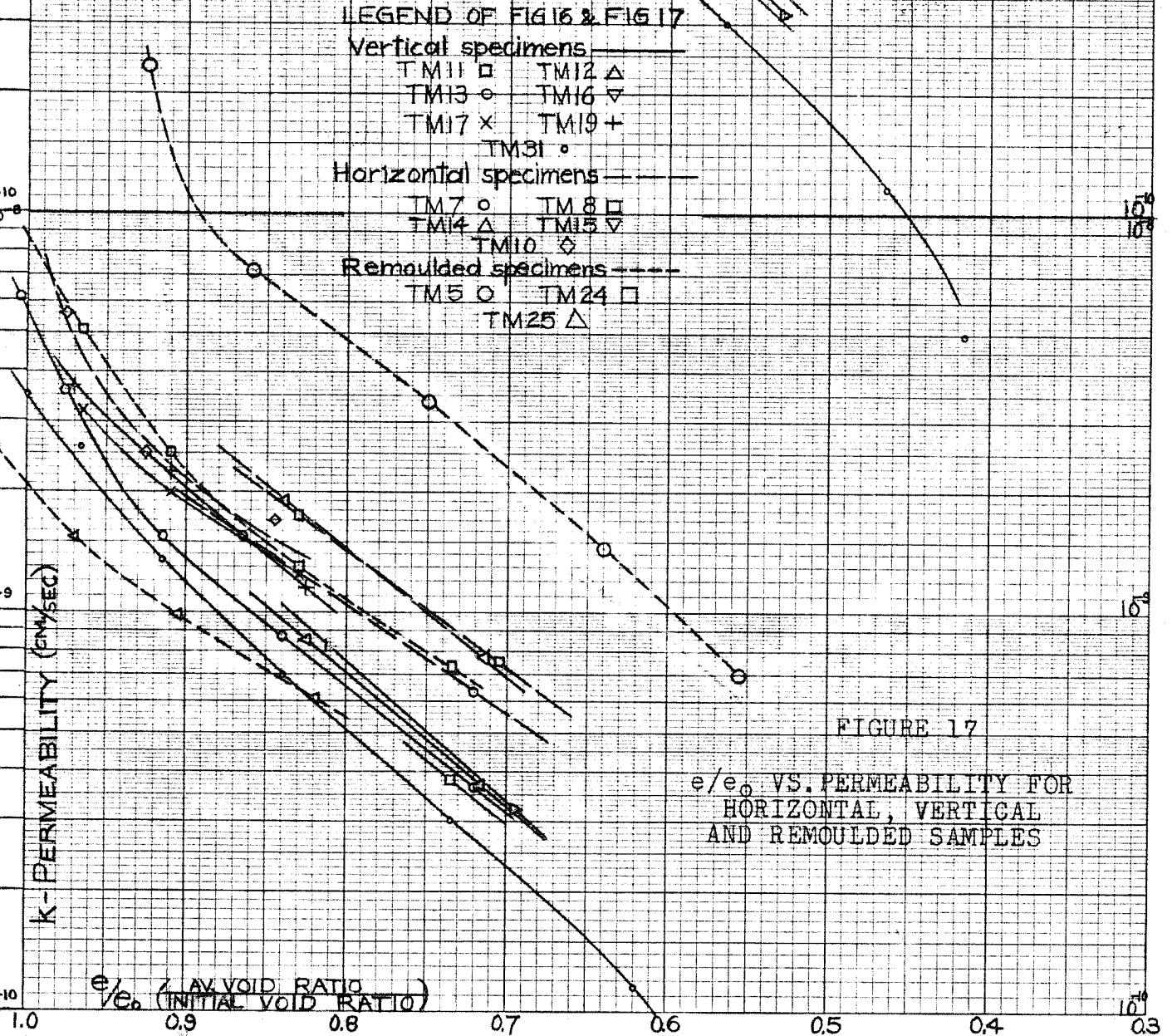
TM14 △ TM15 ▽

TM10 ◇

Remoulded specimens - - - -

TM5 ○ TM24 □

TM25 △



correspond to that of TM 7, which was also a silty sample, draining in the horizontal direction. TM 19 also showed high permeabilities, but this sample was fissured, and these irregularities could account for its high values.

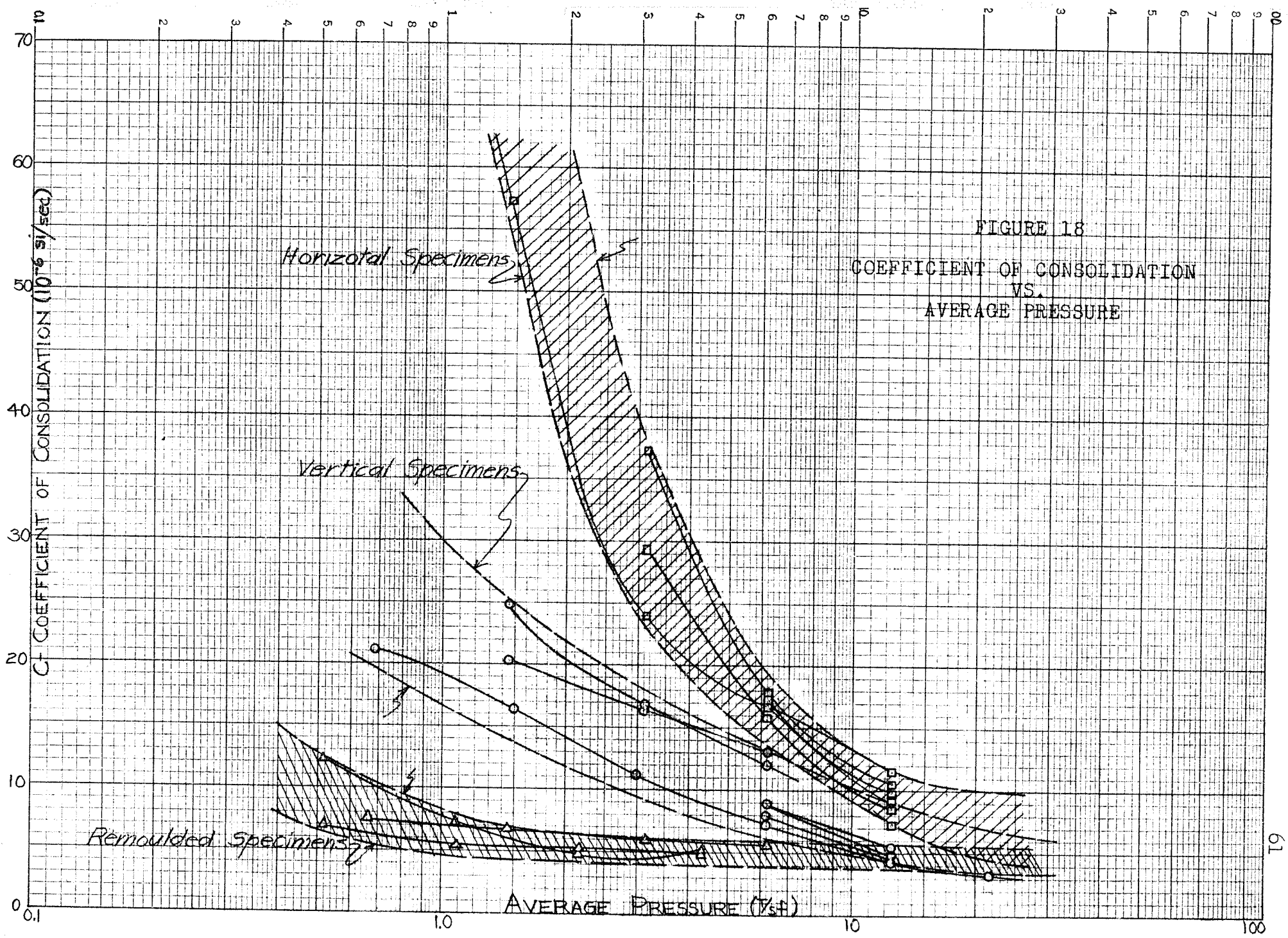
Figure 17 displayed the variation of permeability in relation to the $\frac{e}{e_0}$ ratio, which caused some of the lines to gather slightly, but the effectiveness of silt in increasing the permeability can still be observed in TM 17 and TM 19.

Coefficient of Consolidation. Figure 18 shows the coefficient of consolidation for many tests in horizontal, vertical, and in remoulded samples. At low pressures the value of C_h was definitely higher than that of C_v , and was discovered for London clays.⁷ The values for the remoulded samples, rather than lying between the two as one would expect, fell slightly below both of them. At high pressures all three groups tended to converge.

IV. SUMMARY

A number of general conclusions and observations regarding the usual compression and consolidation characteristics, as measured in the consolidometer, have been made:

⁷Ward, Samuels, and Butler, "Further Studies of the Properties of London Clays," Geotechnique, Vol. IX, (1959), p. 45.



1. a) Using Schmertmann's method for reconstructing the field compression curves of this clay after it had swollen under a very low pressure, it was found that the virgin compression branch had a slope of 0.91, and intersected the laboratory and remoulded curves at 31% of the void ratio to which the swelling reached.
b) It was determined that the amount of disturbance in a typical laboratory specimen by Schmertmann's method was 38% of the total amount of disturbance for remoulded samples, which seemed too high for specimens cut from a block sample. This fact leads to the belief that disturbance occurred in the field before sampling, or that Schmertmann's method does not apply to a soil with a dispersed structure, whether it swells or not.
2. a) The initial void ratio varied from 1.54 to 1.82, depending upon the amount of silt that the specimen contained. The average void ratio for the block, as determined by a number of specimens, was 1.72. For the silty specimens the average void ratio was found to be 1.58, and for the fat, clayey specimens it was found to be 1.75. This latter group comprised 75% of the total specimens.
b) The effect of the silt content on the compression curves was to displace these curves below those with high clay contents. Otherwise, no adverse effects were indicated in the compression curves.
c) The compression indices for the silty and clayey samples were comparable, and no correlation between CI and e_0 existed.
3. Samples compressed parallel to the laminations yielded compression curves similar to those compressed perpendicular to the laminations.
4. The best method for determining the overburden pressure was a no-swell consolidometer test. The value of overburden pressure was 0.50 T/s.f. for a vertical specimen, and it compared closely to the value of 0.52 T/s.f. calculated according to overburden. A horizontal specimen showed a smaller $p_0 = 0.30$ T/s.f..

5. a) The type of loading employed in the test had no effect upon the compression index, or the location of the virgin compression branch, for samples with similar initial void ratios.
b) The average value of the compression index was 0.83 and varied between .78 and .88.
6. The Casagrande fitting method did not fit this clay very well. The Taylor method fitted slightly better and yielded values of the coefficient of consolidation 1.4 times greater than those of the Casagrande method.
7. The ratio of horizontal permeability to vertical permeability was roughly 2/1. Silty samples caused both horizontal and vertical permeabilities to be quite high.
8. The horizontal and vertical coefficients of consolidation tended to converge at high pressures (greater than 10 T/s.f.), but it was not discovered whether this was caused by the high pressure or the disturbance of the numerous foregoing load applications.
9. Under ordinary circumstances the experimental errors in the coefficients of consolidation and coefficients of permeability were respectively, 8.5% and 13%.

SECTION VI

CONSOLIDATION TEST IN A TRIAXIAL CELL

Because it was believed that the disturbance during a test in a triaxial cell would be less than that created in a consolidometer, an attempt has been made to analyse the consolidation test performed in a triaxial cell. Moreover, it was believed that the increasing importance of consolidated-undrained triaxial tests demanded an analysis of the consolidation that occurs during the first phase of such tests. If such an analysis could be perfected, it would be possible to measure both the compression and consolidation properties of a clay while performing the triaxial test, without the necessity of running an independent consolidation test in the consolidometer.

First, the theory was developed, then some tests that were performed by the investigator were analysed.

I. THE THEORY OF COMBINED AXIAL AND RADIAL CONSOLIDATION

The terms presented hereafter have been listed and defined in the Glossary.

For convenience, the result of the continuity equation of flow:

$$dQ = Q \text{ (inflow)} - Q \text{ (outflow)},$$

should be a positive result even though the actual change in moisture is negative. Therefore, $dQ = Q$ (outflow) - Q (inflow) was used.

Evaluation of Hydraulic Gradients. Halfway between the inner and outer faces of the slice in Figure 19, the hydraulic gradient is $-\frac{\delta h}{\delta r}$, i.e., as r increases h decreases as indicated in Figure 19.

Therefore, to make $Q = k i A dt$ a positive value, $-i_r$ shall be used. Because flow is actually occurring in the negative direction axially, Q would be negative and $-i_z$ must be used to keep the sign correct.

At the inner face,

$$i_r = -\frac{\delta h}{\delta r} + \frac{\delta(-\delta h/\delta r)(-dr)}{2}$$

$$\text{or } i_r = -\frac{\delta h}{\delta r} + \frac{dr}{2} \frac{\delta^2 h}{\delta r^2}$$

and at the outer face,

$$i_r = -\frac{\delta h}{\delta r} - \frac{dr}{2} \frac{\delta^2 h}{\delta r^2}$$

Similarly, at the lower face,

$$i_z = -\frac{\delta h}{\delta z} - \frac{dz}{2} \frac{\delta^2 h}{\delta z^2}$$

and at the upper face,

$$i_z = -\frac{\delta h}{\delta z} + \frac{dz}{2} \frac{\delta^2 h}{\delta z^2}$$

Pore Volume Change. Assuming 100% saturation, the change in the amount of water as given by the continuity equation is also the change in volume of the element.

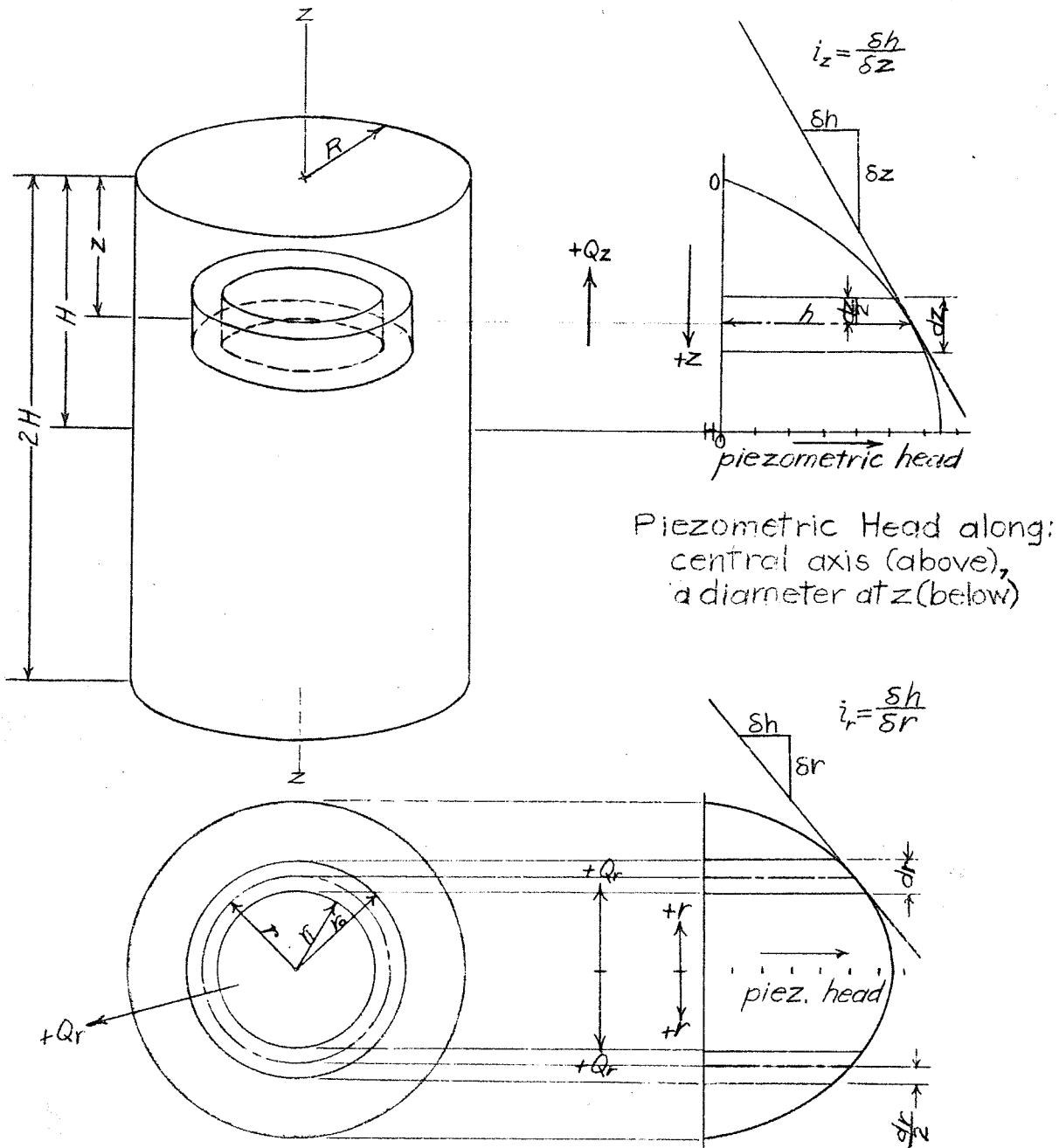


FIGURE 19

PRESSURE DISTRIBUTION WITH THREE DIMENSIONAL DRAINAGE THROUGH A CYLINDRICAL SPECIMEN

In a time element of dt ,

$$(Q_r)_o = k_r \left[\frac{\delta h}{\delta r} + \frac{dr}{2} \frac{\delta^2 h}{\delta r^2} \right] 2\pi r_o dz$$

$$\text{or } (Q_r)_o = 2\pi r_o dz k_r \left[\frac{\delta h}{\delta r} + \frac{dr}{2} \frac{\delta^2 h}{\delta r^2} \right] \text{ at the outer face.}$$

Similarly at the inner face,

$$(Q_r)_i = 2\pi r_i dz k_r \left[\frac{\delta h}{\delta r} - \frac{dr}{2} \frac{\delta^2 h}{\delta r^2} \right]$$

$$dQ_r = (Q_r)_o - (Q_r)_i = 2\pi dz k_r \left[(r_o - r_i) \frac{\delta h}{\delta r} + \frac{dr}{2} \frac{\delta^2 h}{\delta r^2} (r_o + r_i) \right]$$

$$dQ_r = 2\pi dz k_r \left[dr \frac{\delta h}{\delta r} + 2r \frac{dr}{2} \frac{\delta^2 h}{\delta r^2} \right]$$

$$\text{or } dQ_r = 2\pi r dz dr k_r \left[\frac{1}{r} \frac{\delta h}{\delta r} + \frac{\delta^2 h}{\delta r^2} \right]$$

Similarly, $dQ_z = (Q_z)_{\text{upper}} - (Q_z)_{\text{lower}}$

$$\text{or, } dQ_z = k_z \pi (r_o^2 - r_i^2) dz \frac{\delta^2 h}{\delta z^2}$$

Obviously, the total change in volume,

$$\begin{aligned} dV &= dQ_r + dQ_z \\ &= 2\pi r dz dr \left[k_r \left(\frac{1}{r} \frac{\delta h}{\delta r} + \frac{\delta^2 h}{\delta r^2} \right) + k_z \frac{\delta^2 h}{\delta z^2} \right] \dots \dots \dots (1) \end{aligned}$$

But the volume of the element is $2\pi r dz dr$ and the pore volume is $\frac{e}{1+e_o} 2\pi r dz \cdot dr$ at any time represented by the condition "e".

$$\text{Therefore, } \frac{dV}{dt} = \frac{\delta \left(\frac{e}{1+e_o} 2\pi r dz dr \right)}{\delta t}$$

and in an element of time dt ,

$$dV = \frac{2\pi r dz dr}{1 + e_0} \frac{\delta e}{\delta t} \dots \dots \dots (2)$$

Equating (1) and (2),

$$\frac{1}{1+e_0} \frac{\delta e}{\delta t} = k_r \left[\frac{1}{r} \frac{\delta h}{\delta r} + \frac{\delta^2 h}{\delta r^2} + k_z \frac{\delta^2 h}{\delta z^2} \right]$$

$$\frac{\delta e}{\delta t} = \frac{1+e_0}{\gamma_w} \left[k_r \left(\frac{1}{r} \frac{\delta u}{\delta r} + \frac{\delta^2 u}{\delta r^2} \right) + k_z \frac{\delta^2 u}{\delta z^2} \right] \dots \dots \dots (3)$$

Assuming, as did Terzaghi¹, that the void ratio-pressure relationship is a straight line,

$$\frac{de}{dp} = -a, \text{ in which (a) is the coefficient of compressibility for the triaxial method rather than for the consolidometer method.}$$

But, a decrease in pore water pressure means an equal increase in intergranular pressure, i.e., $-du = dp$;

therefore, $de = a du$

$$\text{or } \frac{\delta e}{\delta t} = a \frac{\delta u}{\delta t}$$

Substitution in (3) yields

$$\frac{\delta u}{\delta t} = \frac{(1+e_0) k_r}{a \gamma_w} \left[\frac{1}{r} \frac{\delta u}{\delta r} + \frac{\delta^2 u}{\delta r^2} \right] + \frac{(1+e_0) k_z}{a \gamma_w} \frac{\delta^2 u}{\delta z^2}$$

Basic Differential Equation. If the value $C = \frac{(1+e_0) k}{a \gamma_w}$ replaces the appropriate terms, two coefficients of consolidation are obtained in the fundamental differential equation:

¹Karl Terzaghi, Theoretical Soil Mechanics, (John Wiley and Sons, Inc., New York, 1943) pp. 265-296.

$$\frac{\delta u}{\delta t} = C_h \left(\frac{1}{r} \frac{\delta u}{\delta r} + \frac{\delta^2 u}{\delta r^2} \right) + C_z \frac{\delta^2 u}{\delta z^2} \quad \dots \dots \dots (4)$$

Theorem Combining Radial and Axial Consolidation.

Carillo² showed that, if $u_r = f(r, t)$ is a solution for $\frac{\delta u_r}{\delta t} = C_h \left(\frac{1}{r} \frac{\delta u_r}{\delta r} + \frac{\delta^2 u_r}{\delta r^2} \right)$, and if $u_z = f(z, t)$ is a solution for $\frac{\delta u_z}{\delta t} = C_z \frac{\delta^2 u_z}{\delta z^2}$, then $u = u_r u_z$.

A similar proof can be shown for $U_r = 1 - (u_r/u_0)$ and $U_z = 1 - (u_z/u_0)$. If u_r/u_0 is the solution of

$$\frac{1}{u_0} \frac{\delta u_r}{\delta t} = \frac{C_h}{u_0} \left(\frac{1}{r} \frac{\delta u_r}{\delta r} + \frac{\delta^2 u_r}{\delta r^2} \right) \quad \text{and if } \frac{u_z}{u_0} \text{ is the solution of}$$

$$\frac{1}{u_0} \frac{\delta u_z}{\delta t} = \frac{C_z}{u_0} \frac{\delta^2 u_z}{\delta z^2}; \quad \text{then the whole solution is}$$

$$u/u_0 = (u_r/u_0)(u_z/u_0).$$

The proof is as follows . . .

In the fundamental differential equation (4) divide through by u_0 giving:

$$\frac{\delta(u/u_0)}{\delta t} = C_h \left[\frac{1}{r} \frac{\delta(u/u_0)}{\delta r} + \frac{\delta^2(u/u_0)}{\delta r^2} \right] + C_z \frac{\delta^2(u/u_0)}{\delta z^2}.$$

Replace u/u_0 by the proposed solution of $(u_r/u_0)(u_z/u_0)$

²N. Carillo, "Simple Two and Three Dimensional Cases in the Theory of Consolidation of Soils," Journal of Mathematics and Physics, Vol. 21, pp. 1-5.

$$\frac{\delta(u_r u_z)}{(\frac{u_r}{u_0} \frac{u_z}{u_0}) \delta t} = C_h \left[\frac{1}{r} \frac{\delta(u_r u_z)}{(\frac{u_r}{u_0} \frac{u_z}{u_0}) \delta r} + \frac{\delta^2(u_r u_z)}{(\frac{u_r}{u_0} \frac{u_z}{u_0}) \delta r^2} \right] + C_z \frac{\delta^2(u_r u_z)}{(\frac{u_r}{u_0} \frac{u_z}{u_0}) \delta z^2}$$

$$\text{or } \frac{u_z}{u_0} \frac{\delta(u_r/u_0)}{\delta t} + \frac{u_r}{u_0} \frac{\delta(u_z/u_0)}{\delta t} = C_h \left[\frac{1}{r} \frac{u_z}{u_0} \frac{\delta(u_r/u_0)}{\delta r} \right. \\ \left. + \frac{u_z}{u_0} \frac{\delta^2(u_r/u_0)}{\delta r^2} \right] + C_z \frac{u_r}{u_0} \frac{\delta^2(u_z/u_0)}{\delta z^2} \dots \dots \dots (5)$$

$$\text{But, } \frac{1}{u_0} \frac{\delta u_r}{\delta t} = \frac{C_h}{u_0} \left[\frac{1}{r} \frac{\delta u_r}{\delta r} + \frac{\delta^2 u_r}{\delta z^2} \right]$$

$$\text{and } \frac{1}{u_0} \frac{\delta u_z}{\delta t} = \frac{C_z}{u_0} \frac{\delta^2 u_z}{\delta z^2}$$

The left hand side of (5) becomes

$$\frac{u_z}{u_0} \frac{C_h}{u_0} \left[\frac{1}{r} \frac{\delta u_r}{\delta r} + \frac{\delta^2 u_r}{\delta r^2} \right] + \frac{u_r}{u_0} \frac{C_z}{u_0} \frac{\delta^2 u_z}{\delta z^2}$$

which forms an identity with the right hand side (Q.E.D.).

It has been proved that $\frac{u}{u_0} = \frac{u_r}{u_0} \cdot \frac{u_z}{u_0}$

The degree of consolidation at a depth z , and radius r , is, $U_{zr} = 1 - \frac{u}{u_0}$,

$$\text{Thus, } U_{zr} = 1 - \frac{u_r}{u_0} \frac{u_z}{u_0}$$

and because $1 - \frac{u_r}{u_0} = U_r$ and $1 - \frac{u_z}{u_0} = U_z$,

$$U_{zr} = 1 - (1 - U_r)(1 - U_z)$$

$$\text{or } 1 - U_{zr} = (1 - U_r)(1 - U_z) \dots \dots \dots (6)$$

Equation (6) proves that the problem of combined drainage can be solved by considering the drainage first in one direction, then in the other.

Solution of the Differential Equation.

Let $u_r = F(r) \phi(t)$

$$\text{But } \frac{\delta u_r}{\delta t} = C_h \left(\frac{1}{r} \frac{\delta u_r}{\delta r} + \frac{\delta^2 u_r}{\delta r^2} \right)$$

$$\text{or } F(r) \phi'(t) = C_h \left[\frac{1}{r} \phi(t) F'(r) + \phi(t) F''(r) \right]$$

$$\frac{\phi'(t)}{\phi(t)} = \frac{C_h \left[\frac{1}{r} F'(r) + F''(r) \right]}{F(r)}$$

Obviously a change in the variable on one side of the equation does not affect the other side, and the expression can be written as . . .

$$\frac{1}{C_h} \frac{\phi'(t)}{\phi(t)} = -A^2 = \frac{\frac{1}{r} F'(r) + F''(r)}{F(r)}$$

wherein $-A^2$ is a constant value.

$$\text{Thus, } \phi'(t) = -A^2 C_h \phi(t).$$

By operator methods for differential equations this becomes

$$\phi(t) = C_1 \exp^{-A^2 C_h t} \dots \dots \dots (7)$$

with C_1 being a constant.

$$\text{Also, } -A^2 F(r) = \frac{1}{r} F'(r) + F''(r)$$

$$\text{or, } F''(r) + \frac{1}{r} F'(r) + A^2 F(r) = 0 \dots \dots \dots (8)$$

Let $x = Ar$ and $y = F(r)$

$$r = \frac{x}{A}$$

$$\frac{dr}{dx} = \frac{1}{A}$$

$$\frac{dy}{dx} = \frac{dy}{dr} \frac{dr}{dx} = \frac{1}{A} F'(r)$$

$$\begin{aligned} \frac{d^2y}{dx^2} &= \frac{d(dy/dx)}{dx} = \frac{d(dy/dx)}{dr} \frac{dr}{dx} = \left[\frac{1}{A} F''(r) \right] \frac{1}{A} \\ &= \frac{1}{A^2} F''(r) \end{aligned}$$

In a Bessel Function:

$$x^2 \frac{d^2y}{dx^2} + x \frac{dy}{dx} + (x^2 - m^2)y = 0$$

the foregoing values are substituted.

$$\frac{A^2 r^2}{A^2} F''(r) + \frac{Ar}{A} F'(r) + (A^2 r^2 - m^2) F(r) = 0$$

$$\text{or, } F''(r) + \frac{1}{r} F'(r) + \frac{A^2 r^2 - m^2}{r^2} F(r) = 0$$

If this Bessel Function is of the order zero, $m = 0$, the equation simplifies to equation (8), proving that it is a Bessel Function of zero order:

$$F''(r) + \frac{1}{r} F'(r) + A^2 F(r) = 0$$

whose solution is

$$y = c J_0(x) + b Y_0(x)$$

$$\text{or } F(r) = c J_0(Ar) + b Y_0(Ar) \dots \dots \dots (9)$$

wherein
$$J_0(Ar) = \sum_{m=1}^{m=\infty} \frac{(-1)^m (Ar)^{2m}}{2^{2m} (m!)^2}$$

and $b Y_0(Ar) = 0$ as verified by expanding equation (8) according to the Method of Frobenius.

Consequently, $F(r) = c J_0(Ar) \dots \dots \dots (9a)$

and the combination of (9a) and (7) gives

$$u_r = C_2 \exp^{-A^2 C_h t} J_0(Ar) \dots \dots \dots (10)$$

The solution of the vertical case is well known and as given by Taylor³ is:

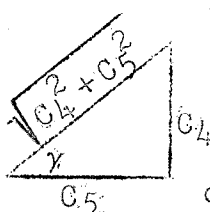
$$u_z = [C_4 \cos(Bz) + C_5 \sin(Bz)] C_3 \exp^{-B^2 C_z t} \dots \dots \dots (10a)$$

wherein B, C₄, C₅, and C₃ are constants.

The solution for pore pressure is . . .

$$u = u_z u_r = C_6 \exp^{-t(A^2 C_h + B^2 C_z)} J_0(Ar) [C_4 \cos(Bz) + C_5 \sin(Bz)]$$

or,
$$u = C_6 \exp^{-t(A^2 C_h + B^2 C_z)} J_0(Ar)$$



or,
$$u = C_7 \exp^{-t(A^2 C_h + B^2 C_z)} J_0(Ar) \sin(Bz + \gamma) \dots \dots \dots (11)$$

³Donald W. Taylor, Fundamentals of Soil Mechanics, (John Wiley and Sons, Inc., New York, 1948), pp. 229-234.

Boundary Conditions. The boundary conditions are,

$$\begin{array}{ll}
 \text{(a) at } t=t, & z = 0 \text{ and } r = r; & u = 0 \\
 \text{(b) at } t=t, & z = 2H & r = r; & u = 0 \\
 \text{(c) at } t=t, & z = z & r = R; & u = 0 \\
 \text{(d) at } t=0, & z = z & r = r; & u = u_0 \text{ (a constant} \\
 & & & \text{usually)}
 \end{array}$$

By the foregoing conditions equation (11) becomes respectively,

$$\begin{array}{ll}
 \text{(a) } 0 = C_7 \exp^{-t(A^2 C_h + B^2 C_z)} & \text{Jo}(Ar) \sin \gamma \\
 \text{(b) } 0 = C_7 \exp^{-t(A^2 C_h + B^2 C_z)} & \text{Jo}(Ar) \sin(2BH + \gamma) \\
 \text{(c) } 0 = C_7 \exp^{-t(A^2 C_h + B^2 C_z)} & \text{Jo}(AR) \sin(Bz + \gamma) \\
 \text{(d) } u_0 = C_7 \text{Jo}(Ar) \sin(Bz + \gamma)
 \end{array}$$

In all cases C_7 appears. Because the solution of (11) is not zero, C_7 cannot be zero. Because u_0 is not zero, in case (d) neither $\text{Jo}(Ar)$, nor $\sin(Bz + \gamma)$ can be zero. Therefore, in case (a),

$$\sin \gamma = 0 \quad \text{and} \quad \gamma = 0$$

and in case (b),

$$\sin(2BH) = 0 \quad \text{and} \quad 2HB = n\pi \quad \text{or} \quad B = \frac{n\pi}{2H}$$

wherein n is any positive integer.

By case (c), $\text{Jo}(AR) = 0$

If the roots of $\text{Jo}(x)$ are $\omega_1, \omega_2, \dots, \omega_k, \dots$, then, $A = \frac{\omega_k}{R}$, wherein the subscript k represents the first, second, etc., roots of the Bessel Equation of zero order.

Equation (11) becomes,

$$u = \sum_{k=1}^{k=\infty} \sum_{n=1}^{n=\infty} C_7 \exp^{-t\left(\frac{\omega_k^2}{R^2} C_h + \frac{n^2\pi^2}{4H^2} C_z\right)} J_0\left(\frac{\omega_k r}{R}\right) \sin\left(\frac{n\pi z}{2H}\right)$$

Or, it may split into its component parts such that C_7 is represented by f_k and f_n :

$$u = \sum_{k=1}^{k=\infty} f_k \exp^{-t\left(\frac{\omega_k^2}{R^2} C_h\right)} J_0\left(\frac{\omega_k r}{R}\right) \sum_{n=1}^{n=\infty} f_n \exp^{-t\left(\frac{n^2\pi^2}{4H^2} C_z\right)} \sin\left(\frac{n\pi z}{2H}\right) \dots \dots \dots (12)$$

According to the boundary condition (d):

$$(u_0)_r = \sum_{k=1}^{k=\infty} f_k J_0\left(\frac{\omega_k r}{R}\right) \dots \dots \dots (13)$$

$$\text{and } (u_0)_z = \sum_{n=1}^{n=\infty} f_n \sin(Bz).$$

This latter constant f_n was solved by Taylor,⁴ and is

$$f_n = \frac{1}{H} \int_0^{2H} (u_0)_z \sin\left(\frac{n\pi z}{2H}\right) dz \dots \dots \dots (13a)$$

But to solve the former, the following procedure is followed:

$$\text{let } x = r/R$$

multiply (13) through by $x J_0(\omega_j x) dx$ and integrate both sides between zero and unity;

$$\int_0^1 (u_0)_r x J_0(\omega_j x) dx = \int_0^1 f_k x J_0(\omega_j x) J_0(\omega_k x) dx$$

The property of orthogonality of a Bessel Function is:

⁴Taylor, loc. cit.

$$\int_0^1 x J_0(\omega_k x) J_0(\omega_j x) dx = \begin{cases} 0 & \text{when } k \neq j \\ 1/2 [J_1(\omega_k)]^2 & \text{when } k = j \end{cases}$$

therefore, $\int_0^1 (u_0)_r x J_0(\omega_j x) dx = 1/2 [J_1(\omega_k)]^2 f_k$

$$\text{or } f_k = \frac{2}{[J_1(\omega_k)]^2} \int_0^1 \frac{r}{R} (u_0)_r J_0\left(\frac{\omega_k r}{R}\right) d\left(\frac{r}{R}\right) \dots \dots \dots (13b)$$

when the required simplification and substitution are made.

Time Factors. The resulting solution is,

$$u = \sum_{k=1}^{k=\infty} \frac{2}{[J_1(\omega_k)]^2} \left[\int_0^1 \left(\frac{r}{R}\right) (u_0)_r J_0\left(\frac{\omega_k r}{R}\right) d\left(\frac{r}{R}\right) \right] \exp \frac{-t \omega_k^2}{R^2} C_h J_0\left(\frac{\omega_k r}{R}\right) \sum_{n=1}^{n=\infty} \frac{1}{H} \left[\int_0^{2H} (u_0)_z \sin\left(\frac{n\pi z}{2H}\right) dz \right] \exp \frac{-t n^2 \pi^2}{4H^2} C_z \sin\left(\frac{n\pi z}{2H}\right) \dots \dots \dots (13c)$$

The equation may be abbreviated by using the time factors

$$T_z = C_z t/H^2 \quad T_r = C_h t/R^2 \quad \dots \dots \dots (13d)$$

$$u = \sum_{k=1}^{k=\infty} \frac{2}{[J_1(\omega_k)]^2} \left[\int_0^1 \left(\frac{r}{R}\right) (u_0)_r J_0\left(\frac{\omega_k r}{R}\right) d\left(\frac{r}{R}\right) \right] \exp^{-\omega_k^2 T_r} J_0\left(\frac{\omega_k r}{R}\right) \sum_{n=1}^{n=\infty} \frac{1}{H} \left[\int_0^{2H} (u_0)_z \sin\left(\frac{n\pi z}{2H}\right) dz \right] \exp \frac{-n^2 \pi^2}{4} T_z \sin\left(\frac{n\pi z}{2H}\right)$$

Degree of Consolidation. The degree of consolidation at any depth z and radius r is . . .

$$U_{zr} = 1 - \frac{u}{u_0} = 1 - \frac{u_r}{u_0} \frac{u_z}{u_0}$$

If $(u_0)_r$ and $(u_0)_z$ are constants equalling u_0 ,
then,

$$U_{zr} = 1 - \left\{ \sum_{k=1}^{k=\infty} \frac{2}{[J_1(\omega_k)]^2} \left[\int_0^1 \frac{r}{R} J_0\left(\frac{\omega_k r}{R}\right) d\left(\frac{r}{R}\right) \right] \right. \\ \left. \exp^{-\omega_k^2 T_r} J_0\left(\frac{\omega_k r}{R}\right) \right\} \left\{ \sum_{m=0}^{m=\infty} \frac{2}{M} \exp^{-M^2 T_z} \sin\left(\frac{Mz}{H}\right) \right\} \dots \dots (14)$$

wherein $m = \frac{n-1}{2}$ and $M = \frac{\pi n}{2}$

Before equation (14) can be simplified any further,
the following mathematical relationship must be studied:

It is known that $\int x J_0(x) dx = x J_1(x)$

$$\text{or } \frac{d(x J_1(x))}{dx} = x J_0(x)$$

similarly if $X = \omega x$,

$$\frac{d(X J_1(X))}{dX} = X J_0(X)$$

or $X J_1(X) = \int X J_0(X) dX$

replacing X by ωx yields

$\omega x J_1(\omega x) = \int \omega x J_0(\omega x) d(\omega x)$

$$\omega x J_1 \omega x = \omega^2 \int x J_0(\omega x) dx,$$

$$\therefore \int_0^1 x J_0(\omega x) dx = \left[\frac{X}{\omega} J_1(\omega X) \right]_0^1 = \frac{1}{\omega} J_1(\omega)$$

But if $x = r/R$, it will be noted that this result can
supplant the integral occurring in equation (14), which be-
comes,

$$U_{zr} = 1 - \sum_{k=1}^{k=\infty} \frac{2}{\omega_k J_1(\omega_k)} \exp^{-\omega_k^2 T_r} J_0\left(\frac{\omega_k r}{R}\right) \\ \sum_{m=0}^{m=\infty} \frac{2}{M} \exp^{-M^2 T_z} \sin\left(\frac{Mz}{H}\right) \dots \dots \dots (15)$$

Equation (15) can be used to study the degree of consolidation at any depth z by measuring the pore pressure at that depth. However, it is customary to work with the average degree of consolidation (U') throughout the sample.

Consequently,

$$1 - U'_r = \frac{\int_0^R \pi r u_r dr}{\int_0^R (u_0)_r \pi r dr} \\ = \frac{\int_0^R r u_r dr}{\int_0^R u_0 r dr} \\ = \frac{\sum_{k=1}^{k=\infty} \frac{2}{\omega_k J_1(\omega_k)} \exp^{-\omega_k^2 T_r} \left[\int_0^R r J_0\left(\frac{\omega_k r}{R}\right) dr \right]}{R^2/2} \quad \begin{matrix} \text{(when } u_0 \text{ is)} \\ \text{(a constant)} \end{matrix}$$

The integral is treated like that in equation (14) and,

$$1 - U'_r = \frac{\sum_{k=1}^{k=\infty} \frac{2}{\omega_k J_1(\omega_k)} \exp^{-\omega_k^2 T_r} \left[\left(\frac{Rr}{\omega_k} \right) J_1\left(\frac{\omega_k r}{R}\right) \right]_0^R}{R^2/2}$$

$$\text{Finally, } U'_r = 1 - \sum_{k=1}^{k=\infty} \frac{4}{\omega_k^2} \exp^{-\omega_k^2 T_r} \dots \dots \dots (16)$$

Similarly,

$$1 - U'_z = 1 - \frac{\int_0^{2H} u_z dz}{\int_0^{2H} u_0 dz}$$

$$\text{and } U'_z = 1 - \sum_{m=0}^{m=\infty} \frac{2}{M^2} \exp^{-M^2 T_z} \dots \dots \dots (17)$$

Equation (16) is the same as that given by Gibson and Lumb.⁵

Combining (16) and (17) according to (6) gives

$$U' = 1 - \sum_{k=1}^{k=\infty} \frac{4}{\omega_k^2} \exp^{-\omega_k^2 T_r} \sum_{m=0}^{m=\infty} \frac{2}{M^2} \exp^{-M^2 T_z} \dots \dots \dots (18)$$

Table II presents the values given by (16) and (17) for various time factors. Figure 20 shows the degree of consolidation plotted against time factor, and Figure 21 shows the degree of consolidation plotted against the square root of the time factor.

II. RESULTS OF TRIAXIAL CONSOLIDATION

Three tests were run in order to confirm the foregoing theory and to ascertain the differences between triaxial consolidation and consolidometer consolidation. Unfortunately, none of three tests proved to be very reliable.

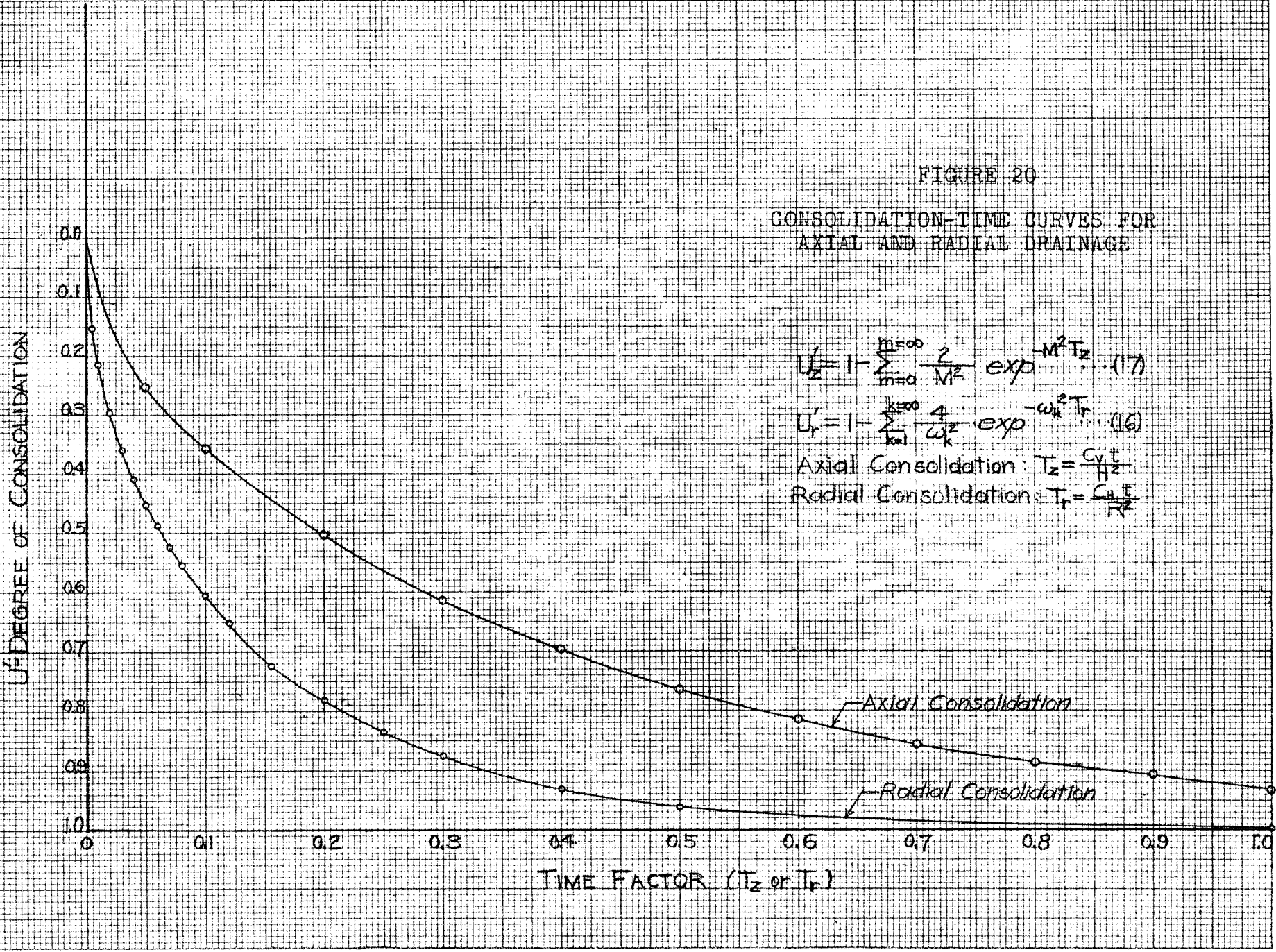
The first test (TM 37) had to be discarded, because the cell pressure was inadvertently released, and the sample failed in shear under the action of the axial load on the

⁵R. E. Gibson and Peter Lumb, "Numerical Solution of Some Problems in the Consolidation of Clay," Proceedings of the Institute of Civil Engineers, (March 1953), Vol. 2, No. 2, part 1.

TABLE II
 AVERAGE DEGREES OF CONSOLIDATION FOR
 VARIOUS TIME FACTOR VALUES

AXIAL DRAINAGE			RADIAL DRAINAGE		
T_z	$\sqrt{T_z}$	U'_z	T_r	$\sqrt{T_r}$	U'_r
0.05	0.224	25.2%	0.005	0.0707	15.4%
.10	.316	35.7	.010	.100	21.5
.20	.447	50.3	.020	.141	29.8
.30	.548	61.3	.030	.173	36.0
.40	.632	69.8	.040	.200	41.0
.50	.707	76.4	.050	.224	45.2
.60	.775	81.6	.060	.245	48.9
.70	.837	85.6	.070	.264	52.3
.80	.894	88.7	.080	.283	55.3
.90	0.949	90.8	.100	.316	60.6
1.00	1.000	93.1	.120	.346	65.1
1.10	1.048	94.6	.160	.400	72.5
1.20	1.095	95.8	.200	.448	78.2
1.50	1.225	98.0	.250	.500	83.7
2.00	1.414	99.4	.300	.548	87.8
3.00	1.732	100.0%	.400	.632	93.2
			0.500	0.707	96.2
			1.00	1.000	99.8%

NOTE: The terms are defined by equations 13d, 16 and 17, and calculations of radial drainage were based upon values from Tables of Functions by E. Jahnke and F. Emde (Dover, New York, 1943), p.154 et seq.

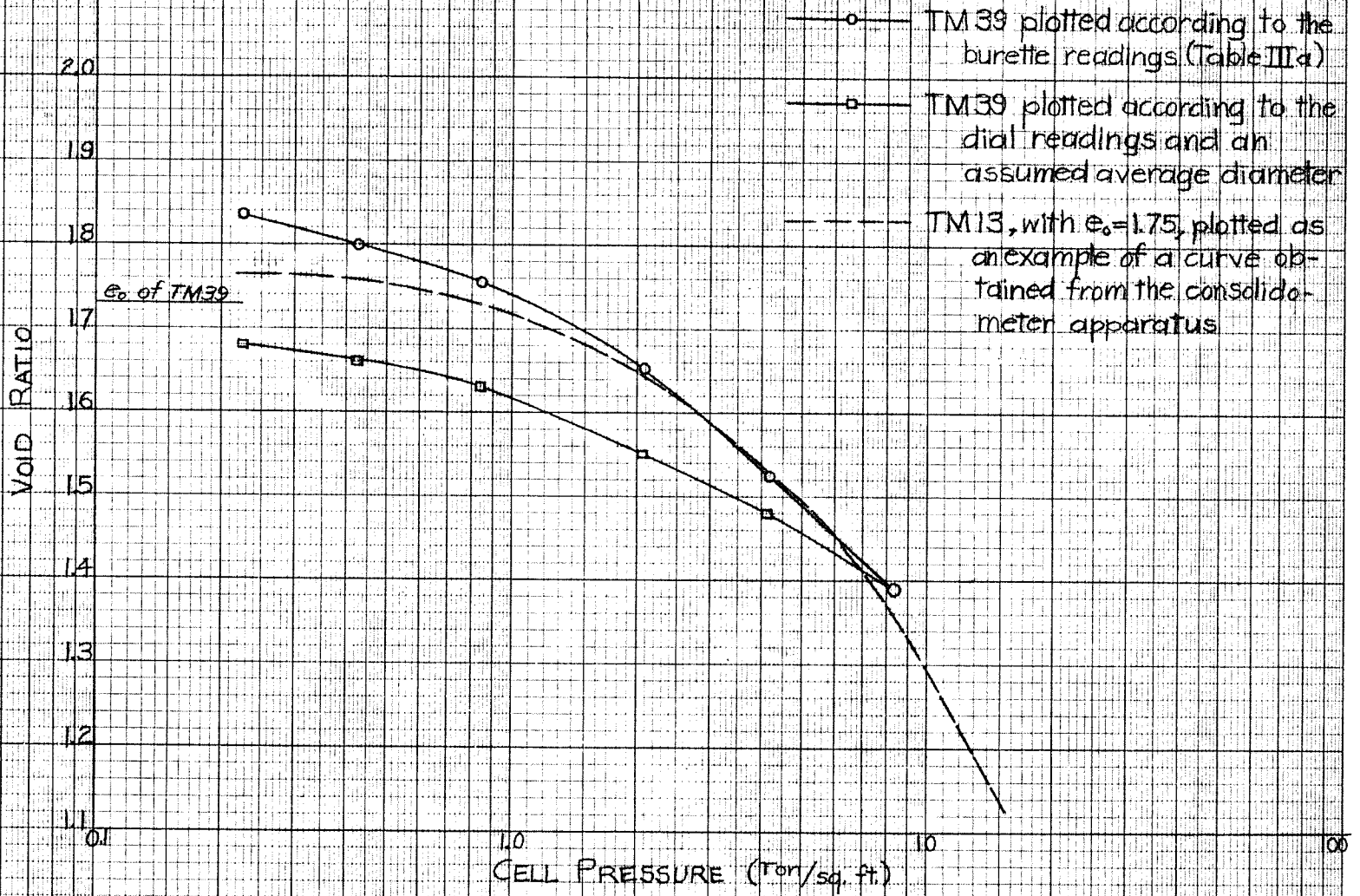


ram, which was not released at the same time. Sample TM 38 did not experience this difficulty. However, it was found that the soft filter paper used as a drain in the radial direction was wholly inadequate, and in fact, drainage was occurring in the axial direction only. Moreover, a substantial leak developed early in the test through the upper burette. As a result, this test was also regarded as a failure.

The third test was by no means perfect. It did not shear and, apart from a leak which developed early in the test, it did not develop any noticeable leaks until the very last day of testing. However, in order to obtain some idea of what can be expected in triaxial consolidation, this last test has been analysed.

Compressibility by Triaxial Consolidation. In order to compare the compression curves in a triaxial cell with those from a consolidometer, in Figure 22 were drawn the e -log p curves according to the burette readings, according to the deflection readings and a mean diameter, and according to sample TM 13 from a consolidometer test. It will be noticed that the use of the deflections alone did not give a comparable curve at all. However, the use of the burette readings for drawing the compression curve yielded fairly good agreement with that of TM 13. Nevertheless, the agreement was not perfect.

FIGURE 22
 COMPRESSION CURVES IN
 THE TRIAXIAL CELL
 FOR TM 39



It will be noticed that they coincide between the pressures of 2 and 6 T/s.f. However, the curve, according to the burette readings, rises well above at lower pressures and slightly above at higher pressures. The latter divergence is reasonable, in view of the fact that consolidation was not permitted to finish due to the leak that developed during the last loading increment.

The divergence at lower pressures is difficult to understand. After the initial leak had been stopped no tendency to swell was observed at low pressures in the triaxial cell. Why then should the curve yield higher void ratios? The only explanation that seems plausible is that the leak which developed when the sample was first set-up introduced sufficient water into the sample to swell it. In addition to this initial leakage, progressive seepage through the membranes surely occurred throughout the test. The latter leakage would be a function of time, and because the change in volume was referred to the condition at the end of the test, the effect of this leak would accumulate towards the beginning of the test. Thus the divergence at low pressures can be explained. The effects of leakage certainly require further study before the triaxial method can be accepted.

Because there was no apparent swelling at low pressures in the triaxial cell, no determination of the

overburden pressure could be made. The lack of initial swelling in the triaxial cell has been observed at the University of Manitoba to occur inevitably for all triaxial tests regardless of the confining pressure, but swelling did occur in samples that were unloaded from a high pressure (TM 38). Two explanations exist, (1), this is a phenomenon peculiar to the triaxial test, (2), the disturbance during the set-up of the sample destroys the tendency to swell. Here again, more research is necessary before any conclusions can be drawn.

Consolidation Characteristics in the Triaxial Cell.

Using equation 6, the value of U_r as indicated in Table III(b) for two load increments was ridiculously small. As a consequence, the coefficients of consolidation were unreasonable values. At first it was believed that the theory as previously expounded was incorrect, but reconsideration produced the belief that the horizontal drainage could be so effective that little or no drainage occurred axially. This hypothesis was confirmed by the close agreement between the U and U_z values at the same value of time, as shown in Table III(b). Therefore, the entire drainage would tend to take place radially, rather than in combined action with the axial direction. The only axial drainage that would occur would be that necessary to take

TABLE III(a)

e VS. p COMPUTATIONS TM 39

Time interval (hrs)	Load on pan (lbs)	Corrected cell pressure		Axial press (psi)	Upper burette(ccs)		Lower burette(ccs)		total vol chg dV (ccs)	de = $\frac{dV}{V_s^a}$	e void ratio
		(psi)	T/sf		corr. rdg	dVu	corr. rdg	dVl			
-	0	0	0	0.3	14.65	6.25	19.2	6.1	12.35	0.57	1.96 ^b
20	0.1	3.1	0.225	3.5	13.4	5.0	17.8	4.7	9.7	0.445	1.835
47	0.2	5.9	0.425	6.45	12.8	4.4	17.55	4.45	8.85	0.41	1.80
22	0.3	11.7	0.84	12.05	12.4	4.00	17.0	3.9	7.9	0.365	1.755
22	0.8	28.9	2.08	29.7	11.25	2.85	15.9	2.8	5.65	0.26	1.65
44	1.6	57.6	4.15	58.8	9.45	1.45	14.55	1.45	2.9 ^c	0.135	1.525
7,40 ^d	3.1	115	8.3	116.7	-	0	13.1	0	0	0	1.39

$$av_s = \frac{W_s}{Gy_w} = \frac{60.62}{2.79} = 21.7 \text{ ccs.}$$

^bBy actual measurements, the initial void ratio of the sample was 1.73.

^cDue to leak $dy = 2dV_l$.

^dLeakage developed in final pressure increment and one had previously occurred in the membranes before the first increment was terminated, but this leak was stopped by the addition of a third membrane.

TABLE III(b)

T_v and T_h COMPUTATIONS TM 39

Drain- age time (mins)	J av press (psi)	corr'td dial rdgs (ins)	dl defln (ins)	dL L ₀ ^a	H ₂ vert path (ins ²)	dV (ccs)	dV V ₀ ^a	Deg of Consoh.			r ^{2c}	Time Factors ^d	
								U	U _z	U _r ^b		T _r	T _z
460		.3475	0	0	$\left[\frac{2.01}{2}\right]^2$	0	0	1.00	1.00		.505		
85 0	115	.3721 .3967	.0246 .0492	.0122	1.04	1.05	.020	.54 0	.50 0	.08 0	.510	.004	0.197
2640 38 0	57.6	.4330 .4550 .4785	.1075	.0535	0.902	4.15	.079	1.00 .52 0	1.00 .50 0	.04 0	.517	.002	0.197

^aat end of test: L₀ = 2.01^m; r₀ = 1.42/2; V₀ = 52.3 ml.

$$bU_r = 1 - \frac{1 - U}{1 - U_z}$$

$$c r^2 = r_0^2 \frac{1 + dV/V_0}{1 + dL/L_0}$$

^dTime Factors obtained from Figure 20. The values of T_r should be larger than T_z to yield a higher Ch.

moisture from one part of the sample to a freely running varve along which the drainage would be completed. Consequently, the assumption has been made that the drainage for the specimen in question is wholly radial drainage.

On this basis the consolidation characteristics for the 57.6 p.s.i. cell pressure have been calculated as follows;

$$C_h = \frac{T_r R^2}{t}$$

according to Figure 23, $t_{50} = 38$ mins., or 2,280 seconds.

$$R^2 = 0.517 \text{ sq.in.}$$

$$T_r = 0.0632 \text{ (from Fig. 20, p. 81)}$$

$$\text{therefore, } C_h = \frac{.0632 \times .517}{2280} = 14.4 \times 10^{-6} \text{ s.i./sec.}$$

$$e_o = 1.65, \text{ and } e_{av.} = 1.58$$

$$a_h = \frac{(2.45 - .5) \times 21.7}{288 \text{ psi}} = 3.12 \times 10^{-3} \text{ s.i./lb.}$$

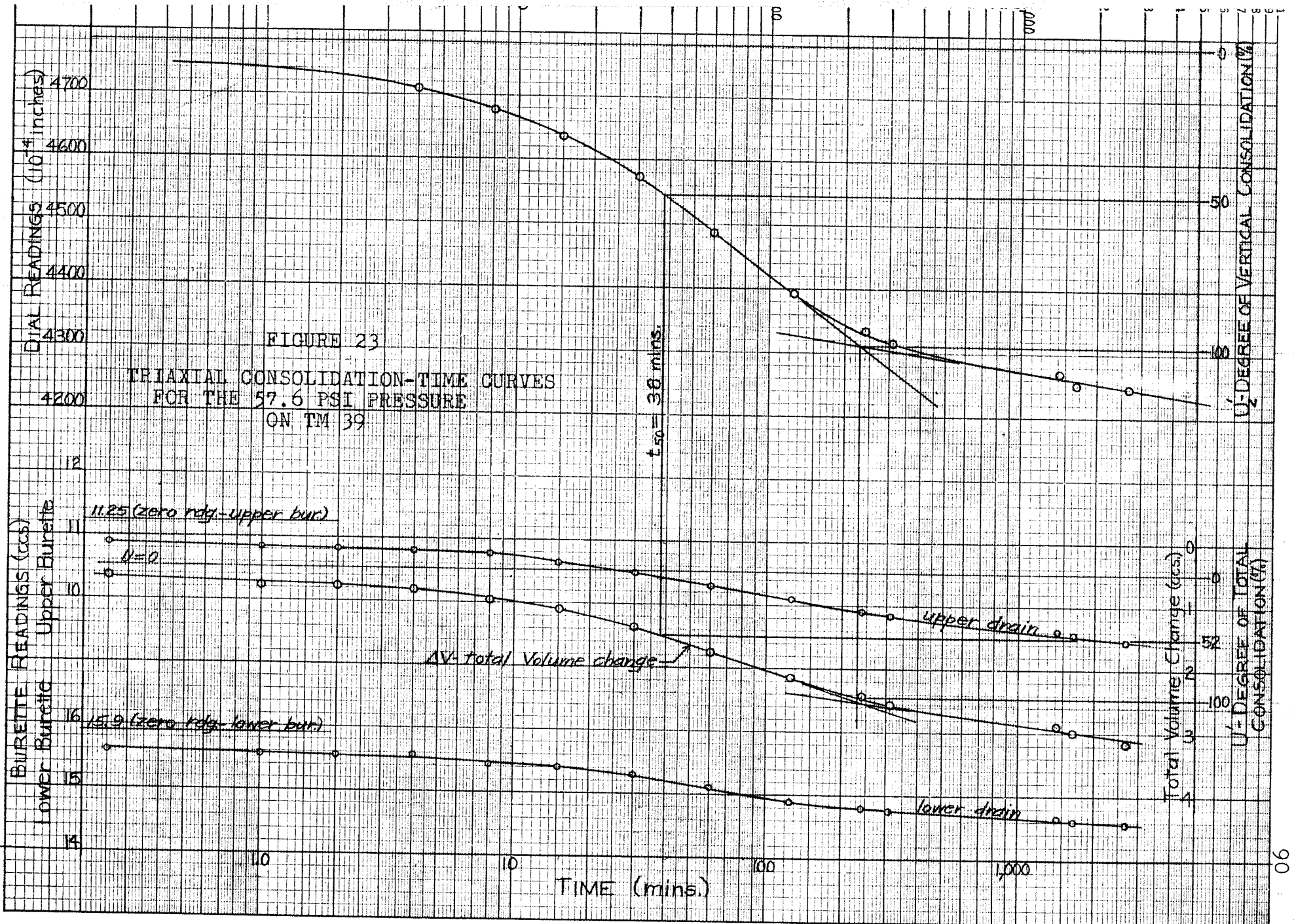
(see Table III(a), p. 87)
(for $d_e = dV/dV_s$.)

$$\gamma_w = 0.0361 \text{ lb./cu.in.}$$

$$\text{therefore, } k_h = \frac{14.4 \times 3.12 \times .0361}{2.65} \times 10^{-9} \times 2.54 = 1.6 \times 10^{-9} \frac{\text{cm.}}{\text{sec.}}$$

Both C_h and k_h were lower than those values obtained at similar void ratios in the consolidometer test. However, these values are at least comparable to those values, and k_h is slightly larger than the k_v 's obtained from the consolidometer test. Moreover, the coefficient of consolida-

*Values represent primary consolidation only. See Fig. 23.



tion is always low in the triaxial cell.⁶ This fact would seem to indicate that the assumption of total drainage in the radial direction is a valid one.

III. DIFFICULTIES WITH THE TRIAXIAL METHOD

A number of difficulties were encountered in the three tests run by the investigator. No doubt more would have occurred had more tests been run. Nevertheless, these difficulties and possible solutions of them have been recorded hereafter.

Special regulating devices for handling the exceptionally high pressures had to be obtained. Moreover, the equipment had to be so constructed as to be used safely under such high pressures.

Despite all precautions taken to remove air from the sample and the components of apparatus adjacent to it, air bubbles were still observed flowing through the connection to the cap. Either a great deal of air was left in the apparatus after assembly, or it permeated through the membranes from the cell fluid.

⁶Allan W. Bishop and D. J. Henkel, The Measurement of Soil Properties in the Triaxial Test, (Edward Arnold Ltd., London, 1957); and P. W. Rowe, "Measurement of the Coefficient of Consolidation of Lacustrine Clay," Geotechnique, Vol. IX, (1959), p. 107

It has been found that the membranes did prevent very large leaks, and two membranes over the sample were sufficient to run a consolidation test for a week or ten days. However, during the set-up of the sample it was not unusual to puncture the membranes with holes that created tremendous leaks despite the tiny size of these holes. This occurred in the last sample; a third membrane was added, and it proved to be effective in preventing further leaks.

Difficulties in setting up the sample in the cell caused disturbances of the specimen. The effect of such disturbances may have been such as to prevent the initial swelling, and a great deal of care, indeed skill, must be used during the assembly of the sample in the cell.

Measurements of the length of the sample taken at the start and finish of the test showed that the change in length, as indicated by the dials, was too large. In the sample TM 39 that was analysed, this change was .2595 in. according to the dial, and only .177 in. according to direct measurements. However, the filter paper had a certain amount of compressibility that could account for about .0150 inches. This left a discrepancy of .0675 inches, some of which could be attributed to the swelling of the sample before the last membrane was applied, but the dial readings did not indicate that the swelling was this large.

Consequently, it seems that in future a great deal of care must be taken to check the changes in length throughout a test.

As shown in Figure 24, the point of 100% consolidation did not really appear for the last pressure increment. Although only seven hours were devoted to consolidation, this was found to be an adequate time for the previous increments, as was verified by the time-curve in Figure 23, p. 90. This unusual occurrence would seem to be the result of the leak which occurred in the upper drain, although it is not quite clear why the sample should continue to deflect during such a leak.

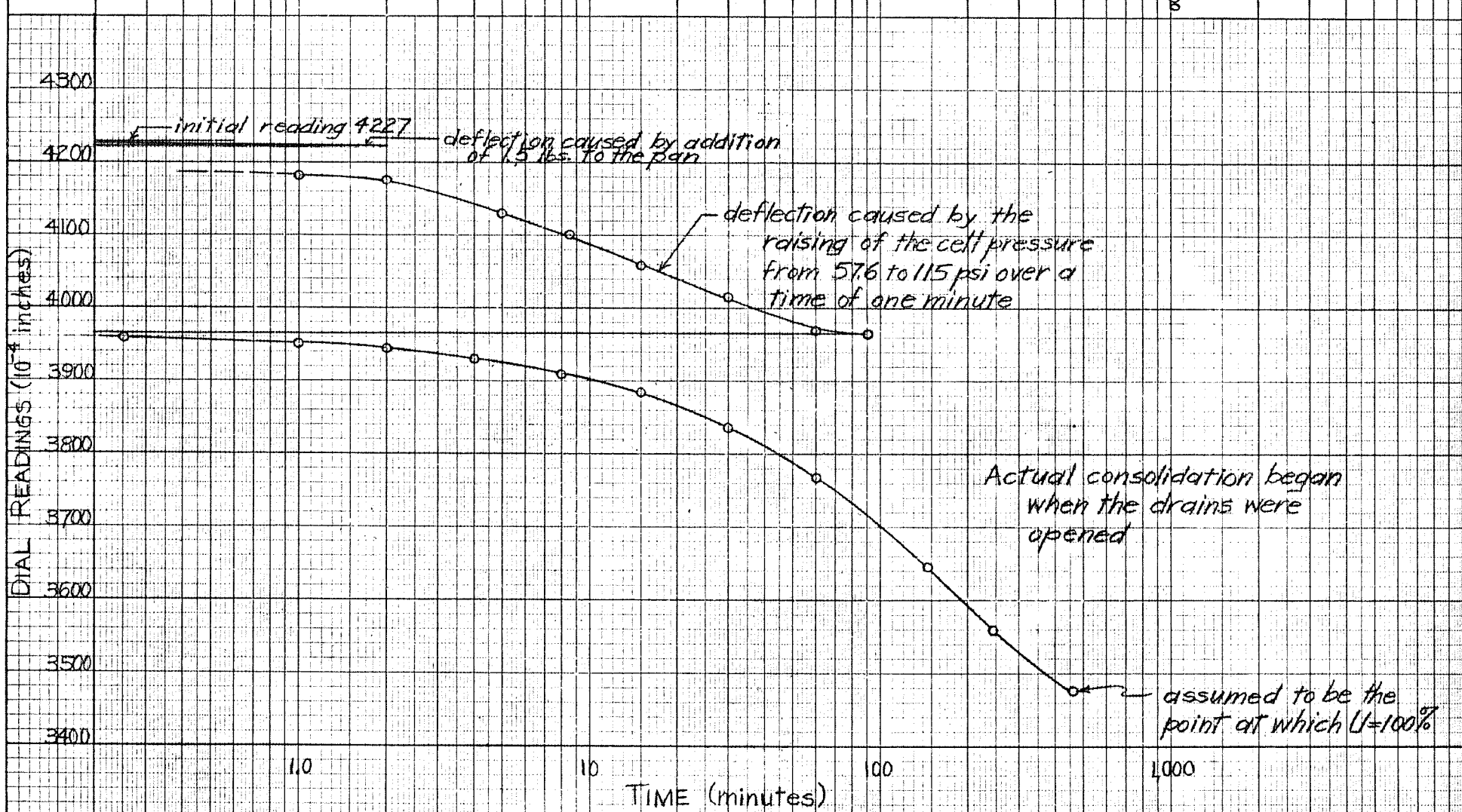


FIGURE 24
 DEFLECTION-TIME CURVES FOR THE
 115 PSI CELL PRESSURE ON TM39

SECTION VII

EFFECTS OF LOADING CYCLES

It has been shown in this section that repeated cycles of loading and unloading between two constant limits had a definite effect upon the compression curve of the soil. An attempt to determine the effects upon the consolidation characteristics under the same circumstances was also made.

I. EFFECT OF CYCLING UPON COMPRESSION PROPERTIES

It has been shown in previous sections that the re-compression branch for this clay had no predominately flat portion. This is typical of the local clays. It was felt that this flattened portion might be produced by repeated loading, and once this was obtained, Casagrande's construction¹ would become possible. Moreover, it was believed that an elastic condition might be approached such that the curve would not be affected by further cycling.

Effect upon Compression Curves. In clays of other regions, a recompression branch passes slightly to the

¹A. Casagrande, "The Determination of the Preconsolidation Load and its Practical Significance," Proceedings First International Conference on Soil Mechanics, Cambridge, Mass., (1936), Vol. 3, pp. 60-64.

left of the overburden pressure, which is signalled by a sharp break in the curvature immediately before this condition is approached. It then strikes the virgin compression branch shortly thereafter.

However, for this clay the typical result as shown in Figure 25 with sample TM 31, did not show any sharp break in curvature. What did occur was a curve-shift, which was the progressively downward trend of the hysteresis loops as the number of cycles increased. The curve-shift for samples TM 10 and TM 18 is demonstrated in Figure 26, in which the loops have been drawn for TM 10, but only the end points have been shown for TM 18.

The first effect of this shift was upon the preconsolidation pressure. Because the straightline portion of the e -log p curve, after shifting was apparently parallel to and coincident with the virgin compression branch of a sample that did not undergo any shifting, it seemed reasonable to expect the preconsolidation pressure to appear to be farther to the right, that is to say, at a higher pressure. For specimen TM 10 the approximate shift was 2 T/s.f.. This would seem to indicate that a clay which has been presumed to be highly preloaded might in fact not have been preloaded at all, but the apparent preloading could simply have been a manifestation of a great deal of curve-shift that has occurred at the overburden pressure. As a con-

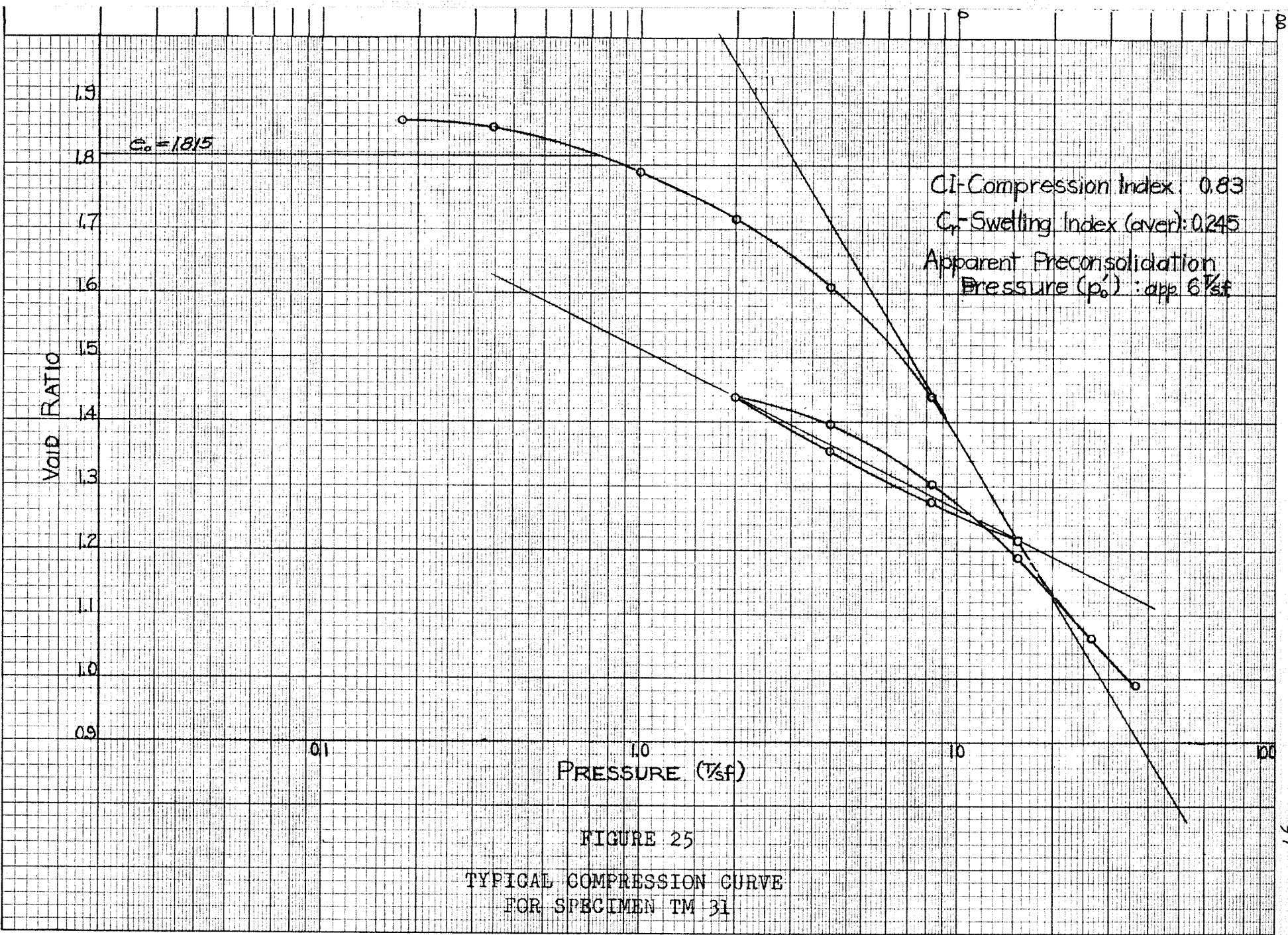
Void Ratio

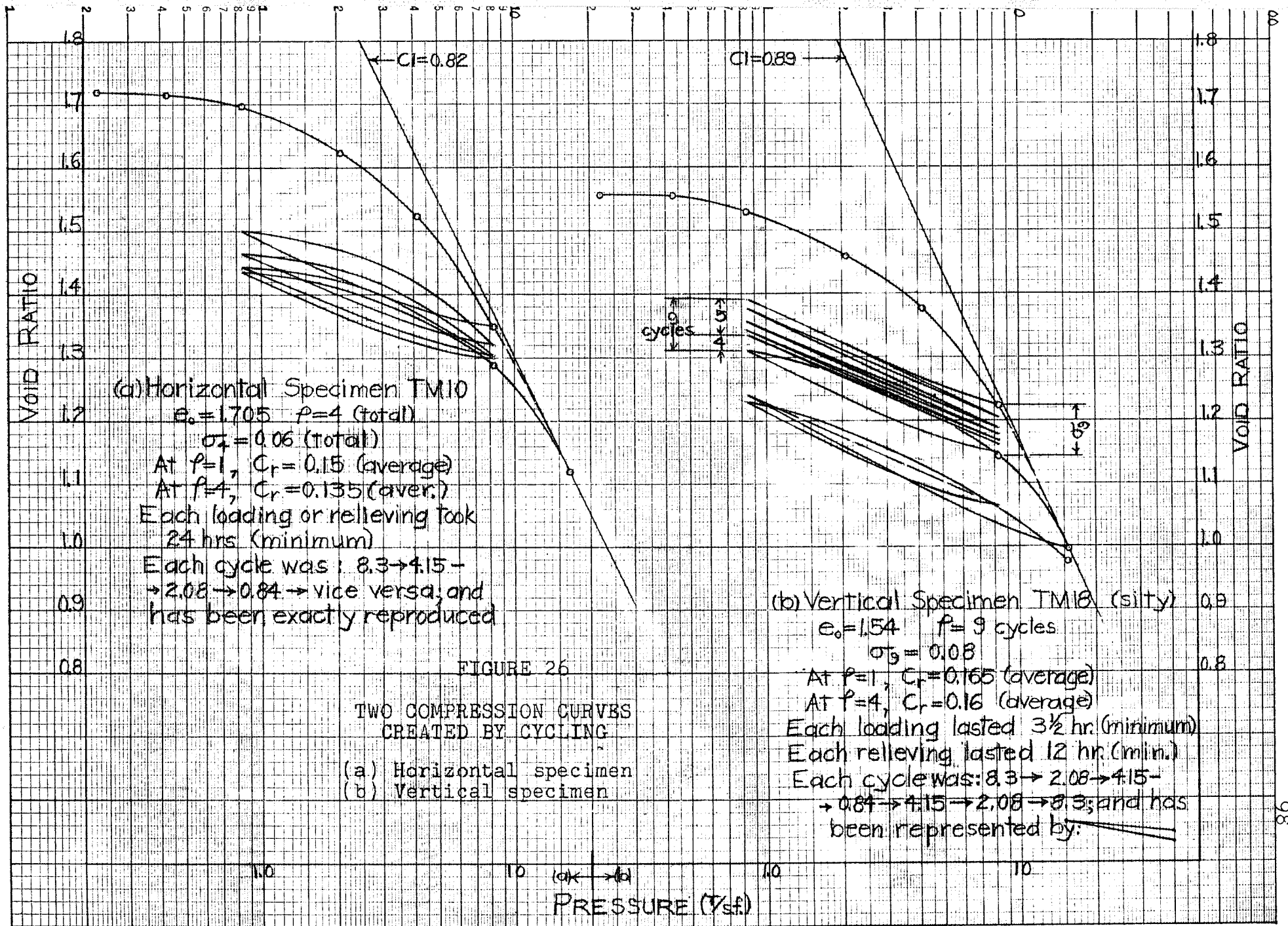
$e_0 = 1.815$

CI-Compression Index: 0.83
C_r-Swelling Index (aver): 0.245
Apparent Preconsolidation Pressure (p'₀): app 6 1/2 tf

Pressure (1/2sf)

FIGURE 25
TYPICAL COMPRESSION CURVE
FOR SPECIMEN TM 31





(a) Horizontal Specimen TM10
 $e_0 = 1.705$ $p = 4$ (total)
 $\sigma'_z = 0.06$ (total)
 At $p=1$, $C_r = 0.15$ (average)
 At $p=4$, $C_r = 0.135$ (aver.)
 Each loading or relieving took
 24 hrs (minimum)
 Each cycle was: 8.3 → 4.15 →
 → 2.08 → 0.84 → vice versa, and
 has been exactly reproduced

(b) Vertical Specimen TM10 (sity)
 $e_0 = 1.54$ $p = 9$ cycles
 $\sigma'_z = 0.08$
 At $p=1$, $C_r = 0.165$ (average)
 At $p=4$, $C_r = 0.16$ (average)
 Each loading lasted 3½ hr. (minimum)
 Each relieving lasted 12 hr. (min.)
 Each cycle was: 8.3 → 2.08 → 4.15 →
 → 0.84 → 4.15 → 2.08 → 0.84, and has
 been represented by:

FIGURE 26
 TWO COMPRESSION CURVES
 CREATED BY CYCLING
 (a) Horizontal specimen
 (b) Vertical specimen

sequence of the shift, the recompression branch would seem to be smoother and extend to a higher pressure.

Magnitude and Causes of Curve-shift. A plot of the curve-shift at 8.3 T/s.f., as compared with the number of cycles has been presented in Figure 27. The values for Figure 27 were obtained from Table IV, where the slopes of the rebound curves were listed too. A number of factors could have influenced this shift. They were;

- 1) the magnitude of the load increments,
- 2) the difference between the upper and lower limits of pressure in the loop (loading cycle),
- 3) the number of minor cycles within the major loop,
- 4) the magnitude of the highest pressure,
- 5) the irregularities of the sample.

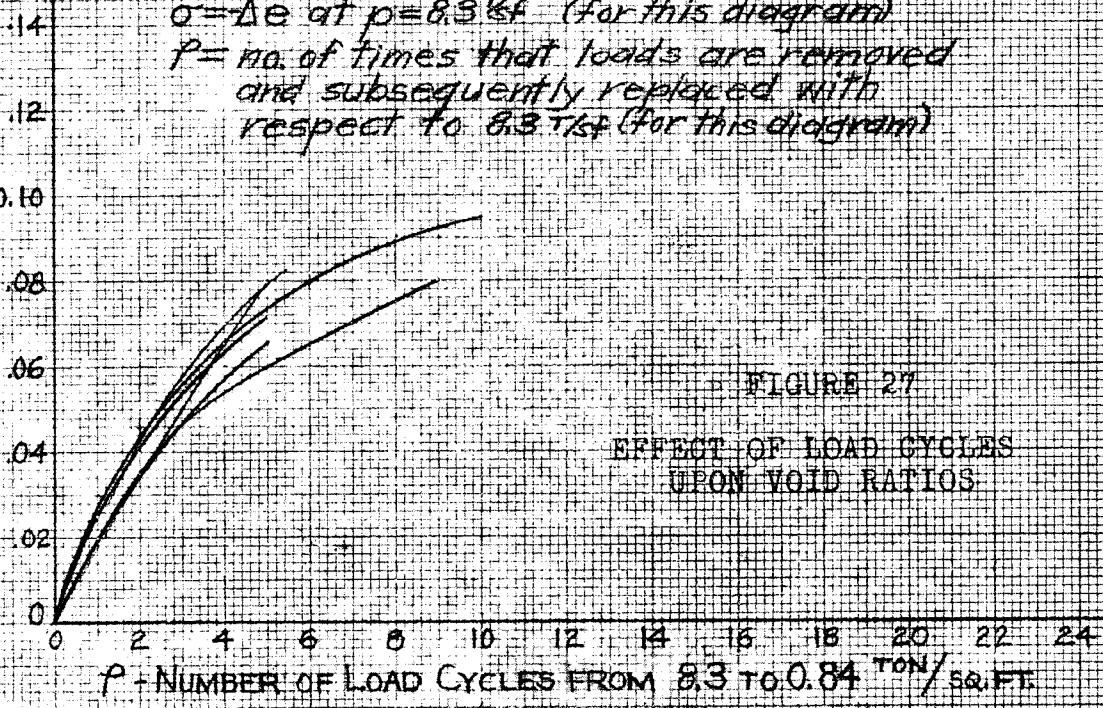
Samples TM 18 and TM 19 employed load increments that were twice as large as usual, although the number of loadings or unloadings remained the same throughout the loop; (example, 0.84 to 4.15 T/s.f., rather than 0.84 to 2.08 T/s.f.).

Figure 28 showed that the curve-shift for TM 18, a silty sample, coincided exactly with TM 17, another silty sample, but that TM 19 gave more shift. However, TM 19 was not as comparable as TM 18, because in TM 19 the loading was achieved so rapidly that usually complete swelling was not allowed, and as a result, greater shifting was anticipated. Moreover, the fact that TM 20, which had an extra large load increment (0.68 to 8.3 T/s.f), did not increase

IF SHEET IS READ THE OTHER WAY (VERTICALLY), THIS MUST BE LEFT-HAND SIDE.

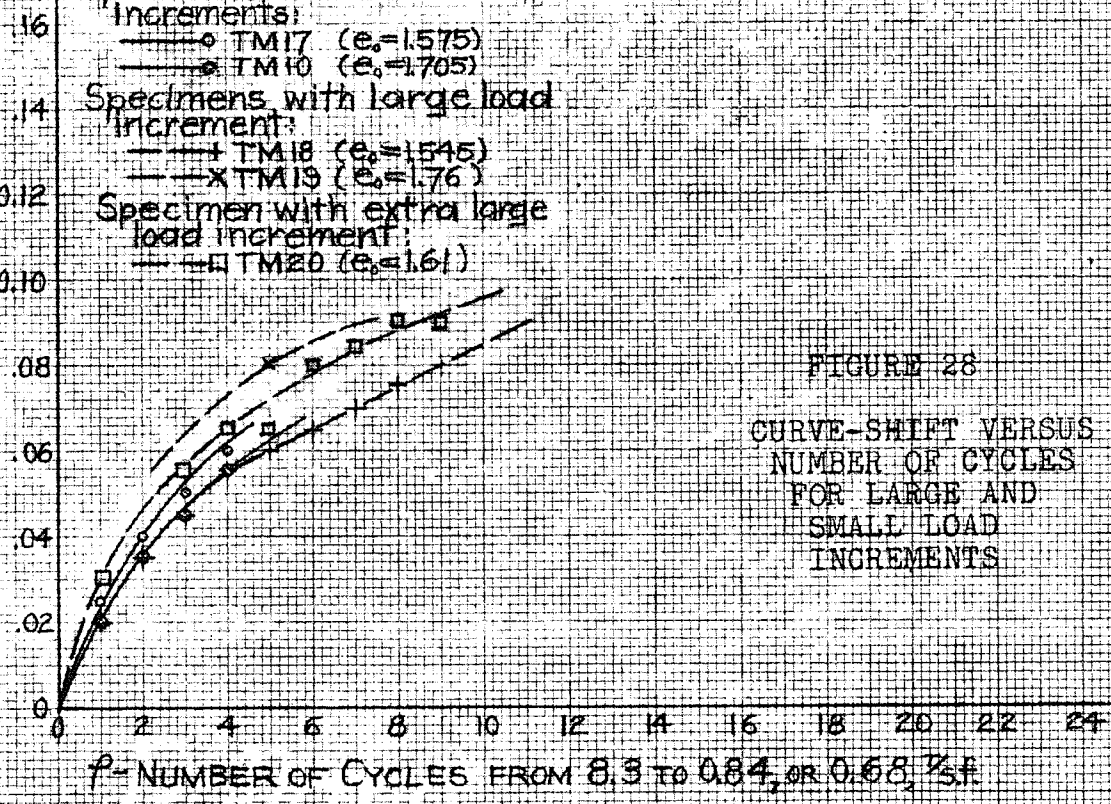
σ_c - CURVE-SHIFT
(Amount of downward displacement of the e -log p curve at 8.3% due to cycling)

$\sigma_c = \Delta e$ at $p = 8.3\% f$ (for this diagram)
 P = no. of times that loads are removed and subsequently replaced with respect to 8.3% f (for this diagram)



Specimens with usual load increments:
 —○— TM17 ($e_0 = 1.575$)
 —●— TM10 ($e_0 = 1.705$)
 Specimens with large load increment:
 —+— TM18 ($e_0 = 1.545$)
 —x— TM19 ($e_0 = 1.76$)
 Specimen with extra large load increment:
 —□— TM20 ($e_0 = 1.61$)

σ_c - CURVE-SHIFT AT 8.3% f



THIS MARGIN RESERVED FOR BINDING.

TABLE IV
EFFECTS OF CYCLING UPON VOID RATIO AND REBOUND

Specimen	Field void ratio %	Type of test	Remarks	Limits of cycle (T/s.f.)	No. of cycles p	Av. swell index Cr	Curve shift σ	e_p^a		
TM 1	1.805	poor test	horizontal direction	2.88-.295	1	.125	0	1.65		
TM 2	1.88	fair test	horizontal	2.88-.295	2	.12	.01	1.705		
TM 3	1.715	fair test	horizontal 18 hrs dried	2.88-.295	1	.125	.01	1.58		
					2	.125	.02			
TM 10	1.705	good test	horizontal silty	8.3 -.84	1	.15	.03	1.355		
					2	.145	.045			
					3	.14	.05			
					4	.135	.06			
TM 17	1.575	excellent	vertical silty fissured	8.3 -.84	1	.185	.02	1.23		
					2	.185	.035			
					3	.185	.045			
					4	.18	.055			
TM 18	1.545	excellent no secondary consolidation silty and fissured	vertical	16.6-.22	1/2	.21		1.02		
					8.3 -.84	1(1) ^b	.165	.02	1.23	
						2(3)	-	.035		
						3(4)	-	.045		
						4(6)	.16	.055		
						5(8)	-	.06		
						6(10)	-	.065		
						7(12)	-	.07		
						8(13)	-	.075		
						9(14)	.16	.08		
						16.6-.84	1(2)	.185		.02
							12(2 $\frac{1}{2}$)	.18		-

TABLE IV (continued)

Specimen	Field void ratio e_0	Type of test	Remarks	Limits of cycle (T/s.f.)	No. of cycles ρ	Av. swell index C_r	Curve shift σ	e_p^a
TM 19	1.76	excellent	vertical	8.3-.84	1/2	.24	-	1.36
			incomplete consolid'tn		4 1/2 (8)	-	.065	
			slightly silty and fissured		5 (9)	.21	.08	
				16.6-.22	1/2	.255	-	1.105
TM 20	1.61	excellent	vertical	8.3-.68	1	.18	.03	1.21
			silty and fissured		2	.18	.07 ^c	
					3	.195 ^c	.055	
					4	.17	.065	
					5	.17	.065	
					6	.17	.08	
					7	.17	.085	
					8	.165	.09	
					9	.165	.09	
			16.6-.68	1/2	.20	-	0.985	
TM 21	1.75	excellent	vertical	8.3-.84	1	.22	.025	1.385
			silty and		2	.22	.04	
			slightly fissured		3	.215	.055	
			2-1/2 hrs. dried		4	.215	.07	
				16.6-.415	1/2	.245	-	1.13
TM 22	1.46	excellent	vertical	8.3-.84	1	.16	.02	1.215
			small silt		2	.16	.035	
			and fissured		3	.16	.045	
			18 hours dried		4	.16	.055	
				16.6-.22	1/2	.18	-	1.05

a e_p represents the void ratio at the highest pressure in the loop from which the first cycle began.

b numbers in brackets represent the total number of cycles including subordinate cycles within the major loops.

c these values believed to be in error.

the shifting significantly, seemed to imply that the size of the load increment did not have a significant effect upon the magnitude of the curve-shift.

Sample TM 20 was permitted to swell more than one cycle of pressure (8.3 to 0.68 T/s.f.), and it was found that the shifting occurred slightly faster than in ordinary samples, although not significantly so, (see Figure 28, p.100). Consequently, it seemed that the magnitude of the relieving pressure, as compared to that from which relieving occurred, had no significant influence upon the rate of curve-shifting.

In Figure 29, it has been shown that the number of minor cycles within the major loop did not cause the curve-shifting to increase at all. Here, the shifting of specimens TM 18 and TM 19, which were both cycled within the major loops, was plotted against the total number of minor cycles (two minor cycles per major loop, approximately); whereas, the other specimens were plotted against the number of major cycles. The resulting curves for the two highly cycled specimens (TM 18 and TM 19) actually fell below those for the ordinary specimens. The indication was that the number of major loops that were formed was more important in the curve-shifting than was the total number of cycles.

In Figure 30 the curve-shift at $\rho = 4$ was plotted against the void ratio, either the field void ratio (e_0), or the value from which cycling was begun. The results of this figure were not very complete, but the indication seemed to be that the higher the pressure of consolidation from which cycling began, the greater was the amount of curve-shifting. Furthermore, it was noticed that higher void ratios at any pressure gave a slightly greater curve-shift.

Consequently, it would seem that the shift was almost wholly due to the magnitude of the highest pressure in the cycle. The reason for this was probably the secondary consolidation, which would be somewhat greater for larger pressures than for smaller ones. As a result, the shift at higher pressures would also be higher.

The only factor that could not have been considered, due to the great deal of time required for the analysis of this phenomenon, was the effect of the number of loadings and unloadings within a cycle. However, sample TM 20 had only one of each for each cycle, and because the fewer loadings did not yield less shifting as compared with the shifting by six loadings for other tests, it can be concluded that the greater number of loadings did not affect the curve-shift at all.

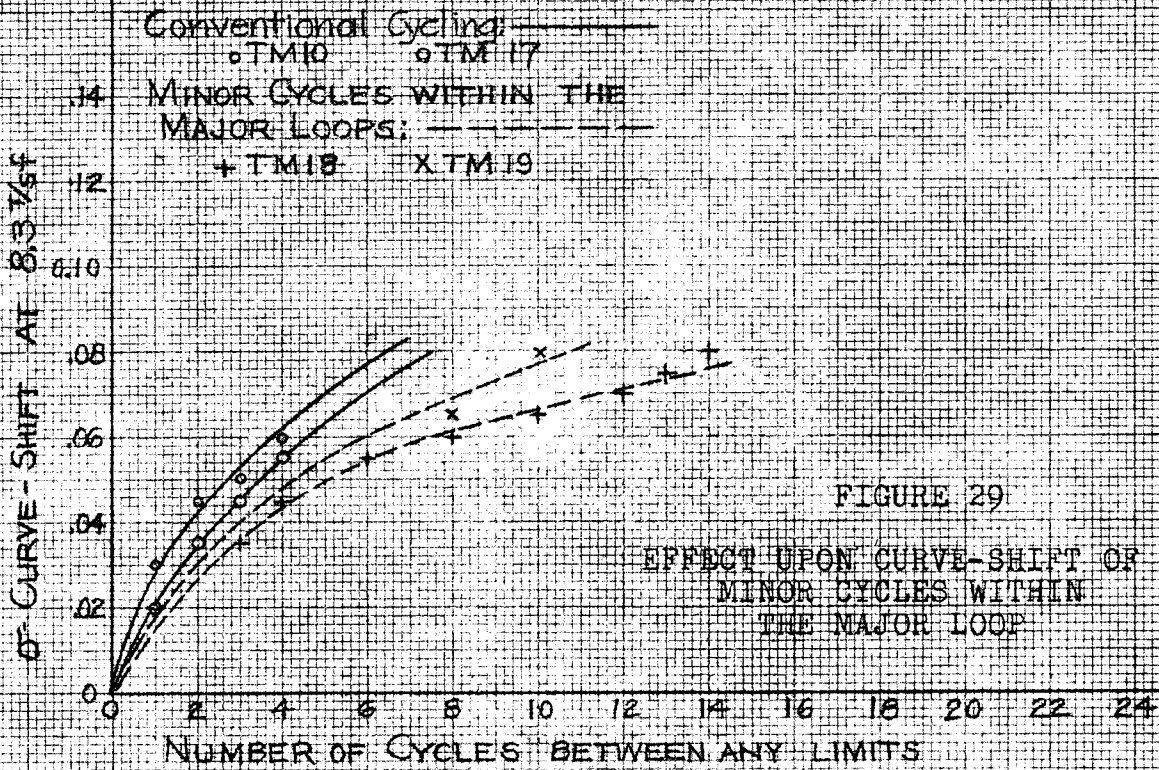
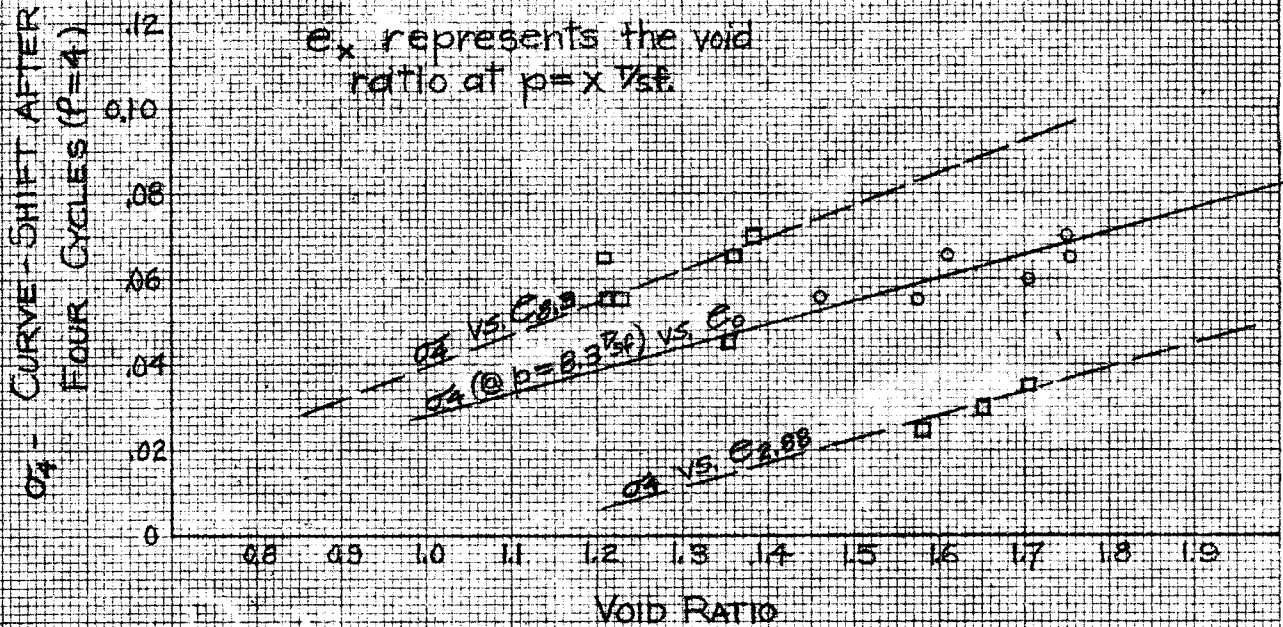


FIGURE 29

EFFECT UPON CURVE-SHIFT OF MINOR CYCLES WITHIN THE MAJOR LOOP

FIGURE 30
 EFFECT OF VOID RATIO UPON THE CURVE-SHIFT



IF SHEET IS READ THE OTHER WAY (VERTICALLY), THIS MUST BE LEFT-HAND SIDE.

THIS MARGIN RESERVED FOR BINDING.

Flaking of the Sample. Another possible cause for shifting which was not mentioned previously, because it is not a fundamental influence, was flaking. It was noticed that after a couple of cycles, almost all the samples began to peel off small flakes, which found their way into the surrounding medium of the consolidometer dishes. Because shifting had occurred prior to this, it was felt that this could not be a cause, although it could easily be a contributing factor. An attempt was made to ascertain what the error in the void ratio would be for sample TM 19, which seemed to be the sample with the largest amount of flaking.

weight of flakes = 0.03 grams (wet).

It was impossible to accumulate all the flakes, therefore, the aforementioned wet weight was considered to be the dry weight for all the flakes.

loss in height of solids due to flakes =

$$\frac{\text{weight of flakes (gms.)}}{G \times \gamma_w \times A(\text{sq. cm.}) \times 2.54} =$$

$$\frac{.03}{2.79 \times 1 \times 11.25 \times 2.54} = 0.0004''$$

therefore, $H_s = .2095 + 0.0004 = .210$

therefore, error in $d_e = \frac{.0400}{.2095} - \frac{.0400}{.2100} = 0.191 - .1905 \doteq 0.001$

This value is small and represented the most severe conditions. It may be seen that flaking had no effect upon the curve-shift.

Flattening of the Loops. An analysis of the average swelling index for each loop of all the samples indicated that as the number of cycles increased, the value of the swelling index decreased slightly. After nine cycles of sample TM 20, it had decreased from 0.18 to 0.165, and for sample TM 18, from 0.165 to 0.16, also after nine cycles. This decrease was small, but it seemed to indicate that some sort of flattening of the loops tended to occur as the number of cycles increased.

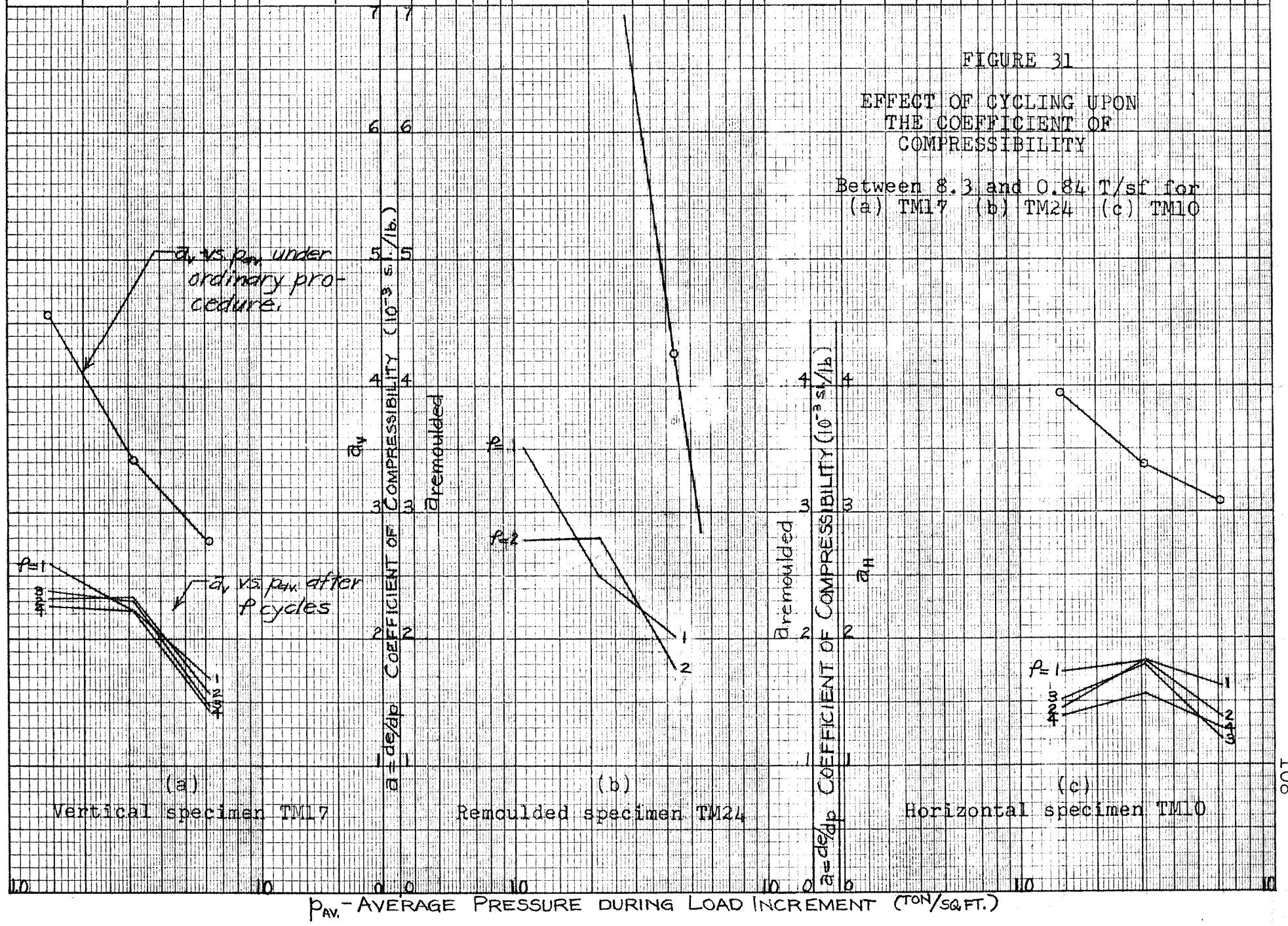
What the limit of either this flattening or of the curve-shift would have been, could not be ascertained, due to the small number of cycles performed in these analyses. To increase the number of cycles would have required a great deal of time.

Further evidence of flattening was shown in Figure 31, which is a plot of coefficient of compressibility (α) against the average pressure. It will be observed that (α) tended to decrease as the number of cycles increased. At the odd point this tendency was destroyed, due to the irregularities in the time allowed for consolidation. The value for the coefficient of compressibility as plotted in this diagram, combined the effects of both primary and secondary compression. Because the primary compression did not show this same tendency to decrease, it was concluded that the flattening was a product of the secondary compression.

FIGURE 31

EFFECT OF CYCLING UPON
THE COEFFICIENT OF
COMPRESSIBILITY

Between 8.3 and 0.84 T/sf for
(a) TM17 (b) TM24 (c) TM10



II. EFFECTS OF CYCLING UPON CONSOLIDATION CHARACTERISTICS

The relationships between the coefficients of consolidation and permeability, and the cycles, proved to be extremely erratic. No pattern was observed to exist.

Figure 32 indicated that the value of the coefficient of consolidation was sometimes higher, sometimes lower, and sometimes a combination of both in relation to the values obtained before cycling was begun. Specimen TM 10 was particularly unusual. The cause for the great variation in this result was the extreme variation in the time of 50% consolidation, because the thickness of the sample changed little and was, therefore, only a minor influence.

Like the coefficient of consolidation, the coefficient of permeability was similarly very erratic. The results of k with cycling were shown in Figure 33 for the three types of samples: vertical, horizontal, and remoulded. Because permeability is a function of the coefficient of consolidation, it was concluded that the vagaries in k can be attributed to the inconsistencies in the time of 50% consolidation.

In some cases the dissimilarities between the permeabilities during the cycles and the standard permeability relationship were rather small, and it was believed that they could lie within the range of experimental error.

FIGURE 32

EFFECT OF CYCLING UPON THE COEFFICIENT OF CONSOLIDATION

(a) TM17 (8.3 to 0.84 T/sf)

(b) TM10 (8.3 to 0.84 T/sf)

(a) Vertical specimen (TM17)

Time of 50% Consolidation (mins)

$\frac{P_2}{P_1}$	146	312	6.2	12.5
0	13.0	15	17	28
1	11.0	12.0	13.0	—
2	14.0	16	12.0	—
3	14.0	15	11.5	—
4	12.0	16	12.5	—

C_v - COEFFICIENT OF CONSOLIDATION (VERTICALLY)

C_v - COEFFICIENT OF CONSOLIDATION (VERTICALLY)

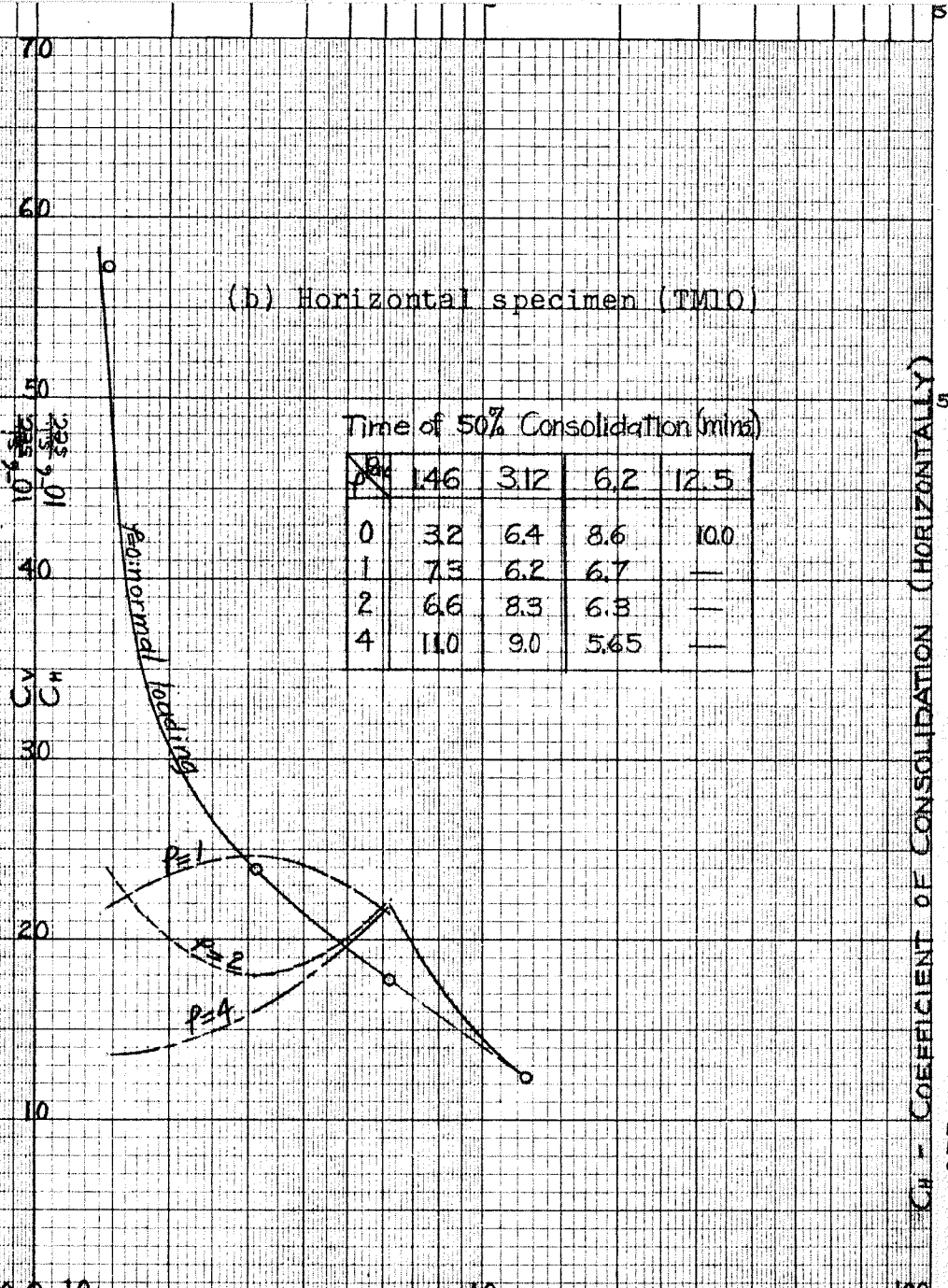
C_h - COEFFICIENT OF CONSOLIDATION (HORIZONTALLY)

P_{AV} - AVERAGE PRESSURE DURING CONSOLIDATION (T/s.f.)

(b) Horizontal specimen (TM10)

Time of 50% Consolidation (mins)

$\frac{P_2}{P_1}$	146	312	6.2	12.5
0	32	64	8.6	10.0
1	73	6.2	6.7	—
2	66	8.3	6.8	—
4	11.0	9.0	5.65	—



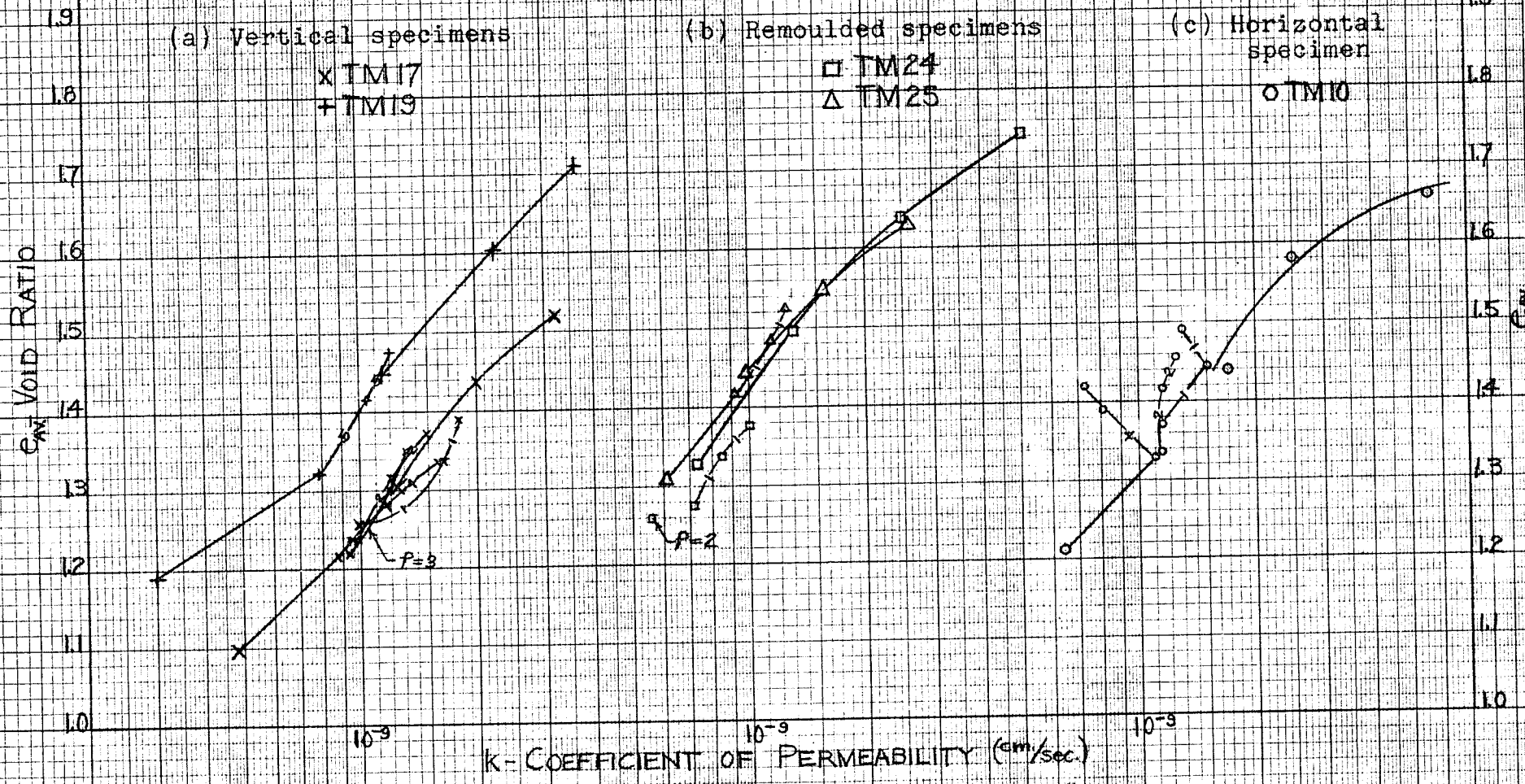


FIGURE 33

EFFECT OF CYCLING UPON THE
 COEFFICIENT OF PERMEABILITY

e vs k for normal loading ○—○
 e vs k during cycles ○— p —○

Therefore, an analysis of the experimental error for the fifth cycle and lowest load increment of sample TM 19 was made:

Due to the flatness of the test-time curve after a few

cycles, $E_t = \frac{2.5 \times 100}{18.5} = \pm 13.5\%$ which is an increase of 5% over the value under normal circumstances.

$$E_H^2 = \pm 0.2\%$$

$$E_C = \pm 13.7\%$$

also, due to the flatness,

$$E_a = .8\% + \frac{.0004 \times 100}{.0099} = \pm 4.8\%$$

therefore, $E_k = 13.7 + 4.8 + .2 = \pm 18.7\%$.

It will be noticed that the error in both C and k has been increased five per cent over what it would have been in an ordinary consolidometer test (see page 58). This large experimental error has explained the dissimilarities in all specimens except TM 10, in which the results were extremely unruly.

If TM 10 had agreed as closely as the other specimens, it could have been concluded that the cycling effect upon the consolidation characteristics was not large enough to overcome any experimental error, and consequently, that the consolidation characteristics were not influenced by cycling.

III. SUMMARY

Although cycling did not seem to have much effect upon the consolidation characteristics of a clay, it certainly influenced the compression properties. It caused progressively downward shifting of the compression curve (curve-shift), the extension of the recompression branch to a higher pressure, and a slight flattening of the hysteresis loops.

From the number of tests conducted, it would seem that the downward shifting is a function of the secondary consolidation under the heaviest load in the cycle, and that such factors as sample irregularities, size of load increments, and minor cycles within the major loops, did not appreciably affect the magnitude of the curve shift. However, these latter conclusions are nothing more than indicators of what might be the case, because the exigencies of time precluded an extensive analysis on this particular aspect of the thesis.

SECTION VIII

SWELLING PROPERTIES

In order to complement the research on cycling, this section was devoted to the study of swelling properties in a general way. This research provided values of the swelling index, which was useful in finding the preconsolidation pressure.

I. DETERMINATION OF SWELLING INDICES

Two samples, TM 26 and TM 27, having closely agreeing initial void ratios, were used to plot the swelling, or rebound, curves shown in Figure 34. It will be noticed that the rebound curves were not straight lines, but were concave at the lower ends for swelling from high pressures, and became convex beginning at the overburden pressure. These irregularities required some explanation.

Explanation of Rebound Curves. The existence of the concavity was probably due to friction.¹ The inflection at the preconsolidation pressure and the resulting convex curvature seem to be quite definite occurrences.

¹Donald W. Taylor, "Research on Consolidation of Clays," Massachusetts Institute of Technology publication of the Department of Civil and Sanitary Engineering, (1942), Serial 82.

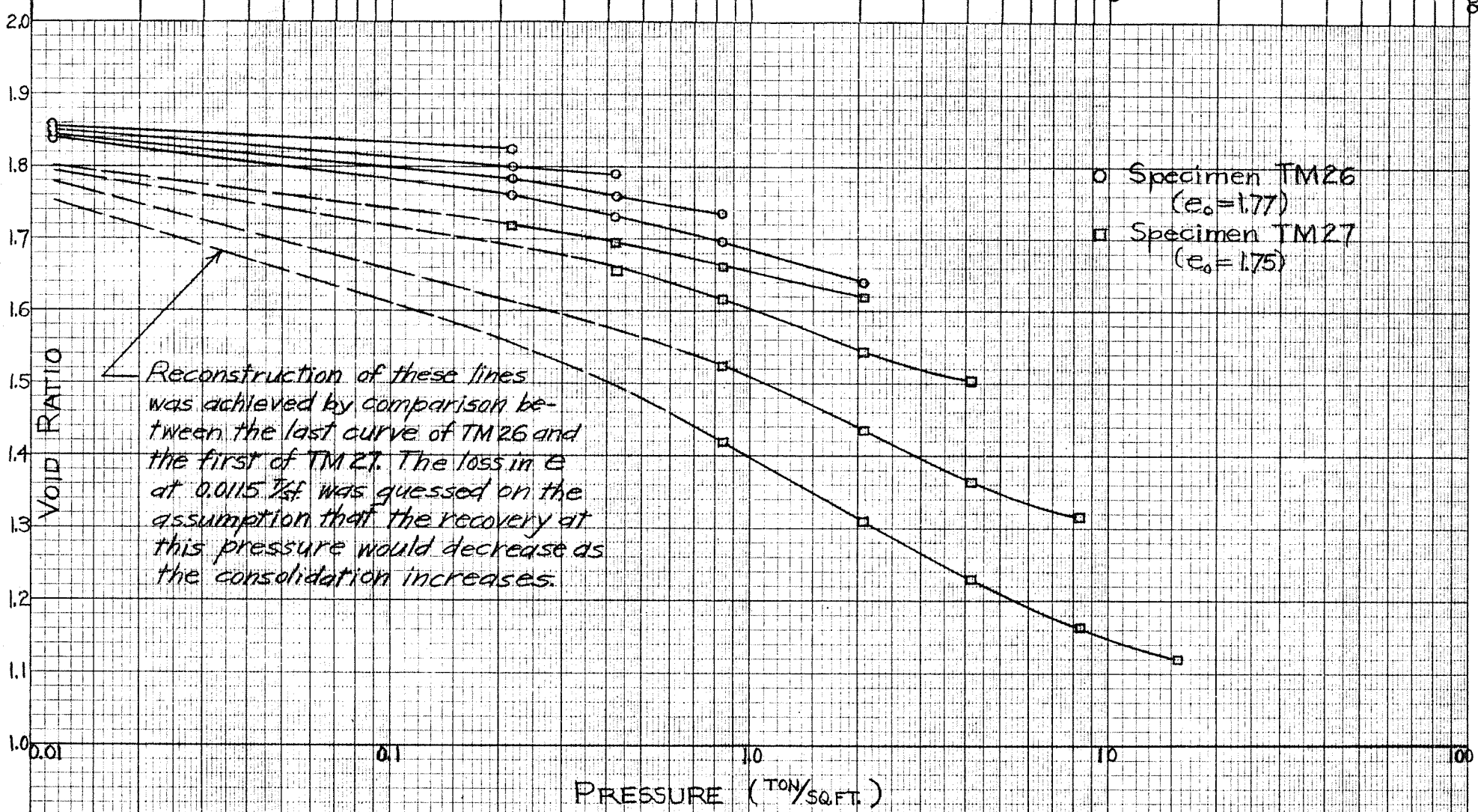


FIGURE 34
 REBOUND CURVES FROM
 VARIOUS VOID RATIOS
 (Vertical specimens)

The fact that this change appeared near the overburden pressure, implied that secondary consolidation was in some way a factor.

In order to explain this occurrence, it was necessary to consider the process of consolidation. During primary consolidation the load increment was transferred from the pore water to the granular and solid-liquid phase. This portion of the process was characterized by the expulsion of pore water, which permitted more intimate packing between the solid elements. For clays of dispersed structure, such as this one, most individual particles would have repelled one another.² Where an end to face type of contact occurred, such as is common in flocculated clays, the particles would have tended to bend and possibly rotate as primary consolidation was completed.

Then secondary consolidation occurred and was characterized by the adjustment of the system to the aforementioned electro-chemical and mechanical forces, which came into full play when primary consolidation had terminated. If the secondary consolidation were not permitted to occur, any particles that were influenced primarily by mechanical forces, would have sprung back almost elastically if the load had been released. In addition, the

²G. H. Bolt, "Physico-Chemical Analysis of the Compressibility of Pure Clays," Geotechnique, Vol. VI, No. 2, p. 86.

natural repulsion between the clay particles would have contributed to the resulting upheaval. The summation of the two was the observed swelling.

At pressures less than the overburden pressure, this flattening of the rebound curve has already occurred, because secondary compression in the field has had a great deal of time in which to develop fully. By comparison with pressures below the overburden pressure, the amount of secondary consolidation has been insignificant in the laboratory, even though the clay might have been overconsolidated a certain extent. Section VII has indicated that this clay has possibly not been preloaded at all. In either case, the rebound curves would have been very steep at these high pressures. However, in time, as the secondary consolidation progresses, these curves will flatten until they correspond with the rebound curves at pressures below p_0 . Thus, the flat portions of the curve would be the true rebound curves under field conditions, and the steep branches would only represent temporary conditions that occur in the laboratory.

Because this clay was not flocculated in structure, the effect of the mechanical forces in producing the steep part of the rebound curve was not as great as it would be in such clays. Nevertheless, it has been shown that a great deal of caution is required in analysing rebound

curves.

Swelling-time Curves. A possibility of incomplete swelling at the lower pressures might also have contributed to the flattening of the slope of the swelling curve. Therefore, it was necessary to study the swelling-time behaviour.

The swelling versus the logarithm of time relationships were plotted in Appendix B for samples TM 26 and TM 27. These curves resembled the compression-time curves insofar as they were mirror images. In Figure 35, some typical curves have been plotted for TM 26. It will be observed that for all the load increments involved in swelling, the upper change in curvature had been surpassed. The ensuing straight line seemed to continue forever, and consequently, it was very difficult to ascertain at what point swelling terminated.

A number of features have been observed in these plots. Firstly, the final straight line portion began at a later time whenever the relieving pressure was low; secondly, the slope of this line was steeper at such pressures. Finally, the higher the pressure of consolidation went before swelling, the longer it took to reach this straight line for any particular swelling increment. Consequently, it would seem that the total pressure-relief, that is to say, the difference between the consolidation

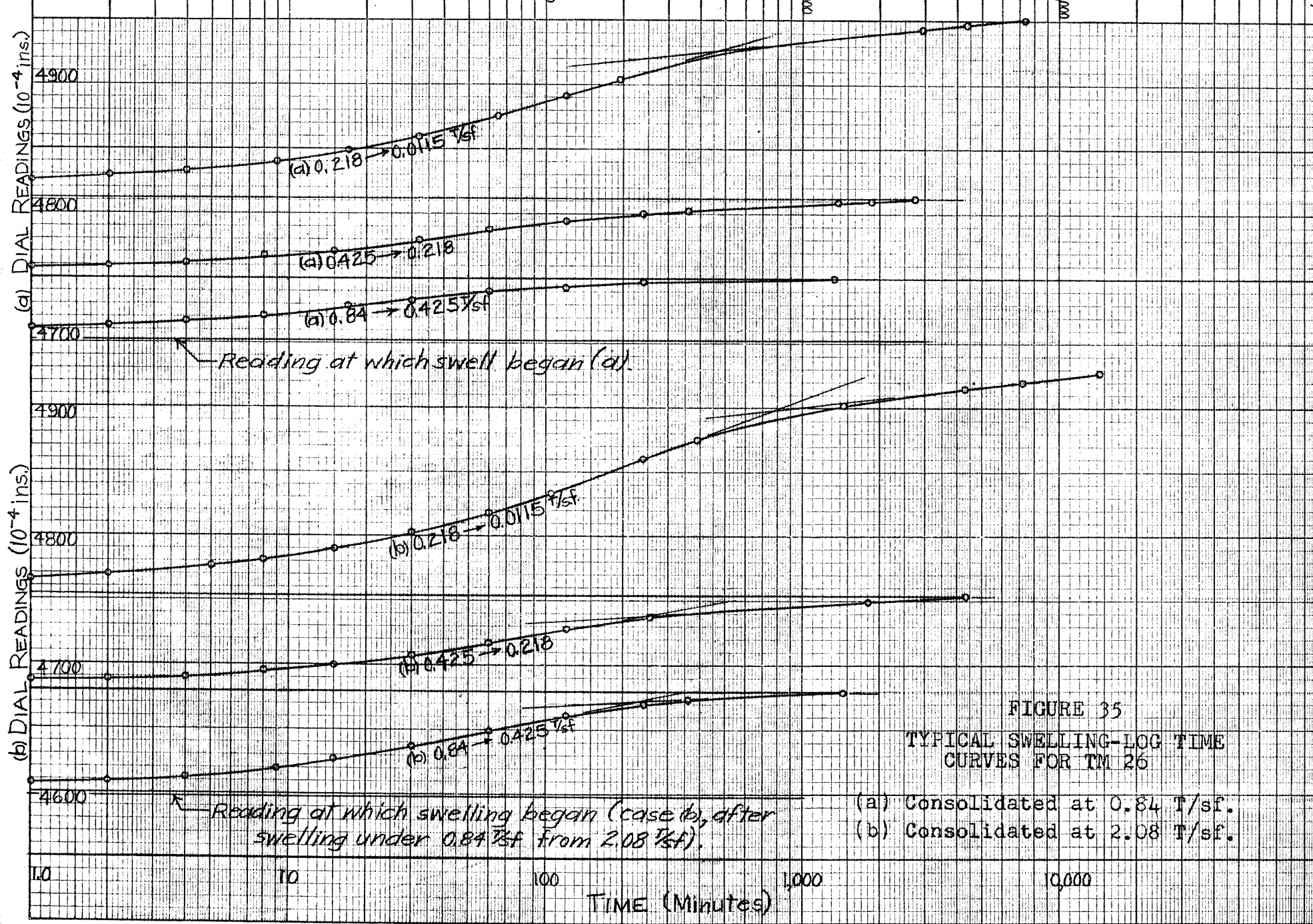


FIGURE 35
TYPICAL SWELLING-LOG TIME
CURVES FOR TM 26

- (a) Consolidated at 0.84 T/sf.
- (b) Consolidated at 2.08 T/sf.

pressure and relieving pressure, had a bearing upon the outcome of the swelling-time curves, as far as any particular swelling increment was concerned.

Figures 36 and 37 present the arithmetic and square root of time plots respectively. The latter resembled the compression-root-of-time-curve as would be expected. These curves showed more clearly that swelling was almost completed when the straight line portion on the log plot was reached, but the question still remained as to what constituted complete swelling.

The Swelling Index. Figure 38 shows three different values for C_r plotted against $\frac{e_r}{e_0}$. Curve 1 represents the average values of C_r ; curve 2 represents the steepest portion of the swelling curve, and curve 3 represents the flattest portion. Curves 1 and 3 were almost straight lines; however, curve 2 tended to show decreasing values for the swelling index when $\frac{e_r}{e_0}$ approached 0.75. Perhaps this fact indicates that at low void ratios the swelling index tends to become a fairly constant value.

All curves seemed to strike the zero-abscissa at e_r/e_0 between 1.09 and 1.10, meaning that the clay would not swell beyond a value of $e = 1.1e_0$.

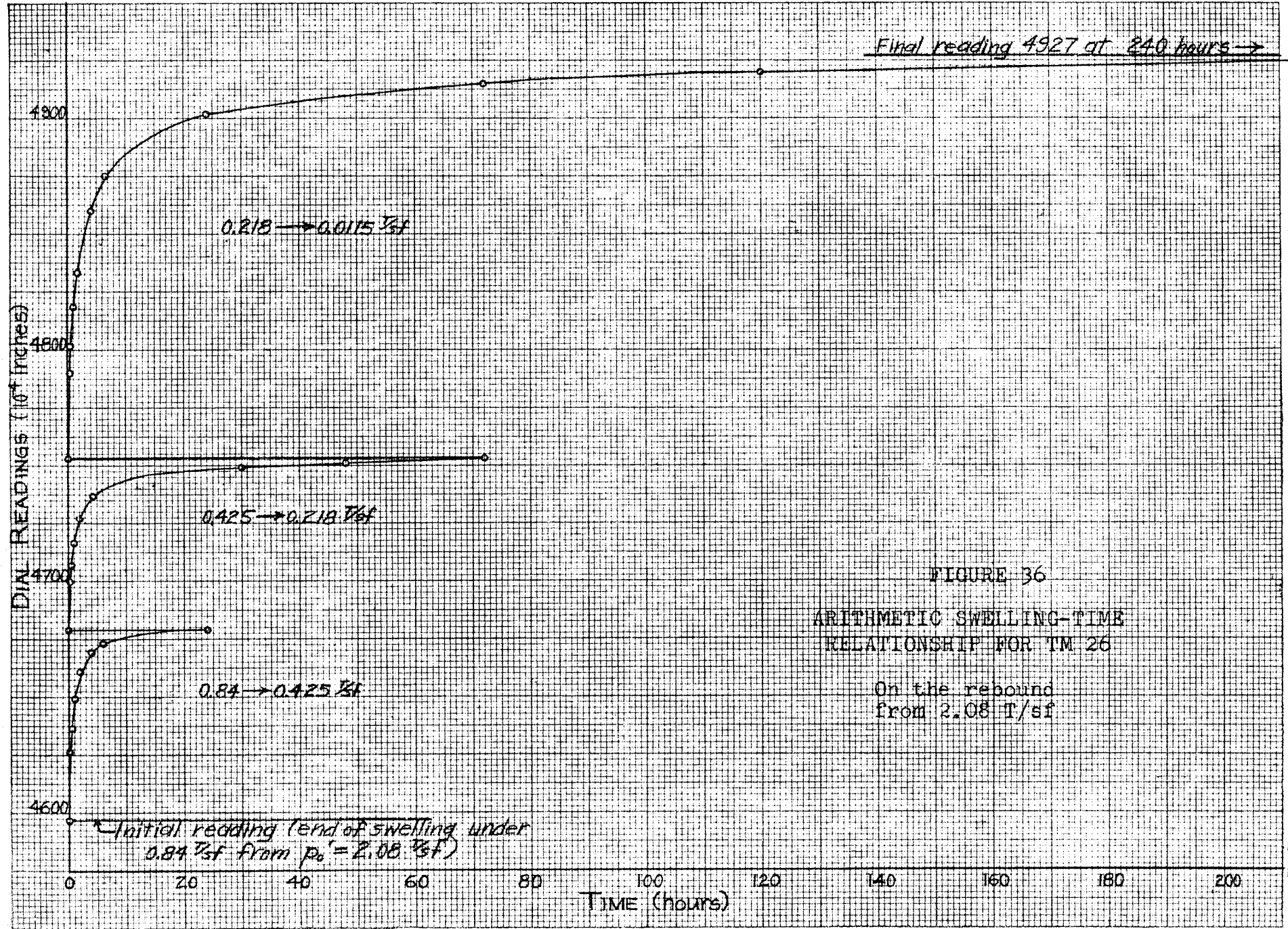


FIGURE 36
 ARITHMETIC SWELLING-TIME
 RELATIONSHIP FOR TM 26
 On the rebound
 from 2.08 T/sf

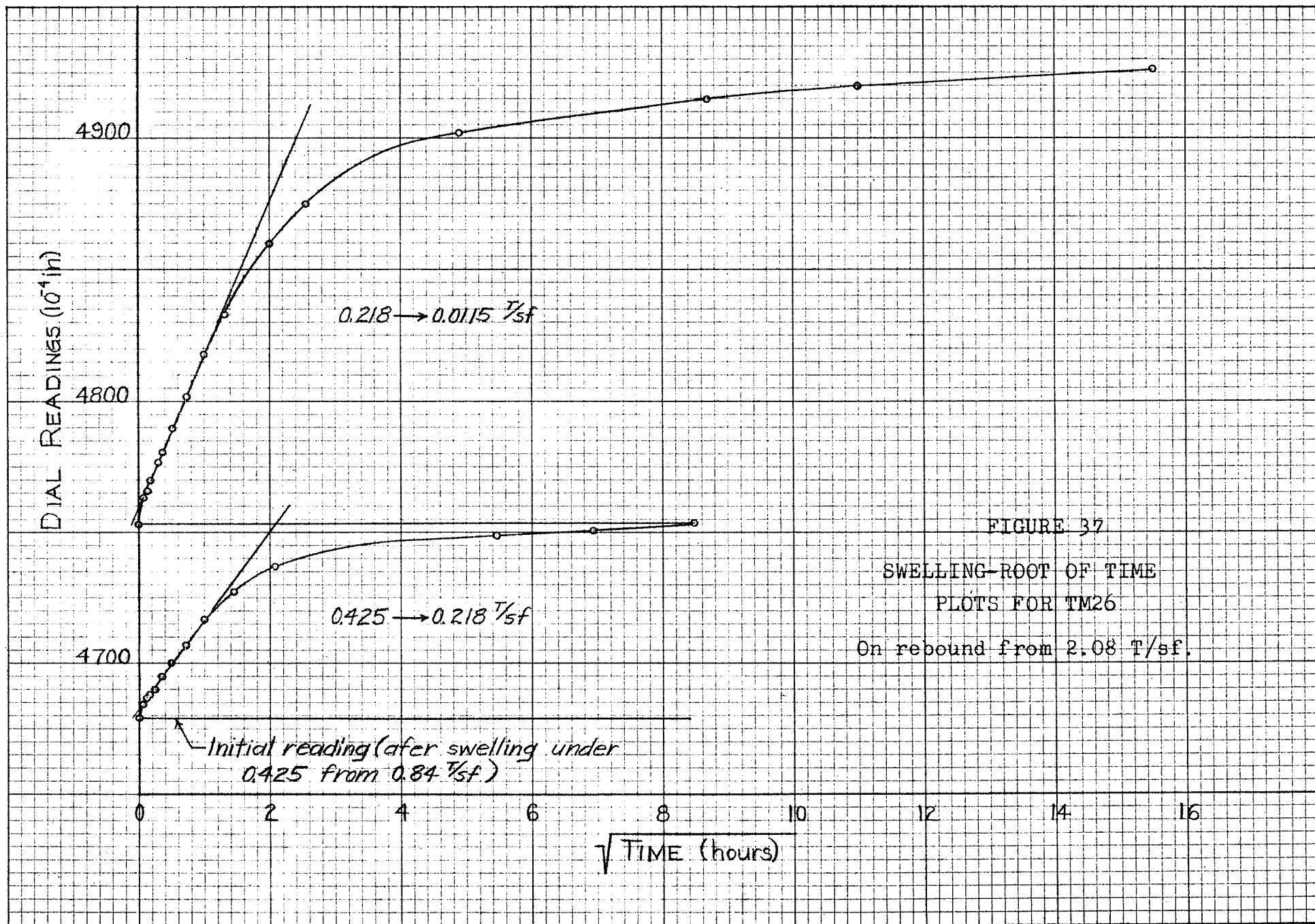


FIGURE 37
 SWELLING-ROOT OF TIME
 PLOTS FOR TM26
 On rebound from 2.08 T/sf.

FIGURE 38

SWELLING INDEX VS. e_r/e_0

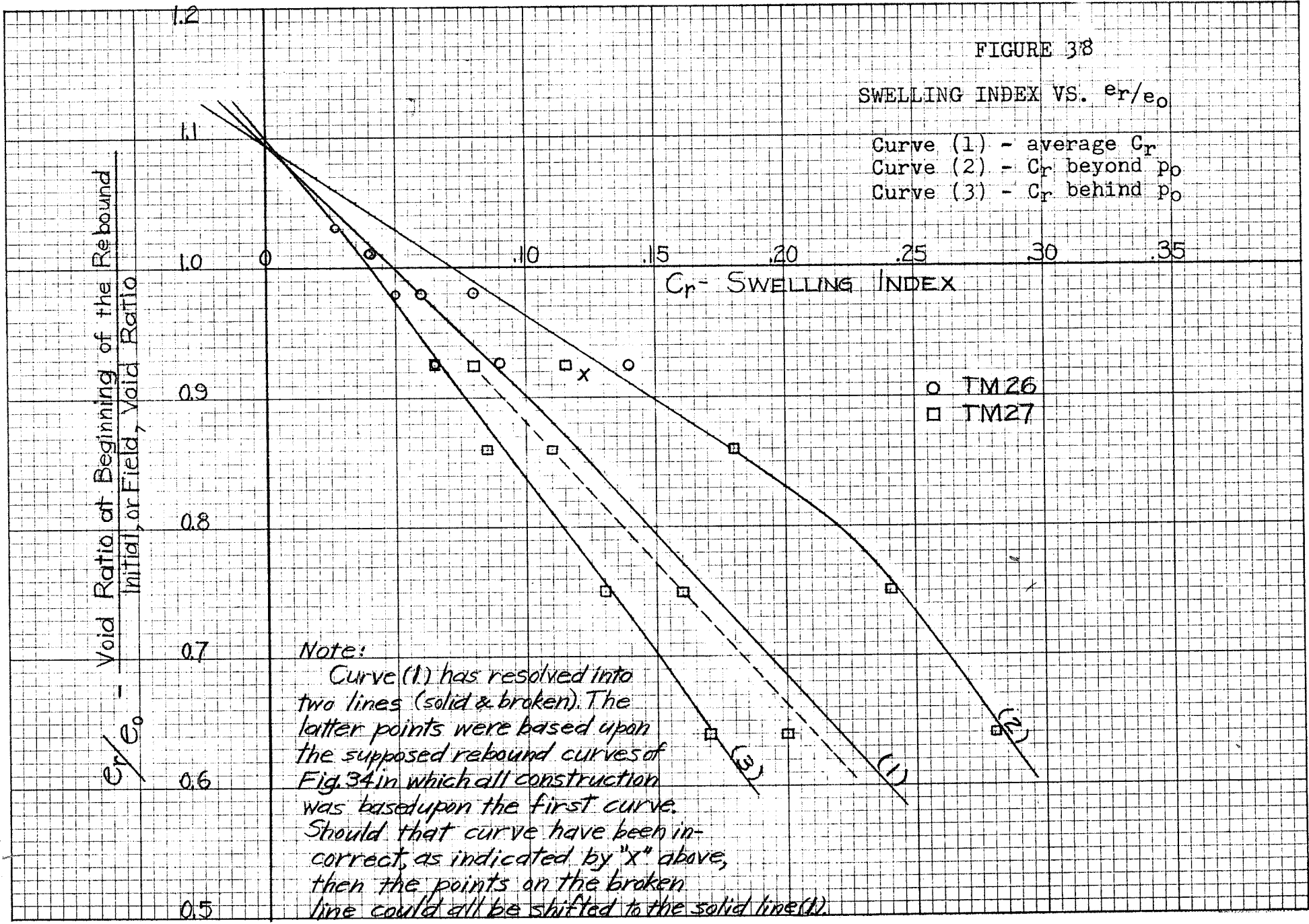
Curve (1) - average C_r
 Curve (2) - C_r beyond p_0
 Curve (3) - C_r behind p_0

e_r/e_0 - Void Ratio at Beginning of the Rebound
 Initial, or Field, Void Ratio

C_r - SWELLING INDEX

○ TM26
 □ TM27

Note:
 Curve (1) has resolved into two lines (solid & broken). The latter points were based upon the supposed rebound curves of Fig. 34 in which all construction was based upon the first curve. Should that curve have been incorrect, as indicated by "x" above, then the points on the broken line could all be shifted to the solid line (1).



II. FACTORS INFLUENCING SWELLING

The factors affecting the swelling-time curves have already been discussed. The remaining factors governing the swelling have also been considered hereafter in a general manner.

Sample Disturbance during Swelling. For sample TM 26 at zero load, the void ratio would be:

$$110\% \text{ of } 1.77 = 1.95.$$

However, tests on samples permitted to swell outside the consolidometer, TM 35 and TM 36, yielded void ratios under no load as high as 2.15 and 2.21 respectively, even though the initial void ratios were comparable to those of TM 26. The difference would presumably be attributed to disturbances or friction in the consolidometer that inhibited the swelling, even at a very low load. Thus, it would seem that the results for the swelling indices were probably somewhat low as they were given by the consolidometer, and greater swelling can be expected in the field under similar circumstances.

Cycling in the Field. Nothing significant could be observed to be caused by cycles insofar as swelling is concerned. Typical test time-curves for TM 17 and TM 20 are plotted in Appendix B, but the results are somewhat incon-

clusive. The only possible effect of cycling was the slight flattening of the rebound curve, which seemed to verify the contention that secondary consolidation has been responsible for the curve shift phenomena. This fact is more readily understood when it is recalled that on page 117 it was explained how secondary compression caused the rebound curve to flatten, as did the hysteresis loops of Section VII.

Orientation of Laminations. The results of swelling on saturated and partially dried specimens plotted in Figure 39 on page 126 seemed to indicate at first that horizontal swelling exceeded the vertical. However, the results for samples TM 35 and TM 36 showed that the swelling in the vertical direction was usually two to three times greater than that in the horizontal direction for samples permitted to swell freely in all directions from the undisturbed state. However, the trends also indicated that a situation in which the horizontal swelling could exceed the vertical, or at least equal it, might arise. This fact was demonstrated by an upward curving of the lines, comparing horizontal to vertical volume dimension increases, for TM 35 and TM 36. Moreover, specimens TM 28 and TM 29, vertical and horizontal specimens respectively, coming from the same position in the block of clay, swelled exactly equal amounts. Therefore, it was concluded that

FIGURE 39
SWELLING CAUSED
BY DESSICATION

PER CENT INCREASE IN VOIDS DUE TO SWELLING

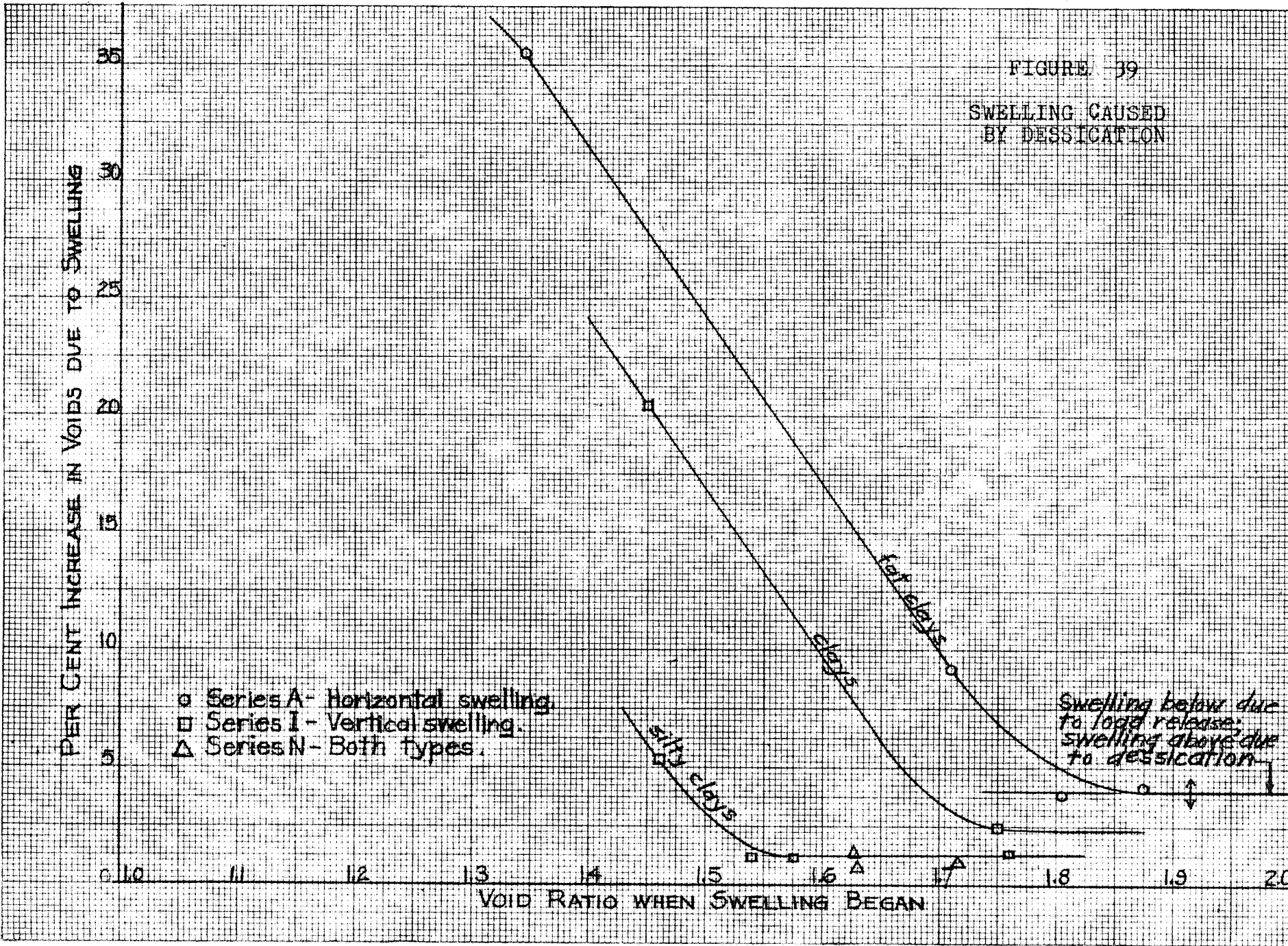
- Series A - Horizontal swelling.
- Series I - Vertical swelling.
- △ Series N - Both types.

Swelling below due
to load release;
swelling above due
to dessication

fat clays
silty clays

1.0 1.1 1.2 1.3 1.4 1.5 1.6 1.7 1.8 1.9 2.0

VOID RATIO WHEN SWELLING BEGAN



the apparently greater swelling of the horizontal samples, as shown by Figure 39, was actually a manifestation of the tremendous ability to swell by the clay minerals contained in samples used for series "A".

Drying of the Samples. Most samples that have been mentioned up to this point, were almost completely saturated, and accordingly, no effect of drying was to be expected in the swelling properties.

The results of attempts to find a relationship between the initial void ratio and swelling for partially dried clays are shown in Figure 39. The results were somewhat inconclusive, and consequently, not much can be said on their behalf.

III. SUMMARY

The following tentative conclusions were made as a result of the brief swelling analysis made in this section:

1. The slope of the rebound curve (C_r) increased as the void ratio (e_r) decreased.
2. The slope of the swelling curve flattened out when the relieving pressure was less than the overburden pressure, and this flattening was caused by secondary consolidation.
- 3a). Swelling for any particular increment took longer when the preconsolidation pressure was high.
- 3b). Increments of swelling at low pressures took longer to complete than those at high pressures.

4. No method exists to ascertain when complete swelling had occurred.
5. Sample disturbance in the consolidometer seemed to reduce greatly the total amount of swelling at very low loads.
6. Load cycles in the field did not seem to have a significant influence upon swelling, except to flatten the rebound curve a slight amount after numerous cycles. This observation verified the belief that secondary consolidation was a factor in the curve-shift during cycling.
7. The orientation of laminations did not seem to affect the swelling in certain cases, although in general, the vertical swelling should have exceeded that of the horizontal by two or three times.
8. Dessication of specimens caused a void ratio decrease which was regained when water was re-admitted, and caused large amounts of swelling to be observed.

SECTION IX

SUMMARY OF CONCLUSIONS

The general nature of this thesis prevented any definite conclusions from being made. Further research will be necessary on all the aspects before any general rules of behaviour of the local clay can be made. Furthermore, other local samples will require testing, to ensure that they follow the same trends as any one block of clay.

Nevertheless, some fairly conclusive remarks can be made;

- 1) The slope of the virgin compression branch was unaffected by the silt content, the amount that the sample swelled, the loading procedure, or the orientation of the laminations.

The average value for the compression index of the clay used was $0.83 \pm .05$.

- 2) Pockets or layers of silt, howsoever small they were, created two groups of specimens with distinctly different initial void ratios. The lower group, comprising silty specimens, yielded an average e_0 of $1.58 \pm 2.5\%$; the higher group yielded an average e_0 of $1.75 \pm 4\%$. The overall average of all samples was 1.72.

Silt did not affect the compression properties other than a downward displacement of the entire e -log p curve, but it did cause specimens to drain more freely in all directions.

- 3) The only method for determining the overburden pressure in a highly preloaded clay, or, in a clay highly disturbed by cycling, was with a no-swell type of test.

The overburden pressures for samples compressed para-

parallel to the laminations (horizontal specimens), were slightly lower than those for vertical specimens.

4. Taylor's fitting method was superior to that of Casagrande for this clay, although neither one could be described as being perfect.

In one case the value for the coefficient of consolidation by Taylor's method was 1.4 times as large as it was by Casagrande's method.

- 5) The errors for the coefficients of consolidation and permeability were respectively 8.5 and 13 per cent. The cycling caused the compression time-curves to flatten and produced errors of 13.5 and 18.5 per cent, respectively.
- 6) Horizontal permeability was twice as large as vertical permeability. The permeability of remoulded specimens was roughly an average of the horizontal and vertical permeabilities.
- 7) The swelling time-curves were mirror images of the compression time-curves, and produced slopes corresponding to the secondary consolidation slopes of the latter.
- 8) Swelling at low pressures required more time to finish, and the final slope (as mentioned in 7), was steeper. The greater the preconsolidation load, the longer swelling took at any particular load increment.

It may be definitely stated that a downward shifting of the compression curve was caused by the cycling of loads in the consolidation test. It has also been shown that flaking of the sample during the test was not a significant contributor to this shifting. Other indications regarding cycling were also discovered:

- 1) The major factor influencing the curve-shift seemed to be the magnitude of the highest pressure in the load-cycle. The higher the pressure, the greater was the shifting.

Furthermore, the greater the void ratio at which cycling began, the greater was the curve-shift.

- 2) Cycling did not seem to influence the consolidation characteristics.
- 3) The hysteresis loops produced by cycling seemed to flatten very slightly as the number of cycles increased.

Consolidation tests run in the triaxial cell did not prove to be very satisfactory. The difficulties of preventing leakage, of assembling the sample in the cell, and of controlling the pressure, proved to be very great indeed. The only definite conclusion regarding the measurements of the consolidation characteristics by this method was that radial drainage predominated, and that analysis on the basis of radial drainage yielded the correct values of k_h and C_h .

A number of unanswered questions regarding the triaxial method persisted:

- 1) How much seepage occurred through the membranes?
- 2) Why did the sample not swell under a low pressure from the undisturbed state?
- 3) Why did leakage seem to prolong the process of consolidation?
- 4) How much disturbance was created during the assembling of the specimen in the cell?
- 5) What were the true volume and dimension changes throughout the test?

Further research will be required in order to answer these questions, and to confirm the rather vague conclusions

regarding curve-shift. Before more investigation on curve-shift can be conducted, a criterion for defining complete swelling must be developed. It is to be hoped that the findings of this thesis will provide insight into these investigations.

BIBLIOGRAPHY

- Allan, H., and A. W. Johnson, "The Results of Tests to Determine the Expansive Properties of Soils," Proceedings Highway Research Board, Vol. 16, (1936).
- Alpan, I., "An Apparatus for Measuring the Swelling Pressure in Expansive Soils," paper 1a1, Proceedings of the Fourth International Conference on Soil Mechanics and Foundation Engineering, London, 1957.
- Barron, Reginald A., "Consolidation of Fine-Grained Soils by Drain Wells," Proceedings of American Society of Civil Engineers, No. 6, part 1, June, 1947, Vol. 73, p.811.
- Biot, Maurice A., "General Theory of 3-D Consolidation," Journal of Applied Physics, (1942), Vol. 12, p. 155.
- Bishop, Allan W., and D. J. Henkel, The Measurement of Soil Properties in the Triaxial Test, (Edward Arnold Ltd., London, 1957).
- Bolt, G. H., "Physico-Chemical Analysis of the Compressibility of Pure Clays," Geotechnique, Vol. VI, No. 2, (1956), p. 86.
- Carillo, N., "Simple Two and Three Dimensional Cases in the Theory of Consolidation of Soils," Journal of Mathematics and Physics, Vol. 21, (1942), pp. 1-5.
- Casagrande, A., "The Determination of the Preconsolidation Load and its Practical Significance," Proceedings First International Conference on Soil Mechanics, Cambridge, Mass., (1936), Vol. 3, pp. 60-64
- Cooling, L. F., and A. W. Skempton, "A Laboratory Study of London Clay," paper No. 5270, Journal of the Institution of Civil Engineers, Vol. 17, No. 3, January, 1942, p. 251.
- Finn, William D., and Bjorn Strom, "Nature and Magnitude of Swell Pressure," Proceedings Highway Research Board, Vol. 37, (1958)
- Gibson, R. E., and D. J. Henkel, "Influence of Duration of Tests at Constant Rate of Strain on Measured Drained Strength," Geotechnique, Vol. IV, (1954), pp. 6-15.

- Gibson, R. E., and Peter Lumb, "Numerical Solution of Some Problems in the Consolidation of Clay," Proceedings of The Institution of Civil Engineers, Vol. 2, No. 2, Part 1, (March, 1953)
- Grim, Ralph E., Clay Minerology, (McGraw-Hill Book Co. Inc.), 1953.
- Haefeli, R., "On the Compressibility of Preconsolidated Soil Layers," paper 1d4, Proceedings of Second International Conference on Soil Mechanics and Foundation Engineering, Vol. I, p. 42.
- Haefeli, R., and G. Amberg, "Contribution to the Theory of Shrinking," Proceedings Second International Conference on Soil Mechanics and Foundation Engineering, Vol. I, p. 13.
- Hamilton, J. J., and C. B. Crawford, "Improved Determination of Preconsolidation Pressure of a Sensitive Clay," Special technical publication No. 254, published by American Society for Testing Materials, of the Sixty-Second Annual Meeting Papers, (1959), p. 254.
- Heidema, P. B., "The Bar-linear Shrinkage Test and the Practical Importance of Bar-linear Shrinkage as an Identifier of Soils," Proceedings of the Fourth International Conference on Soil Mechanics and Foundation Engineering, London, 1957.
- Holtz, W. G., and H. J. Gibbs, "Engineering Properties of Expansive Clays," paper 516, Proceedings of A.S.C.E., Vol. 80, October, 1954.
- Koppejan, A. W., "A Formula combining the Terzaghi Load-Compression Relationship and Buisman Secular Time Effect," paper 1d8, Proceedings of Second International Conference on Soil Mechanics and Foundation Engineering, Holland, Vol. III.
- Lambe, T. W., "The Permeability of Fine-Grained Soils," Symposium on Permeability of Soils, presented to the Fifty-Seventh annual meeting of A.S.T.M., June 15, 1954. A.S.T.M. Special technical publication No. 163.
- Lambe, T. W., "The Structure of Inorganic Soil," Proceedings of A.S.C.E., 1953, Vol. 79, No. 315

- Langer, Karl, "The Influence of the Speed of Loading Increment on the Pressure Void Ratio Diagram of Undisturbed Laboratory Soils, Proceedings of the International Conference on Soil Mechanics and Foundation Engineering, No. D9, Vol. II.
- McDowell, Chester, "Interrelationship of Load, Volume Change, and Layer Thicknesses of Soils to the Behaviour of Engineering Structures," Proceedings Highway Research Board, Vol. 35, (1956).
- Mitchell, James K., "The Fabric of Natural Clays and its Relation to Engineering Properties," Proceedings Highway Research Board, Vol. 35, (1956).
- Naylor, A. H., and I. G. Doran, "Precise Determination of Primary Consolidation," paper 1d2, Proceedings Second International Conference on Soil Mechanics and Foundation Engineering, Vol. I, p. 34.
- Newland, P. L., and B. H. Allely, "A Study of the Consolidation Characteristics of a Clay," Geotechnique, Vol. X, No. 2, (June, 1960).
- Progress Report on Research on the Consolidation of Fine-Grained Soils, (1936). Proceedings of the International Conference on Soil Mechanics and Foundation Engineering, paper D14, Vol. II, p. 138
- Richart, F. E., Jr. "A Review of Theories for Sand Drains," paper #1301, Proceedings of A.S.C.E., Journal of Soil Mechanics and Foundations, Vol. 83, SM 3, (July, 1957).
- Rowe, P. W., "Measurement of the Coefficient of Consolidation of Lacustrine Clay," Geotechnique, Vol. IX, (1959). p. 107.
- Russell, Worsham and Andrews, "Influence of Initial Moisture and Density on the Volume Change of Typical Illinois Soils," Proceedings Highway Research Board, Vol. 26, (1946).
- Rutledge, P. C., "Relation of Undisturbed Sampling to Laboratory Testing," paper No.2229, A.S.C.E. Transactions, Vol. 109, (1944), p. 1155.
- Seed, H. B., and C. K. Chan, "Thixotropic Characteristics of Compacted Clays," Proceedings of A.S.C.E., Journal of Soil Mechanics and Foundations Division, paper 1427, Vol. 83, S.M.4, (Nov., 1957).

- Schmertmann, John H., "The Undisturbed Consolidation Behaviour of Clay," paper No.2775, Transactions of American Society of Civil Engineers, Vol. 120, (1955). p. 1201.
- Taylor, Donald W., Fundamentals of Soil Mechanics, (John Wiley and Sons, Inc., New York, 1948).
- Taylor, Donald W., "Research on Consolidation of Clays," Massachusetts Institute of Technology publication of the Department of Civil and Sanitary Engineering, 1942, serial 82.
- Terzaghi, Karl, "Undisturbed Clay Samples and Undisturbed Clays," Journal of the Boston Society of Civil Engineers, Vol.XXVIII, No. 3, (July, 1941).
- Terzaghi, Karl, Theoretical Soil Mechanics, (John Wiley and Sons, Inc., New York, 1943).
- Van Zelst, T. W., "An Investigation of the Factors Affecting Laboratory Consolidation of Clay," Proceedings of Second International Conference on Soil Mechanics and Foundation Engineering, paper 11c4, Vol. VII, p. 52.
- Ward, W.H., S.G.Samuels, and Muriel E. Butler, "Further Studies of the Properties of London Clay," Geotechnique , Vol. IX, (1959).
- Warkentin, Dr. B. P., and M. Bozozuk, "Shrinking and Swelling Properties of Two Canadian Clays," unpublished bulletin prepared as submission to the Fifth International Conference of Soil Mechanics and Foundation Engineering to be held in Paris, July, 1961. (July, 1960).

APPENDIX A

DESCRIPTION OF TEST SERIES

APPENDIX A

TESTING SERIES

A summary of the series, the object of each, the date performed, and the specimens involved, are as follows:

"A" series. To study the effects of drying upon swelling in the horizontal direction.

Dec., 1959, (poor tests, because apparatus compression was not considered).

- TM 1 chocolate-clay.
- TM 2 chocolate-clay.
- TM 3 chocolate-clay air dried 18 hours.
- TM 4 chocolate-clay air dried 74 hours.

"B" series. To study the effects of cycling in the horizontal direction (parallel to laminations).

June, 1960, (fair tests, because laminations at slight angle to trimming of sample).

- TM 10 chocolate-clay with silt pocket at one end of the sample.

"C" series. To run two tests in the horizontal direction at right angles to one another.

July, 1960, (fair tests).

- TM 7 chocolate-clay.
- TM 8 chocolate-clay.

"D" series. To compare the effects of a no-swell test in the horizontal direction with a standard consolidometer test.

July, 1960, (fair tests)

- TM 6 chocolate-clay with visible silt pockets,
swelling restricted.
- TM 9 as above, fissured with free-swelling in a
standard test.

"E" series. To study the effects of remoulding at
various moisture contents upon the consolidation character-
istics.

(good tests).

- TM 5 August, 1960, remoulded at a high moisture con-
tent
- TM 24 Dec., 1960, sample remoulded by kneading at
slightly above field moisture content.
- TM 25 Dec., 1960, remoulded by kneading at less than
the field moisture content.

"F" series. To find the compression characteristics
in the vertical direction under various types of loading in-
crements.
August, 1960, excellent tests, (all chocolate-clay samples).

- TM 11 a load greater than the overburden pressure
immediately applied.
- TM 12 swelling permitted as usual; then a load
greater than the overburden pressure applied.
- TM 13 standard test.
- TM 16 no-swell test.

"G" series. To find the consolidation characteristics
in a horizontal direction with specimens near those ob-
tained for the "F" series.

August, 1960, excellent tests, chocolate-clay samples.

- TM 14 parallel to X-X axis.
- TM 15 slightly fissured, parallel to Y-Y axis.

"H" series. To study the effects of cycling in the
vertical direction.

Dec., 1960, excellent tests.

- TM 17 chocolate-clay with small silt pockets. This sample cycled in conventional manner, i.e., swelling was treated in the same manner as compression.
- TM 18 as for 17. Unconventional cycling was used, e.g. the loads on the pan were in sequence 2, 10, 5, 20, 5, 10, and 2 again. It was hoped in this manner to make the effects of cycling visible twice as fast.
- TM 19 chocolate-clay, the cycling was similar to that of 18, except that the loading was performed rapidly, and in many cases 100% consolidation was not achieved. It was hoped by this method to accelerate the manifestations that accompany cycling.
- TM 20 chocolate-clay with visible silt pockets. The cycling loads were from 2 to 25 to 2 again.

"I" series. To study in conjunction with series "H" the effects of air drying upon the swelling.

Sept., 1960. excellent tests.

- TM 21 chocolate-clay with silt pockets 2-1/2 hours air dried.
- TM 22 chocolate-clay with silt pockets 18 hours air dried.
- TM 23 chocolate-clay with silt pockets 74 hours air dried.

"J" series. To determine the swelling curves in a vertical direction.

Dec., 1960, excellent tests.

- TM 26 chocolate-clay allowed to swell under no load.
- TM 27 chocolate-clay allowed to swell against the brake, after which it was loaded quickly to 2.08 T/s.f., as in a no-swell test.

"K" series. To study the horizontal and vertical swelling characteristics together.

Jan., 1961, excellent tests.

- TM 28 nuggety, mottled, brown-grey clay sample parallel to the vertical axis.
 TM 29 nuggety, brown-grey clay sample parallel to the horizontal axis.
 TM 30 nuggety, mottled brown-grey clay with visible silt pockets parallel to the vertical axis and slightly air dried.
 TM 32 chocolate-clay parallel to the vertical axis.

"L" series. To study the tri-dimensional swelling and shrinkage processes on samples independently of the consolidometer by measuring dimension alterations with deflection dials (vertical changes) and calipers (diametrical changes).

Dec., 1960, good tests (all chocolate-clay).

- TM 33 shrinkage specimen.
 TM 34 shrinkage specimen.
 TM 35 swelling specimen.
 TM 36 swelling specimen.

"M" series. To study the swelling and consolidation characteristics in the triaxial cell.

Dec., 1960, poor tests.

- TM 37 sample failed.
 TM 38 excessive leakage.
 TM 39 chocolate-clay, fairly good sample.

"N" series. To study the compression and consolidation characteristics in a vertical direction on an excellent sample at high pressures.

Feb., 1961.

- TM 31 chocolate-clay.

Unless otherwise specified, the foregoing series were all consolidometer tests of the standard kind. Only the "L" and "M" series were not consolidometer tests.

APPENDIX B

ADDITIONAL SWELLING-TIME CURVES

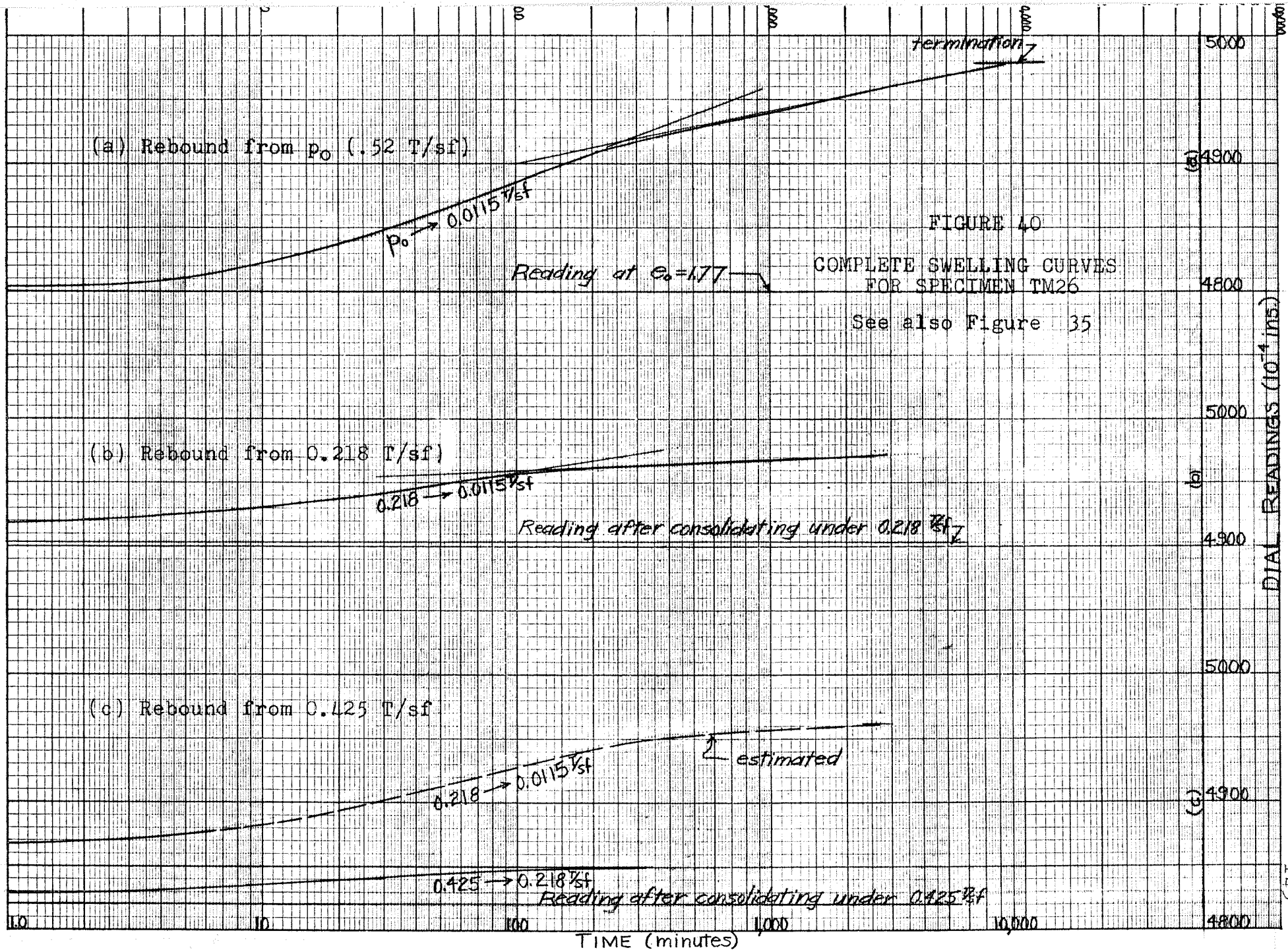


FIGURE 40

COMPLETE SWELLING CURVES
FOR SPECIMEN TM26

See also Figure 35

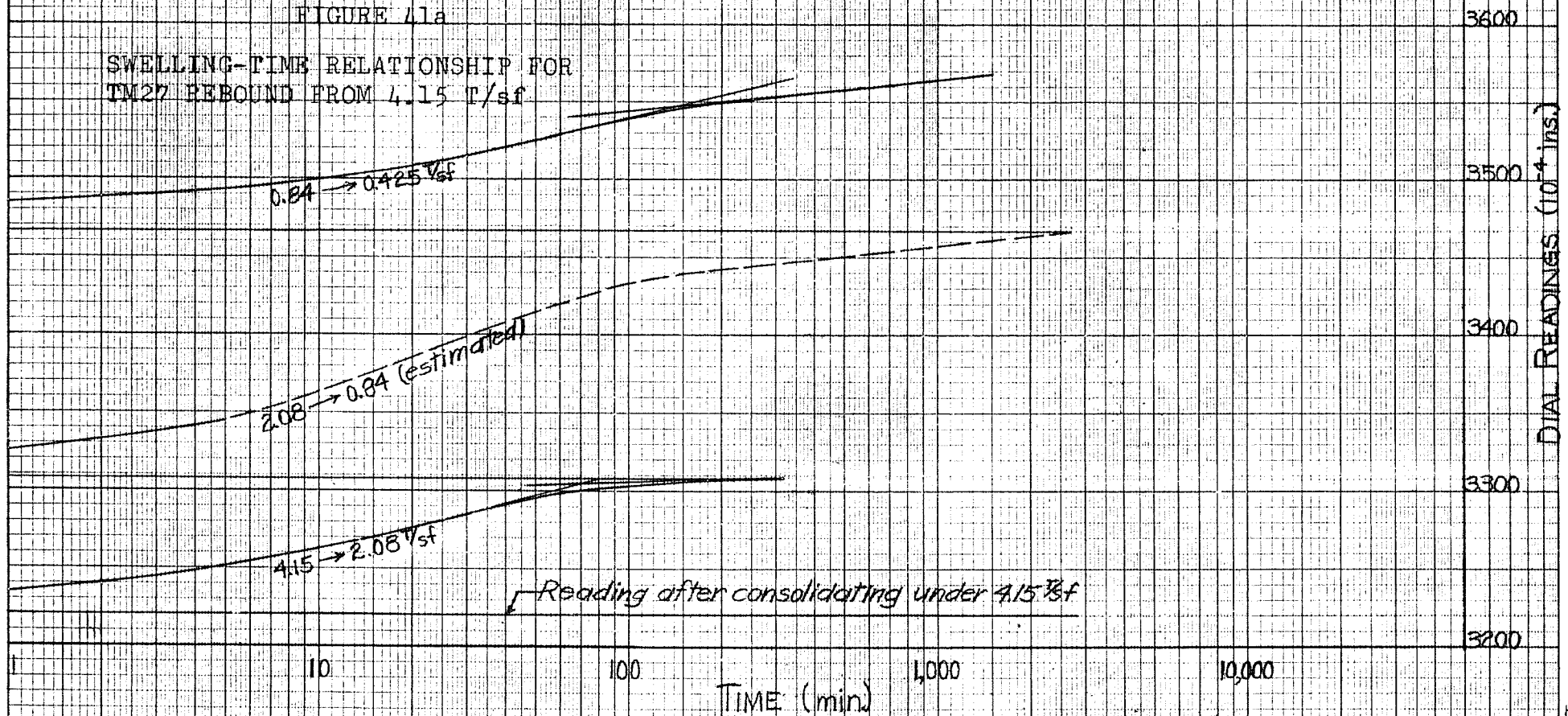
FIGURE 4J

COMPLETE SWELLING CURVES
FOR SPECIMEN TM 27

- (a) Rebound from 4.15 T/sf
- (b) Rebound from 8.3 T/sf
- (c) Rebound from 16.6 T/sf

FIGURE 4Ja

SWELLING-TIME RELATIONSHIP FOR
TM27 REBOUND FROM 4.15 T/sf



DIAL READINGS (10^{-4} ins.)

TIME (min)

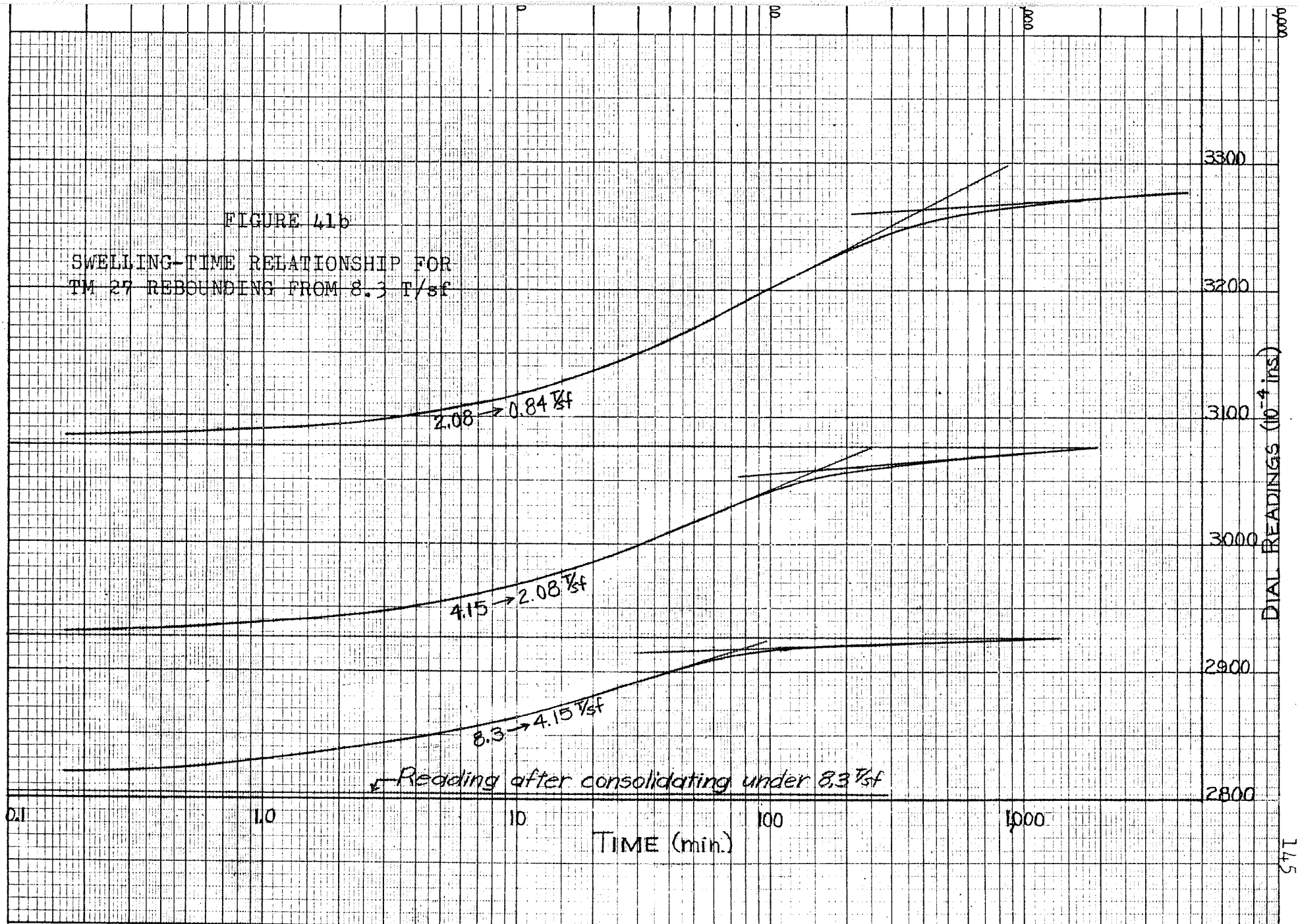


FIGURE 41c

SWELLING-TIME RELATIONSHIP FOR
TM 27 REBOUNDING FROM 16.6 T/sf

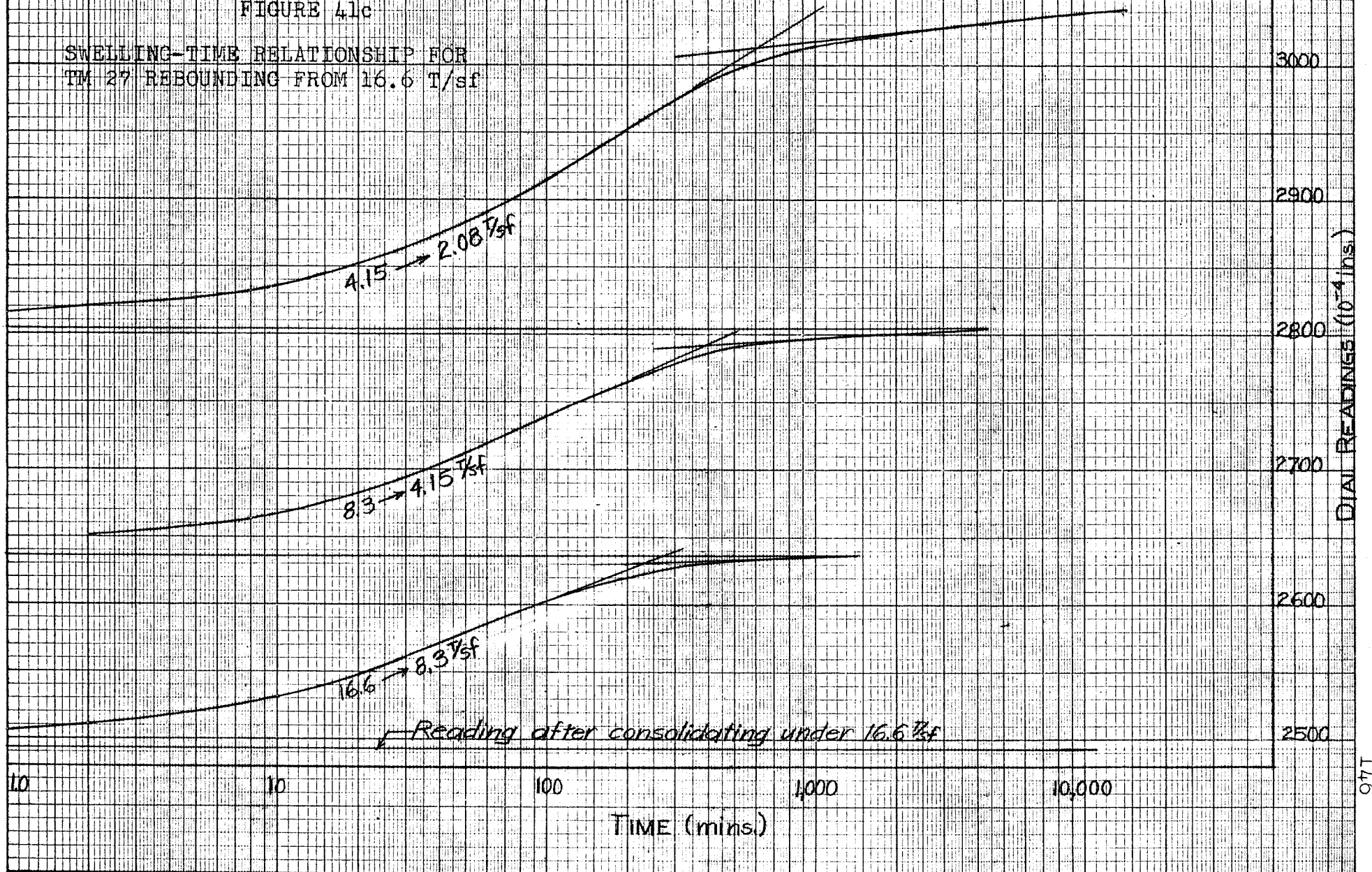


FIGURE 4.2

TWO SETS OF SWELLING CURVES
FOR TM 17 DURING CYCLES
(a) $\rho=1$ (b) $\rho=3$

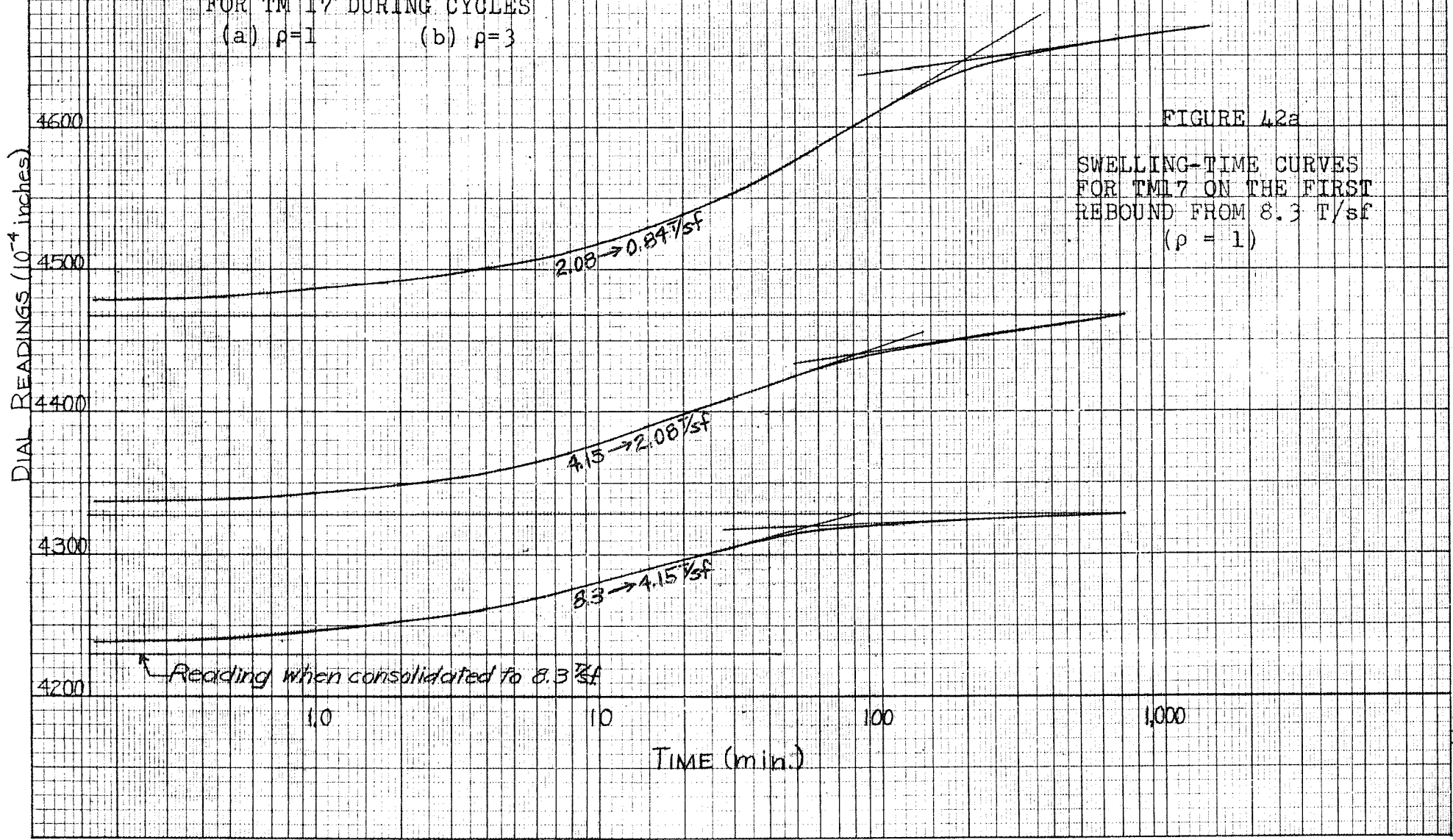
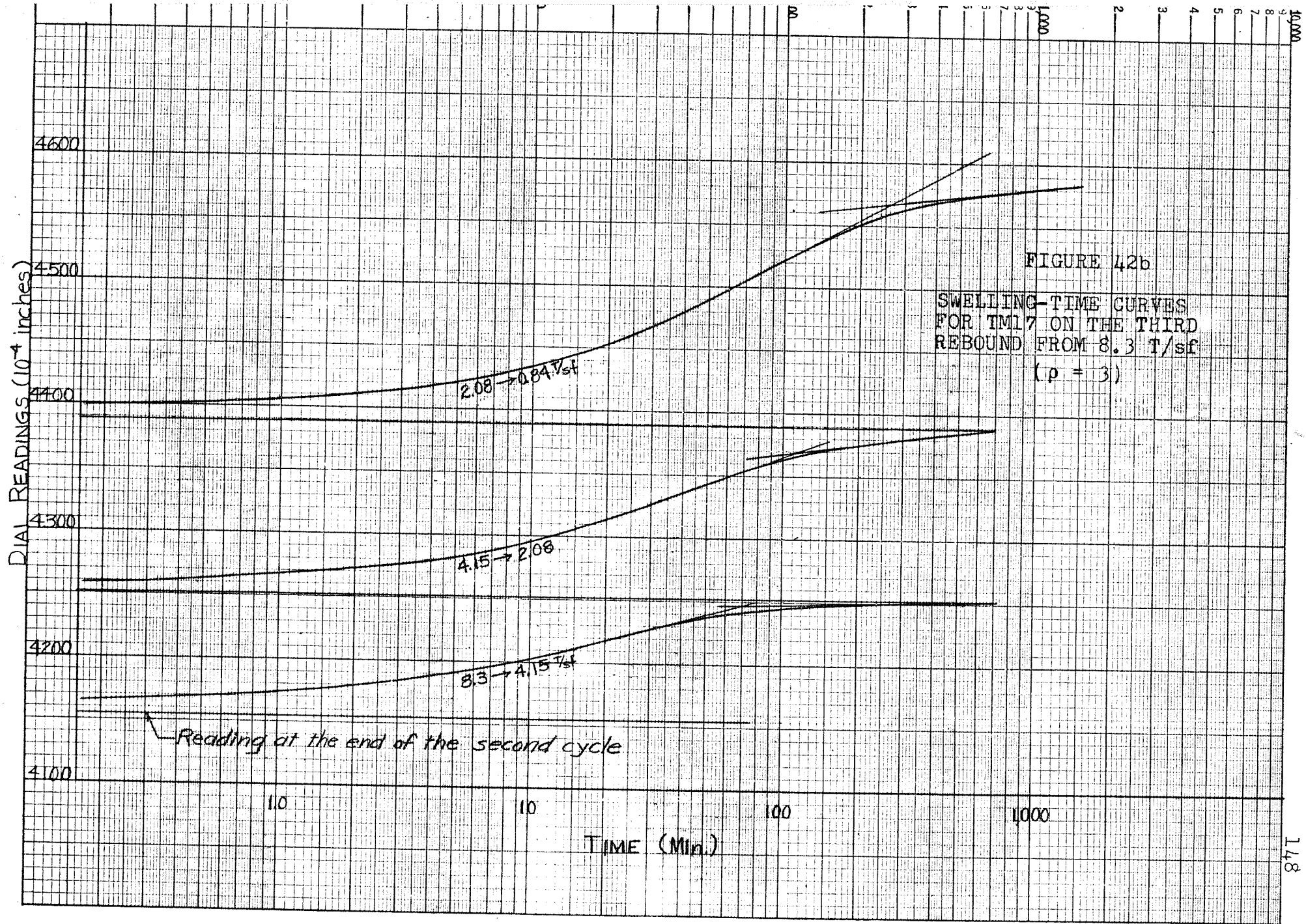
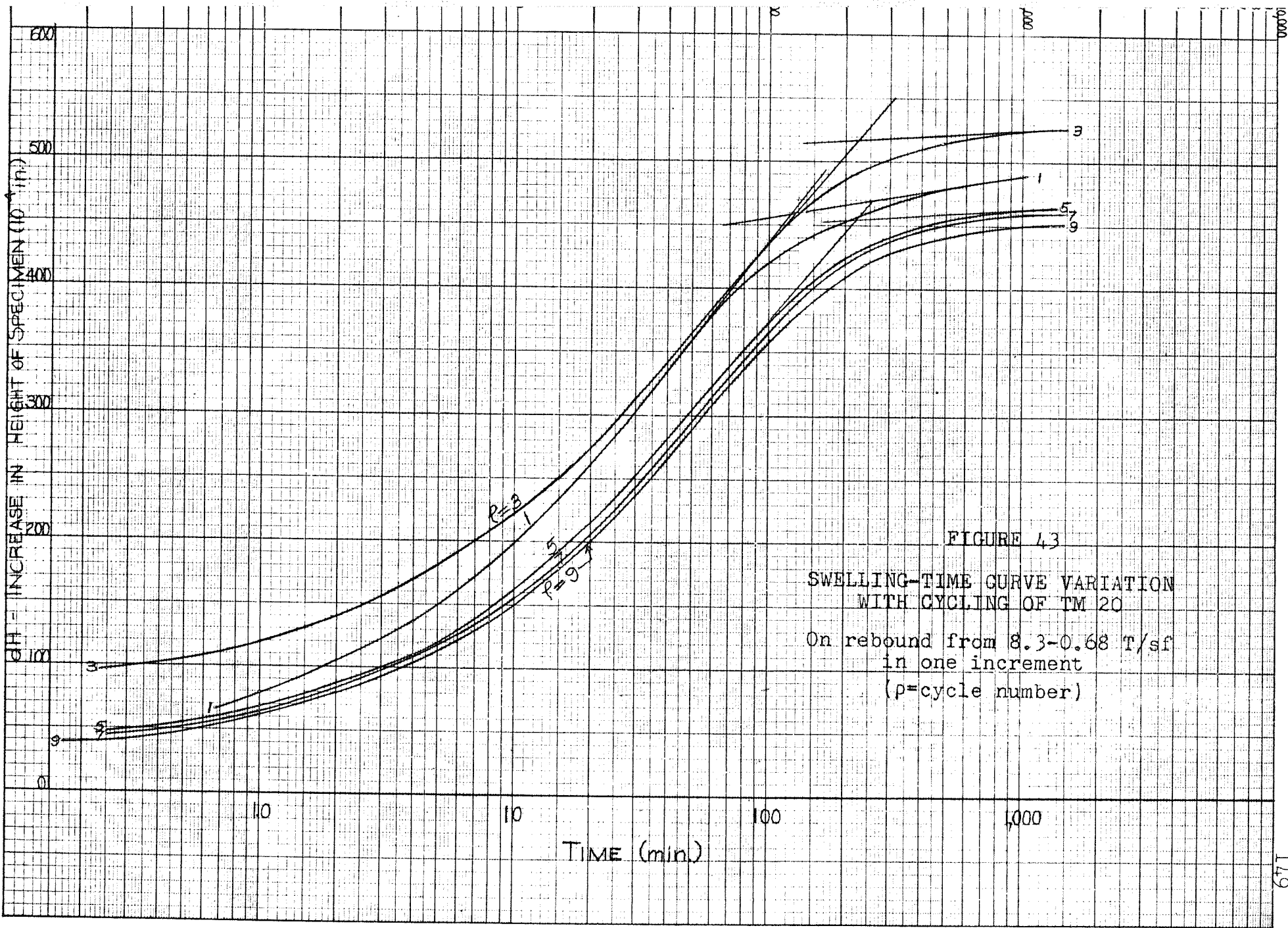


FIGURE 4.2a

SWELLING-TIME CURVES
FOR TM17 ON THE FIRST
REBOUND FROM 8.3 T/sf
($\rho = 1$)





INDEX

- Air bubbles, 91
- Air compressor, 26
- Allely, B. H., 24
- Apparatus deflections, 22, 23
- Assembly,
 - of specimens in consolidometer, 24
 - of specimens in triaxial cell, 27, 31
- At-rest condition, 49
- Atterberg limits, 18, 19

- Bessel Function, 72,
 - form of, 72
 - orthogonality, 75
 - series for, 73
 - roots of, 74
- Bishop, A. W., 12, 91
- Bolt, G. H., 14
- Bond theory of Terzaghi, 9
- Boundary conditions, of triaxial drainage, 74
- Burettes, 29, 30
- Butler, W. H., 13, 60

- Calibration,
 - of pressure gauges, 28
 - of springs on consolidometers, 19
- Carillo, N., 69
- Casagrande, A., 10, 41, 57, 95
- Cell pressures, 26, 27
- Classification tests, 18, 19
- Clay, description of, 16
- Clay content, effect of, 62
- Clay minerology, 13
- Coefficient,
 - of compressibility, 3, 12, 68, 107
 - of consolidation,
 - calculations of, 57
 - definition of, 3
 - effects on, cycling, 109, disturbance of sample, 7
 - fitting methods, 57
 - horizontally, 86
 - in triaxial cell, 8, 12, 86
 - of permeability, 3, 58, 63, 89, 109
- Colloids, content of, 19
- Compressibility of clays, 9, 14, 83
- Compression curve, 2, 45, 50, 62, 113
- Compression index, 3, 9, 38, 45, 52, 62

- Consolidation characteristics, 3, 9, 112
- Consolidometer
 - description of, 20
 - loading process, 25
 - standard test, 12, 25, 124
- Continuity equation of flow, 64, 65
- Counter weights, 22
- Crawford, C. B., 9, 11
- Curve-shift, 95, 99, 101, 104, 128
- Cutting tool, 22, 28
- Cycling tests, 2

- Darcy's Law, 4, 65
- Degree of consolidation, 10, 70, 76, 78, 79
- Depth of sample, 16
- Dessication, 127
- Differential thermal analyses, 13
- Dispersed structure, 1, 116
- Disturbance, 5, 34, 40, 62
- Doran, I. G., 10

- Electron microscope, 13
- Elmwood, 16
- e-log p curve, 2, 12, 42, 83, 96
- Equipment, 7
- Errors, 57, 63, 112

- Field,
 - compression curve, 40, 62
 - swelling, 117
- Filter paper, 22, 24, 25, 26, 83
 - drains, 8, 30, 31, 83
 - type recommended, 30
- Fissures, 16
- Fitting methods, 10, 53, 55, 63
- Flaking of samples, 106
- Flattening of curves, 107
- Floating ring consolidometer, 8
- Flocculated clays, 116
- Flow line, 18, 19
- Flow through a soil, 4
- Free swell test, 13
- Friction, 7, 114, 124
- Frobenius, method of, 73

- Gibbs, H. J., 14
- Gibson, R. E., 79
- Grain sizes, 19
- Grim, R. E., 13

Haefeli, R., 10
Hamilton, J. J., 9, 11
Henkel, D. J., 91
Holtz, W. G., 14
Horizontal drainage, 86
Horizontal specimens, 13
Hydraulic gradients, 65
Hysteresis loops, 96, 107

Increment of load, 9, 25, 99
Increment ratio, 25
Initial void ratio, 42, 43, 62
Irregularities in sample, 41 99

Laboratory testing, 7, 10
Lake Agassiz, 1
Lambe, T. W., 1
Laminations, (see varves)
Langer, K., 8
Lateral pressure, 8
Leaks, effects of, 83, 85, 93
Leda clays, 11
Length of specimens, 22, 92
Liquid limit, 18, 19
Load increment ratio, 25
Loading devices, 20, 30
Log of time fitting method, 10, 53
Lumb, P., 79

Magnitude, of curve-shift, 99, 113
Mechanical advantage of consolidometers. 20, 22
Membranes, 92
Mitchell, J. K., 14
Moisture content of sample, 17

Natural log of time fitting method, 10
Naylor, A. H., 10
Newland, P. L., 24
Normal consolidation, 12, 50
No-swell test, 25, 47, 49

Oedometer (see consolidometer)
Operator method of integration, 71
Orientation,
 of laminations, 89, 125
 of minerals, 14
O-rings, 31
Osmotic pressure, 14
Overburden pressure, 3, 47, 49, 62
Overconsolidated clays, 12, 50, 96

Pan loads in triaxial consolidation, 27
Permeability, 3, 58, 63, 89, 109
Plastic limit, 18, 19
Plasticity index, 19
Pore pressure, 54, 68, 76
Preconsolidated clays, 12, 50, 96
Preconsolidation pressure, 3, 6, 10, 41, 96
Primary consolidation, 10, 11, 116
Pressure,
 gauges, 27
 in triaxial cell, 26, 27
 regulators, 26, 27
Profile of ground, 16

Rate of loading, 62
Rebound curve, 6, 10, 114
Recompression, 10, 95
Relieving load (pressure), 10, 101, 118
Remoulding clays, 6, 35, 38
Rowe, P. W., 8, 13, 60, 91
Rutledge, P. C., 5

Sample, 16, 17
 effects of disturbance, 5, 6, 34, 38
Saturation, 7, 17
Samuels, W. H., 13, 60
Schmertmann, J. H., 6, 34, 38, 52, 63
Secondary compression, 9, 11, 104, 107, 117
Seepage, 2
Settlements, 2
Shift (see curve-shift)
Shrinkage limit, 18, 19
Silt content, 43
 effect of, 42, 47, 58, 62, 63
Size of specimens, 28, 30
Solid bond theory, 9
Specific gravity, 18, 19
Spring constant, 22
Square root of time fitting method, 10, 55
Stress history, 6
Standard consolidometer test, 25, 47, 50
Structure of clays, 2, 12, 116
Swelling, 13
 effects upon, 14, 117, 124
 clays, 7, 19
Swelling index, 3, 107, 120
Swelling-time curves, 118, 120, 143

Taylor, D. W., 7, 9, 10, 52, 55, 73, 75, 114
Testing techniques, 22, 30
 effects of, 7, 8, 50, 54, 63
Test-time curves, 10, 89, 112
Theoretical consolidation curves, 54, 55, 56
Terzaghi, K., 3, 9, 10, 68
Thicknesses,
 of samples, 6, 13, 30, 109
 effect of in field, 11
Time factors, 76
Time of 50% consolidation, 53, 55, 57, 109
Triaxial test,
 cell, 2, 26
 test techniques, 12, 30
Trimming of specimens, 22, 30

Undisturbed compression curve (see field curve)

Van Zelst, T. W., 6, 35
Varves, 1, 13, 89, 125
Virgin branch and compression curve, 6, 40, 47, 62
Void ratio reduction patterns, 6, 40
Volume changes, 65, 67

Ward, W. H., 13, 60

X-ray diffraction, 13